PEDRO CARMO E SOUZA

EFFECT OF NATURAL VENTILATION ON AIRBORNE DISEASE INFECTION RISK IN LECTURE HALLS

Dissertation submitted to the Architecture and Urbanism Graduate Program of the Universidade Federal de Viçosa in partial fulfillment of the requirements for the degree of *Magister Scientiae*.

Adviser: Joyce Correna Carlo

VIÇOSA - MINAS GERAIS
2024

Ficha catalográfica elaborada pela Biblioteca Central da Universidade Federal de Viçosa - Campus Viçosa

T
S729e
2024

Souza, Pedro Carmo e, 1995-
Effect of natural ventilation on airborne disease infection risk in lecture halls / Pedro Carmo e Souza. – Viçosa, MG, 2024.
1 dissertação eletrônica (111 f.): il. (algumas color.).

Texto em inglês.
Inclui apêndice.
Orientador: Joyce Correna Carlo.
Dissertação (mestrado) - Universidade Federal de Viçosa, Departamento de Arquitetura e Urbanismo, 2024.
Inclui bibliografia.
DOI: https://doi.org/10.47328/ufvbbt.2024.054
Modo de acesso: World Wide Web.

1. Ventilação. 2. Edifícios - Avaliação de riscos. 3. Doenças. 4. Chaminés. I. Carlo, Joyce Correna, 1973-. II. Universidade Federal de Viçosa. Departamento de Arquitetura e Urbanismo. Programa de Pós-Graduação em Arquitetura e Urbanismo. III. Título.

CDD 22. ed. 697.92

Bibliotecário(a) responsável: Euzébio Luiz Pinto CRB-6/3317

PEDRO CARMO E SOUZA

EFFECT OF NATURAL VENTILATION ON AIRBORNE DISEASE INFECTION RISK IN LECTURE HALLS

Dissertation submitted to the Architecture and Urbanism Graduate Program of the Universidade Federal de Viçosa in partial fulfillment of the requirements for the degree of *Magister Scientiae*.

APPROVED:February 23, 2024.

Assent:

gov.br Documento assinado digitalmente
PEDRO CARMO E SOUZA
Data: 02/07/2024 12:40:26-0300
Verifique em https://validar.iti.gov.br

Pedro Carmo e Souza

Author

gov.br Documento assinado digitalmente
JOYCE CORRENA CARLO
Data: 26/03/2024 16:07:56-0300
Verifique em https://validar.iti.gov.br

Joyce Correna Carlo

Adviser

Ad Nemo

ACKNOWLEDGEMENTS

To the Federal University of Viçosa, for the opportunity to complete the postgraduate course.

This study was financed in part by the Coordenação de Aperfeiçoamento de Pessoal de Nível Superior – Brasil (CAPES) – Finance Code 001, under the project number 60419479687, titled "Tecnologias para adaptação de edificações às mudanças no clima"

To the Fundação de Amparo à Pesquisa do Estado de Minas Gerais (FAPEMIG), for granting the scholarship, under the research project number APQ-00872-22, titled "Uso de simulação e ferramentas computacionais no estudo de edifícios naturalmente ventilados"

To my peers and colleagues at LATECAE/UFV, without whom this dissertation would have never been completed.

“It's the questions we can't answer that teach us the most. They teach us how to think. If you give a man an answer, all he gains is a little fact. But give him a question and he'll look for his own answers.”
— Patrick Rothfuss, The Wise Man's Fear.

ABSTRACT

SOUZA, Pedro Carmo e, M.Sc., Universidade Federal de Viçosa, January, 2024. **Effect Of Natural Ventilation On Airborne Disease Infection Risk In Lecture Halls**. Adviser: Joyce Correna Carlo.

This dissertation shows that two calibration indices suggested by ASHRAE to calibrate energy and water demand simulations can be used to calibrate any type of simulation, including natural ventilation. The authors subsequently use these indices to create a calibrated simulation model of a three-story, 30-classroom lecture hall in tropical climate, and by virtue of assessing the air renovation profile of each of its classrooms, also create an airborne disease infection risk matrix for that building, which can be adapted to similar lecture halls. The risk matrix accounts for three different diseases' quanta emission rates, three different occupation rates (10%, 50% and 90% occupation) and classroom permanence times of up to 250 minutes. Findings suggest ventilation chimney height to be more influential to air renovations than temperature difference alone, that higher occupation rates resulted in more air renovations per hour, but also in higher infection risk, and that differently from temperate climate research has shown, tropical classrooms equipped with thermal chimneys can rely on natural ventilation to reduce airborne infection risk to an acceptable threshold.

Keywords: COVID-19. Building Energy Simulation. Measles. Tropical climate. Thermal Chimney.

RESUMO

SOUZA, Pedro Carmo e, M.Sc., Universidade Federal de Viçosa, January, 2024. **Effect Of Natural Ventilation On Airborne Disease Infection Risk In Lecture Halls**. Adviser: Joyce Correna Carlo.

A presente dissertação mostra que dois índices de calibração sugeridos pela ASHRAE para calibrar simulações de consumo de energia e água podem ser utilizados para calibrar qualquer tipo de simulação, incluindo simulações de ventilação natural. Os autores utilizam estes índices para criar um modelo de simulação calibrado de um edifício de três pavimentos, com 30 salas de aula, em clima tropical e, através da avaliação do perfil de renovação do ar de cada uma das salas de aula, criam também uma matriz de risco de infecção por doenças transmitidas pelo ar para esse edifício, a qual pode ser adaptada a outros pavilhões de aulas semelhantes. A matriz de risco considera três taxas de emissão de quanta de doenças diferentes, três taxas de ocupação diferentes (10%, 50% e 90% do total de cadeiras ocupadas) e tempos de permanência em sala até 250 minutos. Os resultados sugerem que a altura da chaminé é mais significante para as renovações de ar do que a diferença de temperatura por si só, que taxas de ocupação mais elevadas resultam em mais renovações de ar por hora, mas também em maior risco de infeção, e que, ao contrário do que os estudos em climas temperados tem demonstrado, as salas de aula tropicais equipadas com chaminés térmicas podem contar com a ventilação natural para reduzir o risco de infecção por doenças aéreas para um limiar aceitável.

Palavras-chave: COVID-19. Simulação Termoenergética. Sarampo. Clima tropical. Chaminé térmica .

LIST OF ILLUSTRATIONS

LIST OF TABLES

LIST OF ACRONYMS AND ABBREVIATIONS

ABNT Associação Brasileira de Normas Técnicas.

ASHRAE American Society of Heating, Refrigeration and Air Conditioning Engineers.

ACH Air Changes per Hour

BES Building Energy Simulation

CAPES Coordenação de Aperfeiçoamento de Pessoal de Nível Superior

CIBSE Chartered Institute of Building Services Engineers

CV(RMSE) Coefficient of Variation of the Mean Squared Error.

CNPq Conselho Nacional de Desenvolvimento Científico e Tecnológico

FAPEMIG Fundação de Amparo à Pesquisa do Estado de Minas Gerais

LBL Lawrence Berkeley National Laboratory

MBE Mean Bias Error

NMBE Normalized Mean Bias Error

NV Natural Ventilation

PVB Pavilhão de Aulas II

UFV Federal University of Viçosa.

UN United Nations.

USDOE United States Department of Energy

WHO World Health Organization

Cwa "Humid Subtropical" according do Koppen-Geiger Classification.

LIST OF SYMBOLS

@	"At".
%	Percentage.
∑	Summation.
∫	Integral.
e	Euler's number.
$\log_a b$	logarithm base "a" of "b".
A⇐B	If "B", then "A".
√x	The square root of "x".
ΔCp	"Delta Cp", the variation of the Pressure Coefficient.
Δt	"Delta t", the variation of temperature.
Q	Flow
°	Degrees
°C	Degrees Celsius
K	Degrees Kelvin
m	metres
m^2	square metres
m^3	cubic metres
cm	centimetres
cm^3	cubic centimetres
kJ	kilojoules
W	Watts
α	Reflectance

SUMMARY

1 INTRODUCTION

As schools and universities transitioned back to in-person learning in the wake of the COVID-19 pandemic, concerns rose as to whether this would entail a rise in infection, since occupation density and “social proximity” had been pointed out as a leading factor in infectivity during the period. (Morawska et al. 2020). Conversely, ventilation had long since been pointed out as an effective disease control method (WHO, 2019. NIGHTINGALE, 1863. MACIEL apud VITRUVIUS, 2006.), and it was known that thermal chimneys improved ventilation in classrooms (OLIVEIRA, 2017). Therefore, we set out to investigate if the classrooms in the Federal University of Viçosa’s largest lecture halls building, which are equipped with thermal chimneys, were well ventilated enough to safely accommodate the returning students.

To this end, we needed not only to understand the mechanics of airborne disease infection, but also and most crucially, the behavior of air in the classrooms of this building. Papers discovered during literature revision spoke about how natural ventilation alone was insufficient for mitigating infection risk in temperate climates (ZIVELONGHI et al., 2020, BUONANNO et al. 2022, RODRIGUES and FELICIANO, 2019.), but the absence of studies on indoor spaces with thermal chimneys, and/or in tropical climates was noticed. In this context, the area of computational simulation presented itself as a method of obtaining natural ventilation metrics, as seen in (LAMBERTS et al 2011, SAKIYAMA et al 2020, O’DONOVAN et al. 2019) and others.

Bhagat et al. (2020), Foster and Kinzel (2021) and others suggest Computational Fluid Dynamics (CFD) for calculating infection risk, but ultimately, applying such a computationally expensive method to such a numerous number of complex interior environments would be incompatible with the limitations of this research project. CFD was used to model outdoor airflow around the building instead, and the interior of the classrooms was modelled through Building Energy Simulation, using software EnergyPlus.(USDOE, 2023)

By delving into the issues of building simulation, especially as pointed out by (CHONG et al. 2021, and RUIZ E BANDERA, 2017), it became clear that ensuring the calibration of the simulation essential to the reliability of the results, as was the correct use of calibration indices suggested by ASHRAE Guidelines (ASHRAE, 2023). We successfully demonstrated the applicability of these indices for natural ventilation simulations, and with a calibrated model, were able to glean from it the ventilation metrics we needed to finally

assess the biological risk faced by would-be occupants of *"Lecture Hall II"* (author's translation). During this process, we also had to tackle issues regarding the microclimate around the building and its discrepancy from the nearby weather station, collected

What follows is a more detailed explanation of the subjects examined by this dissertation, as well as its goal, objectives and structure. We hope to enlighten the reader to these subjects before the later chapters to ensure a clearer understanding of this dissertation as a whole.

Airborne diseases have been a recurring challenge for public health and safety since time immemorial. These diseases are primarily transmitted through minuscule particles that remain suspended in the air for extended periods, frequently in the form of saliva and phlegm aerosols (ZHANG et al., 2020; MORAWSKA et al., 2020, 2009; XIE et al., 2007). The ability of these diseases to propagate through the air has made them a significant concern, calling for thorough research and mitigation measures to ensure the safety of occupants in indoor spaces.

The emergence of the COVID-19 pandemic has heightened this concern, particularly within indoor spaces like classrooms. This global health crisis has underscored the importance of understanding and mitigating the risk of all airborne infections, given the severe consequences of COVID-19. The pandemic has forced a reevaluation of health and safety practices, particularly in educational settings, prompting a need for effective measures to reduce the risk of contagion and improve indoor air quality.

As is logical, one of the oldest and most ubiquitous health problems in human history also has had a known solution for a long time. One of the simplest and most effective means of mitigating the risk of contagion in indoor spaces is through natural ventilation (NV) (VITRUVIUS, apud MACIEL, 2006; NIGHTINGALE, 1863). As a risk mitigation mechanism, NV relies on the inflow of fresh outdoor air and the expulsion of indoor air, diluting potential pathogens and reducing their concentration within enclosed spaces (WELLS, 1955; RILEY, 1978). This natural process can significantly improve indoor air quality, decrease the risk of airborne disease transmission, and mitigate the effects of the so-called "Sick Building Syndrome" (SBS) (REDLICH, SPARER and CULLEN, 1997). Therefore, understanding the effectiveness of NV in classrooms becomes a crucial aspect of mitigating infection risk.

The behavior of air in an enclosed space is highly dependent on its geometry, the size, quantity, and position of its doors and windows as openings, and the location of said

enclosed space, both concerning urban space and its biome. We have chosen to study “PVB” (“*Pavilhão de Aulas II”,* translated from portuguese as *“Lecture Hall II”)*, a three-story tall educational building with 30 classrooms with near identical dimensions and openings in three different façades orientations, all equipped with thermal chimneys, located on the campus of a university in a tropical climate (Köppen-Geiger Cwa. (PEEL et al., 2007)). The high number of classrooms in constant use, the building surroundings, and this building’s classroom characteristics lead us to believe this study shall apply to many similar classrooms in other buildings. More importantly, we suspect the characteristics of this building’s classrooms, namely the presence of thermal chimneys and large vertical openings enabling cross-ventilation, ensure a low risk of airborne contamination with natural ventilation, through elevated air exchange rates. We set out to investigate this suspicion.

1.1 OBJECTIVES

Aim: To quantify the infection risk of three airborne infectious diseases in classrooms of a naturally ventilated, thermal chimney-equipped lecture hall in a tropical climate.

Goal 1: To discuss the applicability of two statistical indices, the NMBE and the CV(RMSE), on the calibration of building simulation models of naturally ventilated spaces.

Goal 2: To review the methods of calibrating building energy models.

Goal 3: To create a calibrated computational building simulation model of PVB, a naturally-ventilated, thermal chimney-equipped lecture hall in a humid subtropical climate.

Goal 4: To obtain an air exchange rate profile for all classrooms in the building throughout the year.

Goal 5: To create a safe usage matrix of PVB, indicating safe occupancy rates and maximum permanence times for its classrooms.

1.2 THEORETICAL FRAMEWORK: Terminology adopted in this work.

1.2.1 Ventilation

In architecture, ventilation is the intentional entry of air into a space, naturally through openings in the sealing elements or by devices such as fans or exhaust fans. This concept contrasts with infiltration, which is similarly the entry of air into a room, but unintentionally, through gaps, faults, or other accidental openings in the building's sealing elements. Mechanical or forced ventilation is generated artificially by instruments such as fans and exhaust fans. On the other hand, natural ventilation is a consequence of natural pressure differences between two or more points in the atmosphere (WHITE, 2011). Natural

ventilation is generally associated with horizontal openings. However, it is essential to note the contribution of vertical ventilation, caused by the difference in temperature (and therefore density) of the air between two points at different heights (OLIVEIRA, 2017), the so-called "chimney effect."

1.2.2 Infection

Airborne transmission of diseases has been understood since ancient times, with early warnings about the harm of winds and the belief that diseases like Malaria were caused by “bad air” (OXFORD LANGUAGES, 2021). In the 19th century, natural ventilation was already recognized as responsible for maintaining a healthy environment and reducing contagion. (VITRUVIUS, apud MACIEL, 2006; NIGHTINGALE, 1863).

The Wells-Riley model, developed in the 20th century, is the basis for studying the risk of airborne transmission (WELLS, 1955; RILEY, MURPHY & RILEY, 1978). This model estimates the probability of contagion in a healthy individual, and later studies expanded it to predict the number of infections based on exposure time. (GAMMAITONI & NUCCI, 1997; BUONANNO et al, 2020) Wells introduced the concept of a "quantum" of contaminating particles, that necessarily infects 63.3% of patients after contact. Wells considers the vector of airborne respiratory diseases to be "Droplet Nuclei," the remnants of evaporated droplets of mucus and saliva that contain infectious agents and float uniformly distributed in an internal space. Riley and his colleagues used this theory to model the transmission of measles. Overall, understanding the mechanisms of airborne transmission is crucial for preventing the spread of diseases.

1.2.3 Simulation

Building Performance Simulation (BPS) aims to create accurate virtual representations of real-world buildings for scientific and practical insights. Calibration, the process of aligning simulation models with actual buildings, is pivotal for model accuracy. However, a 2017 study revealed widespread mis-implementation and reporting of calibration methods, reflecting the confusion surrounding calibration, validation, and verification terminologies (RUIZ e BANDERA, 2017).

Calibration involves adjusting models through data collection and comparison with real-world data, acknowledging inherent simulation inaccuracies. Despite allowable error margins in many BPS applications (ASHRAE, 2014), a persistent "performance gap" between simulations and actual measurements has been noted, often attributed to

uncertainties like approximations and operational variations. Irreducible uncertainties, such as microscopic material variations and future wind pressure coefficients, pose challenges (O'DONOVAN et al, 2019). In sum, calibration in BPS seeks to minimize discrepancies and enhance model reliability, even in the face of unavoidable uncertainties, by applying established guidelines and principles to various parameters and variables.

1.3 STRUCTURE

This dissertation is divided into five chapters, the first of which is this introduction. Each of the subsequent three chapters takes the form of a stand-alone research paper tackling one of the specific objectives of the dissertation, with its own introduction, methodology, results, and conclusions. The final chapter provides conclusions and recommendations in respect to the research project as a whole.

Chapter 2, "The Applicability of NMBE and CV(RMSE) for Calibrating Natural Ventilation Simulations" argues the Normalized Mean Bias Error (NMBE) and the Coefficient of Variation of the Root Mean Square Error (CV(RMSE)) thresholds suggested by ASHRAE Guideline 14 can be used to calibrate simulations of any nature, and subsequently describes the calibration of a model with said guidelines. The model was manually calibrated through five classrooms which exhibit a range of characteristics representative of the whole building. They were monitored while empty in winter and summer conditions with temperature and humidity sensors. The calibration process was based on the work of Lamberts et al (2017), which calibrated a ventilation simulation through temperature.

Chapter 3, "Obtaining the Air Exchange Profile of a Tropical Naturally Ventilated Building through Calibrated Simulation." follows the process of obtaining the air exchange profiles of all classrooms in the building, through data obtained from the calibrated simulation model. The results indicate a healthy building, whose classrooms are heavily influenced by their façade orientation and position relative to the ground.

Chapter 4, "Creating a Safe Use Matrix for a Naturally Ventilated Educational Building in Tropical Climate" evidences the mechanics of infection as seen by the airborne infection probability models devised by William F. Wells (and improved on by Riley et al. (1978) and Gammaitoni and Nucci (1997), and most recently Buonanno et al. (2020). It calculates the risk of infection by three common airborne infections: COVID-19, Tuberculosis and Measles, based on the air exchange rate profile of each classrooms and three occupation scenarios.

The fifth and final chapter presents the overall conclusions of the study, as well as the study's limitations and indications for future work.

1.4 METHODOLOGICAL OVERVIEW

Chapter 2 describes the process of creating a calibrated model of the building in a Building Energy Simulation (BES) software called EnergyPlus. After a literature review to determine the calibration standards and procedures, we demonstrated ASHRAE Guideline 14's NMBE and CV(RMSE) limits to be acceptable and applicable to the calibration process at hand. We subsequently collected data on the building under study. This data was used to create a simulation model of the building in EnergyPlus 22.1 and also to calibrate the said model, ensuring it was the best possible representation of the actual building with respect to BES.

Chapter 3 takes advantage of the assumption that a calibrated simulation model behaves similarly to the object it represents (GU et al., 2007) to quantify the air changes per hour (ACH) inside the classrooms of PVB. We added three occupation scenarios to the simulation model, which already included the typical openings operation schedule. This enabled us to study how the building's classrooms exchange air with the outside environment throughout a typical school weekday, how that behavior changes when classrooms are sparsely populated or more densely occupied, and most importantly, provided air renewal metrics for each classroom.

Chapter 4 builds on the results of the previous chapter to calculate airborne infection risk. This chapter employs the GN-Riley infection model as posed by Buonanno et al. (2020) to calculate the risk of infection by three major airborne diseases for healthy occupants in a classroom, assuming they are in the company of one infected individual. This is done by comparing the rate of emission of infective particles by the infected individual, the ventilation rate (ACH) of the classroom, and the total exposure time to the infected air.

1.5 BIBLIOGRAPHY

BERKELEY, L. *et al. EnergyPlus essentials*. [S.l: s.n.], 2019.

BUONANNO, G.; STABILE, L.; MORAWSKA, L. Estimation of airborne viral emission: Quanta emission rate of SARS-CoV-2 for infection risk assessment. *Environment International*, p. 105794, 2020. Disponível em: <https://doi.org/10.1016/j.envint.2020.105794%20Received>.

L.GAMMAITONI; M.C.NUCCI. Using a mathematical model to evaluate the efficacy of TB control measures. *Emerg. Infect. Dis.*, v. 3, p. 335–342, 1997.

MORAWSKA, L. *et al.* Size distribution and sites of origin of droplets expelled from the human respiratory tract during expiratory activities. *Journal of Aerosol Science*, v. 40, p. 256–269, 2009.

MORAWSKA, L.; MILTON, D. K. It is time to address airborne transmission of coronavirus disease 2019 (COVID-19). *Clinical Infectious Diseases*, v. 71, p. 2311–2313, 2020.

NIGHTINGALE, F. *Notes on hospitals*. 3rd. ed. [S.l.]: Longman, Green, Longman, Roberts and Gre, 1863. p. 187Disponível em: <https://books.google.com/books?hl=en&lr=&id=n5FtEAAAQBAJ&oi=fnd&pg=PA1&dq=good+governance&ots=6UIHTdayhH&sig=sO-wYh6SQrgpIFukLwvBQeCPru8>.

OLIVEIRA, M. M. *Análise da influência de chaminés solares no conforto e na renovação de ar de ambientes interno*. 2017. 2017.

PEEL, M.; FINLAYSON, B.; MCMAHON, T. Updated world map of the Köppen-Geiger climate classification. *Hydrology and Earth System Sciences*, v. 11, p. 1633–1644, 2007.

RILEY, C.E; MURPHY, G.; RILEY, R.L.. AIRBORNE SPREAD OF MEASLES IN A SUBURBAN ELEMENTARY SCHOOL. *American Journal of Epidemiology*, v. 107, p. 421–432, 1978.

REDLICH, C. A.; SPARER, J.; CULLEN, M. R. Sick building syndrome. *Journal of Orthomolecular Medicine*, v. 12, p. 23–27, 1997.

VITRUVIUS. *Vitruvio: Tratado de arquitectura*. [S.l.]: IST Press c2006, [S.d.]. p. 454

WELLS, F. Threshold sanitary ventilation. [S.l.]: Harvard University Press, 1955.

White, F. M. (2011). Fluid mechanics (seventh ed.). (7th ed.). McGraw-Hill.

XIE, X. *et al.* How far droplets can move in indoor environments - revisiting the Wells evaporation-falling curve. *Indoor Air*, v. 17, p. 211–225, 2007.

ZHANG, R. *et al.* Identifying airborne transmission as the dominant route for the spread of COVID-19. *Proceedings of the National Academy of Sciences of the United States of America*, v. 117, p. 14857–14863, 2020.

2 The Applicability of NMBE and CV(RMSE) for Calibrating Natural Ventilation Simulations

2.1 Abstract

Scholars and practitioners in Building Science widely accept ASHRAE Guidelines. Guideline 14 (CHONG et al., 2021), which sets standards for water and energy savings calculations, also recommends a standard for calibrating building energy simulations. This paper provides an overview of methods used for simulation model calibration, with a particular focus on those representing naturally ventilated environments. It evidences the current state of the art by analyzing recent applications of these methods in six recent studies. By examining statistical definitions, we show that one can use the method proposed by ASHRAE to calibrate natural ventilation in computational models. We apply this calibration method to a model of an educational building in tropical weather and achieve sub-2% normalized error thresholds.

Keywords: ASHRAE, Calibration, Building Simulation Models, EnergyPlus

2.2 Introduction

Building Performance Simulation is a field of scientific computing that involves creating a simulacrum of reality from which scientists and practitioners can draw information about actual buildings and environments. As such, one would imagine that guaranteeing the accuracy of these simulacra (in most cases, physics-based mathematical models) would be one of the field's primary concerns since the works based on them are only as reliable as the models themselves. Guaranteeing the accuracy of simulation models is precisely the purpose of calibration.

A 2017 study also found that calibration methods are often wrongly implemented or reported. Ruiz e Bandera (RUIZ and BANDERA, 2017) discusses 58 documents or articles in the energy modeling field where errors have been found regarding the validation process's implementation, conceptualization or nomenclature. This finding corroborates the later study from 2021 (CHONG et al., 2021), which claims the differences between calibration, validation, and verification may escape some readers since the three terms have been used to indicate model-to-building consistency in the literature.

Calibration is the process of adjusting a simulation model to make it more similar to the actual building it is supposed to represent (O'DONOVAN et al., 2019). The first step in calibration is gathering data on the building and comparing the simulation results to the gathered data. By its very nature, simulated results will never be absolutely accurate at all times (CHONG et al., 2021). However, a certain level of error is admissible for most applications of BES, such as measuring energy efficiency, thermal comfort, and even biological safety (ASHRAE, 2014; CHONG et al., 2021).

Even so, constant and recent instances of a "performance gap" (CHONG et al, 2021; O'DONOVAN et al. 2019) between simulated models and actual measurements have been reported. As an illustration, studies as recently as 2018 show an up to 26% difference between two different simulation tools (MANTESI et al., 2018). Chong et al. (2021) say these discrepancies mainly arise from uncertainties, which are attempts at filling in unknown data with approximations and averaged values. Both Chong et al. (2021) and O'Donovan et al. (2019) cite building operation as a significant source of uncertainty, but uncertainty can stem from several sources, some of which are impossible to verify, observe, or correct (DER KIUREGHIAN and DITLEVSEN, 2009.). Examples of this type of uncertainty are the natural microscopic variations in building materials and the wind pressure coefficient at any given instant in the future. For these "irreducible" uncertainties, most calibration guidelines

(ASHRAE, 2023.) suggest acknowledging they are part of the modeling process, identifying them, and quantifying their possible influence on the simulation results.

ASHRAE Guideline 14 is among the most cited of these calibration guidelines (RUIZ e BANDERA, 2017), despite being primarily about measuring water and energy savings. One must ask if the indicators and thresholds suggested by this guideline are useful for calibrating other variables, such as a naturally ventilated model's air exchange rate. If so, how would one do that?

2.3 Objective

The present study aims to discuss the applicability of two statistical indices present in ASHRAE Guideline 14 (ASHRAE, 2023.), the NMBE and the CV(RMSE) to the calibration of building simulation models of naturally ventilated spaces.

2.4 Calibration, Validation, and Verification

Calibration is not the sole method of lending credence to simulation models. Model validation and verification are also processes by which one can ascertain the adequacy of a modeled building for simulation purposes, with marked differences. Verification is testing whether the model is coherent with the modeled object, as far as the simulation is concerned. In other words, a verified model is one that, irrespective of its degree of simplification, completeness, or actual output values, exhibits the same logical structure and behaves the same as the modeled object in the simulated situation (ORESKES, SHADER-FRECHETTE, and BELITZ, 1994.). Calibration, as stated previously, is the process by which one adjusts model parameters to bring model output values closer to a set of measured values (CHONG et al., 2021). At the same time, Validation consists of ascertaining whether a model is a valid and accurate representation of reality beyond just one set of measured values (ORESKES, SHADER-FRECHETTE, and BELITZ, 1994.).

2.4.1 Calibration Criteria

Another concern regards calibration criteria. What is an acceptable level of error when calibrating a model? While it may seem that answers depend on the variable the model is being calibrated against, this article evidences that some error quantification strategies can be universally employed. As an example, we examine an ASHRAE publication that suggests model calibration guidelines that were supposed to be used for energy savings calculations

but have also been used in natural ventilation models (SAKIYAMA et al, 2021; O'DONOVAN et al, 2019).

ASHRAE Guideline 14 primarily talks about how to standardize the measurement of water and energy savings, presumably in buildings where there has been or will be a modification or a retrofit. For that, it suggests three approaches. The "*Retrofit Isolation Approach"* measures the independent variables of the systems and elements of the building directly affected by the retrofit, both before and after installation. While this approach may seem too simple to warrant any calibration, one must understand that measuring energy and water consumption in a system comes with a series of metrological issues. How long to measure for? When to measure? Does it make sense to compare the energy consumption from a colder week to the consumption of a week in summer? Does the number of users in this building affect the measurements? By how much? The list goes on. Therefore, the guideline establishes a calibration protocol and standard, which ensures that the measurements from before and after the retrofit are comparable.

Another problem with the Retrofit Isolation Approach is that sometimes measuring only the systems and sections of the building affected by the retrofit is impossible. That problem is tackled by the "Whole Building Approach." In this approach, the calibrator needs to measure the consumption of the entire building or facility and use inverse methods to infer the energy consumption of the systems affected by the retrofit. With this mathematical model, it is possible to determine the energy and water savings by comparing the model with the post-retrofit consumption and with post-retrofit independent variables, such as weather and occupation. This approach uses calibration to ensure that its inferences about the building consumption are correct and accurately predict the influence of each independent variable on the energy consumption of the building as a whole.

The third and last approach tackles the issue of prediction. With the Whole-Building Calibrated Simulation approach, it is possible to use computer building simulation software, such as EnergyPlus, to build a virtual model of the building. At this stage, it is possible to predict savings by adding the planned retrofit to the simulation model. This savings prediction is only possible if the model accurately describes the building and retrofit. Model calibration and the related verification and validation practices are thus essential to this approach. They are used to ensure that the computational model not only outputs correct consumption values but also is a valid representation of the building, and responds accurately to different input variables as the building itself does.

By their very nature, the models resulting from these approaches can incorporate uncertainty, which is “reasonable doubt” (CHONG et al., 2021) about the accuracy of a model. Guideline 14 highlights three primary sources of uncertainty in a model.

Sampling uncertainty refers to the uncertainty about the period of data collection. If one or both measurement periods (before and after retrofit) are anomalous or differ from the “normal” behaviour of the building, then the model may be inaccurately calibrated. Furthermore, small sample sizes may inaccurately reflect the building consumption.

Equipment uncertainty refers to the calibration of the measuring equipment. Uncalibrated instruments can obviously jeopardise the accuracy of measurement, and therefore the accuracy of the model itself. Guideline 14 lists a series of calibration requirements for this very reason.

Modelling Uncertainty refers to the degree of “inaccuracy” of the model, be it a mathematical or a computational model. While uncertainty is inherent to any model, be it mathematical or computational, a maximum uncertainty level must be established to enable model-reference comparison. Guideline 14 sets that level by stating that a model calibrated with values measured every hour may present an NMBE of 10% at most and a CV(RMSE) of no more than 30%. But what do these numbers mean?

The CV(RMSE) and the NMBE are dimensionless indices for discrepancies between simulated and measured data. The first index cited by Ruiz e Bandera (RUIZ and BANDERA, 2017). cited in ASHRAE Guideline 14-2014 is the Normalized Mean Bias Error (NMBE). Before delving into the NMBE, we must first define its origin, the Mean Bias Error (MBE) which Ruiz e Bandera (RUIZ and BANDERA, 2017) defines as “the average of errors in a sample space”. It can be defined by (eq. 1) (ASHRAE, 2023.)

$$MBE = \frac{\sum_{i=1}^{n}(m_i - s_i)}{n} \qquad \textit{(eq. 1)}$$

Where *i* is the value index, m is the measured value, s is the simulated value, and n is the number of samples (RUIZ and BANDERA, 2017). As can be seen in (eq.1), the MBE equation can yield negative or positive results, depending on whether the simulation model over- or under-predicted results in response to natural conditions. For example, an MBE of -5 on a thermal simulation means that it predicted temperatures that were, on average, 5°C higher than measured on site (RUIZ and BANDERA, 2017).

Normalising the MBE means scaling it up or down so that MBEs can be compared for models of different value scales (RUIZ and BANDERA, 2017). This is done by dividing the MBE by the mean of the measured values ($\underline{m}$). ASHRAE Guideline 14 also suggests adding a p variable, representing the number of adjustable parameters in the model, but for calibration purposes it also suggests that variable to be 0. Therefore, normalising the MBE gives us what is shown in (eq. 2)

$$NMBE = \frac{1}{\underline{m}} \cdot \frac{\sum_{i=1}^{n}(m_i - s_i)}{n - p} \cdot 100\ (\%) \qquad \text{(eq.2)}$$

Equation (eq. 2) quantifies the average percentage by which simulated values differ from the measured values of the same parameter in reality. In other words, one can say that the NMBE is a comparison between the size of the averaged error and the average measured value, as well as the "direction" of that error (positive or negative). In this case, positive values mean the simulation under-predicts conditions, while negative values showcase an overestimate in the model. For a model to be calibrated by ASHRAE Guideline 14, its NMBE must not exceed 5% if working with monthly data or 10% if working with hourly data. Figure 2.1 shows an illustration of that concept.

Figure 2.1— Illustration of the concept of NMBE. How much does the average error compare to the average measurement?

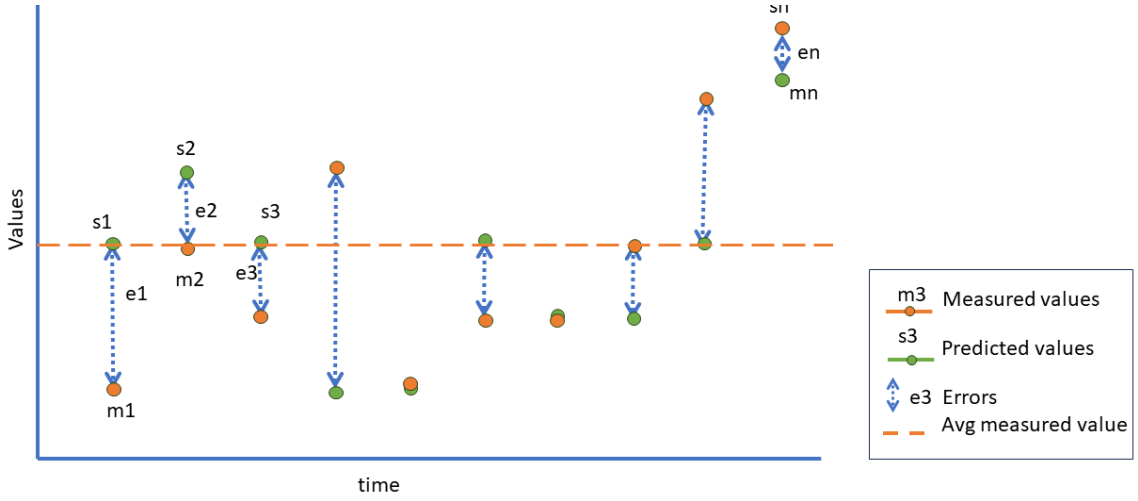

Source: Produced by the author.

One might notice, though, that both these indices are subject to cancellation bias (RUIZ e BANDERA,2017; GOLDBERG, 1991); that is, if there are substantial and opposite discrepancies between the individual data points' biases (errors), the NMBE will still show a small average bias, which can be misleading.

Impervious to this type of error is the second index recommended by ASHRAE Guideline 14, the CV(RMSE), which stands for "Coefficient of Variation of the Root Mean Squared Error" (CHONG et al., 2021). This coefficient can be obtained by (eq. 3).

$$CV(RMSE) = \frac{1}{m} \cdot \sqrt{\frac{\sum_{i=1}^{n}(m_i - s_i)^2}{n-p}} \cdot 100\ (\%) \qquad \text{(eq.3)}$$

With p suggested to be 1 in this case. Stemming from the RMSE or the "Root Mean Square Error", this index can be used to measure if the simulated values are consistent with each other in the same way the measured values are (CHONG et al, 2021; RUIZ e BANDERA, 2017). In other words, it measures by how much the error between the simulation and the measurement varies, and furthermore, how these errors compare to the average measurement. A low CV(RMSE) tells us that even if the simulation has errors, they are small and similar between each other, which may indicate it behaves similarly to the modelled building. On the other hand, a high CV(RMSE) may indicate the simulation is no better than random guessing. Notice that this index measures the absolute distance between simulated and measured values, so it cannot be negative. Figure 2.2 illustrates this concept better

Figure 2.2—The concept of CV(RMSE). If all errors were the same, how big would they be? And how would they compare to the average measurement? Alternatively: How much does the error vary, on average, and how does it compare to the mean measured value?

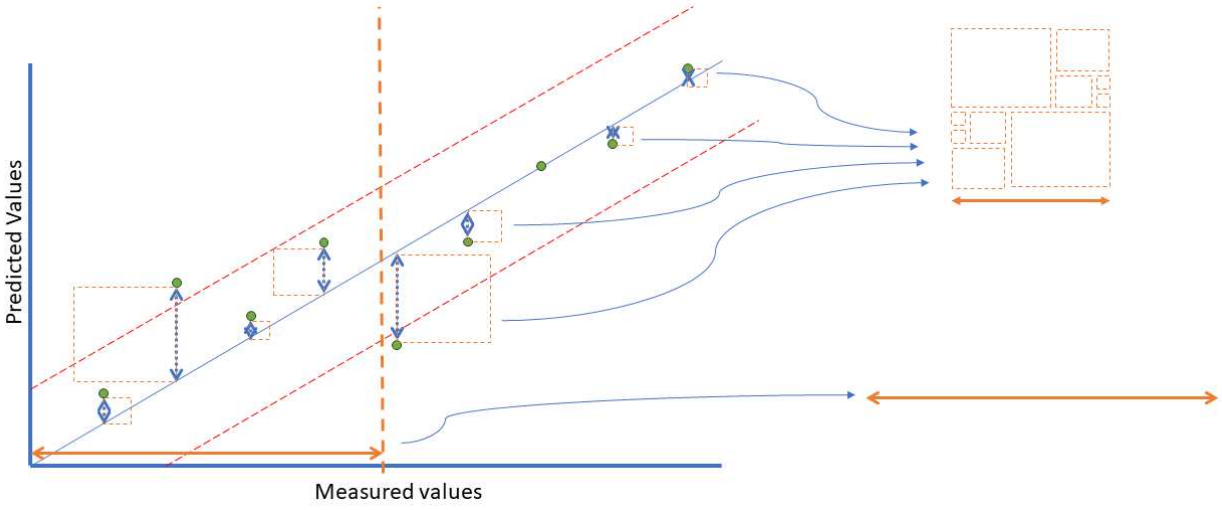

Source: Produced by the author

It is recommended that both the NMBE and the index presented in equation (eq. 3) be used alongside one another (RUIZ and BANDERA, 2017), since they indicate different relationships between the data.

After examining these indices, it becomes clear that the bounds of 10% or lower NMBE and 30% or lower CV(RMSE) suggested by Guideline 14 (ASHRAE, 2023.) can be applied to any type of simulation. This is true because both indices are relative to the measurements, allowing absolute comparison to a single standard. Furthermore, using a relative index tells us more about the simulation than comparing the errors to an absolute value. As an example, if a simulation has an average error of 2°C, and the mean measured temperature is 20ºC, that error is much more significant than it would be if the average measured temperature was 40ºC (an NMBE of 10% versus 5%). This is becoming increasingly relevant as climate change accelerates, and outside temperatures become less and less constant.

2.4.2 Calibration Methods

After understanding the calibration indices and setting targets for these indices, one must focus on how to achieve those targets. Quite a few approaches to calibration have been presented in the literature. In their paper (CHONG et al., 2021) Chong et al. classify them as “automated” or “manual”. The most basic idea of calibrating a model is to iteratively adjust its parameters, run the simulation, and compare the outputs to the measured data (perhaps by employing one of the methods described in section 3). This would very much classify as a manual approach, but better, more optimised ways to do this exist.

Some forms of statistical analysis can greatly improve the efficiency of manual calibration, especially when multiple parameters are involved. One such form of statistical analysis is the Sensitivity Analysis (PICHERY, 2014), which tries to determine the influence of uncertainty in the input variables of the model over the outputs of the model. In BES, this can be used to determine which variables to adjust first to speed up model calibration (CHEN et al, 2019). Local Sensitivity Analysis (SA) tries to “fine-tune” parameters by varying input values in small increments and analysing the outputs, this can be done for example by obtaining the partial differential of an output with respect to an input (PICHERY, 2014). In contrast, Global SA can use linear regression, variance analysis, or sampling methods to determine a hierarchy of model inputs.

Automated methods of calibration rely on computer software to quickly adjust model parameters so that the model output values better match the values observed in the field.

Sakiyama et al. (O'DONOVAN et al., 2019) employ jEplus (jEPlus.org, 2019), an external interface to the well-known BES software EnergyPlus, to run multiple parallel simulations at once, and to automatically and rapidly vary model parameters and extract results.

In addition to this automated interface, the paper uses statistical sampling techniques (specifically, Latin Hypercube sampling) to optimise computing time by simulating only a small representative sample of all the possible model parameter combinations. Sampling methods like Latin Hypercube and Bayesian Inference can be of significant help when testing multiple parameters, as is also shown in (HOU, HASSAN and WANG, 2021). Chong et al. (CHONG et al., 2021) also cite Sensitivity Analysis as a frequently used approach, consisting of a method for determining the influence of individual input variables on the final output of the model. (TIAN , 2013)

Similarly, (ASADI et al., 2019) proposes a methodology that couples a Harmony Search (HS) algorithm with EnergyPlus to create an ever-improving feedback loop, where an initially random combination of parameter values is gradually refined by replacing less optimal values with new values in each loop. This is an optimization-based approach to calibration and can be also done with algorithms such as GenOpt (LBL, 1998), Octopus (VERLINGER, 2012) and Opossum (Opossum Support, 2016).

2.4.2.1 *Analysis of Naturally Ventilated Model Calibration*

We have selected six papers that specifically focus on calibrating naturally-ventilated computational simulation models. The papers selected for analysis in this review were: Sakiyama et al. (2021), O'Donovan et al (2019), Asadi et al (2019), Aparicio-Fernandez et al (2019, Chen et al (2019) and Blazquez, Suaréz and Sendra (2015).

Out of the selected papers, half (SAKIYAMA et al, 2021; ASADI et al., 2019; CHEN et al, 2019) employed some form of automated calibration method, while the other half O'DONOVAN et al., 2019; APARICIO-FERNÁNDEZ, 2019; BLÁZQUES, SUÁREZ and SENDRA, 2015) iteratively adjusted the model manually. Not all of the papers cited ASHRAE Guideline 14, but all used either MBE, NMBE or CV(RMSE) as a way to check model calibration. The works featuring automatic calibration employed optimization-based calibration chose as objectives: minimum CV(RMSE) and NMBE (ASADI et al., 2019), minimum GOF (SAKIYAMA et al., 2021) and minimum MBE (CHEN et al., 2019).

All of the papers considered indoor air temperature in their calibration stages, which coincides with the findings in (CHONG et al., 2021), and the methodology employed by Lamberts (2010) (LAMBERTS et al., 2010). Asadi et al (ASADI et al., 2019) considered

only the temperature setpoints. Relative humidity was only a target on Chen et al (CHEN et al., 2019)

Other calibrated outputs were: ACH (BLÁZQUEZ, SUÁREZ and SENDRA , 2015), Energy consumption (APARICIO-FERNANDEZ et al., 2019), Level of Occupancy (ASADI et al., 2019), Equipment gains (ASADI et al., 2019), lighting gains (ASADI et al., 2019), infiltration (O'DONOVAN et al, 2019; ASADI et al., 2019), window opening (O'DONOVAN et al, 2019; APARICIO-FERNÁNDEZ et al., 2019) and Relative Humidity (CHEN et al., 2019).

2.4.2.2 *Calibration of an Educational Building Model*

We applied the aforementioned calibration techniques in this study to model an educational building on the main campus of the Federal University of Viçosa, Brazil (Köppen-Geiger Cwa climate). The building also referred to as "*Pavilhão de Aulas II"* or *"PVB",* contains 30 classrooms of very similar dimensions facing northwest, southeast and southwest, distributed in three floors and organized around two internal courtyards (Figures 2.3, 2.4, and 2.6). The building is also conveniently close (<300m, Figure 2.7) to the local weather station and directly next to an open-air parking lot, which should influence modelling.

In addition to the classrooms, PVB also houses a snack bar, a kitchen for staff, tutoring classrooms and a computer lab, which have been added to the model. The administrative offices, bathrooms on all three floors, and reception desk, which are also part of the building, have not been modelled. The building is typically in use for the entirety of the school year, which goes from March to December, with a brief two-week pause in July. It is operational from 7 a.m. to 10 p.m. on weekdays, and from 7 a.m. to 12 a.m. on weekends, with the majority of classrooms in use during that time.

We have selected five of these near-identical classrooms to be the focus of our calibration: Rooms 106, 306, 107, 307 and 308 (Figures 3). We selected these as a sample of the building, with classrooms on the top and bottom floors of all three façades. Each classroom measures approximately 7m by 9m, with a 3.25m ceiling, has one set of wooden double doors, two sets of quadruple metal doors, a row of maxim-air windows, and a thermal chimney. Some classrooms are equipped with wall-mounted electrical fans which are seldom if ever used. Since these are inconsistently numbered and placed, and since all electrical equipment and lights remained off during measurement and calibration, these were ignored. Classrooms house 64 to 80 student desks plus the teacher's desk.

2.5 Materials and Methods

2.5.1 Outline

The calibration of this building model was informed by Lamberts et al.'s work (LAMBERTS et al., 2010) as well as ASHRAE guideline 14 (ASHRAE, 2023.). Our approach to calibration is similar to (LAMBERTS et al., 2010; SAKIYAMA et al, 2021; O'DONOVAN et al., 2019) in that we first collected temperature data on the building, then modelled the structure in EnergyPlus, then ran the simulation and compared its temperature output to the measurements. If the differences between the simulation and the measurements were more significant than the limits allowed in (ASHRAE, 2023.), we adjusted the model and simulation and reran it.

2.5.2 Data Collection

We obtained the building's original plans, which significantly sped up the collection of physical dimensions. It was furthermore impractical to gather temperature data on all 30 classrooms in the building, so the authors selected five classrooms (Figure 2.3) on all three façades and the top and bottom floors, which collectively represent the extremes of the environmental conditions experienced by this building's classrooms.

Figure 2.3—Diagram showing the location of the five classrooms (left) and top-down view of the same diagram (right)

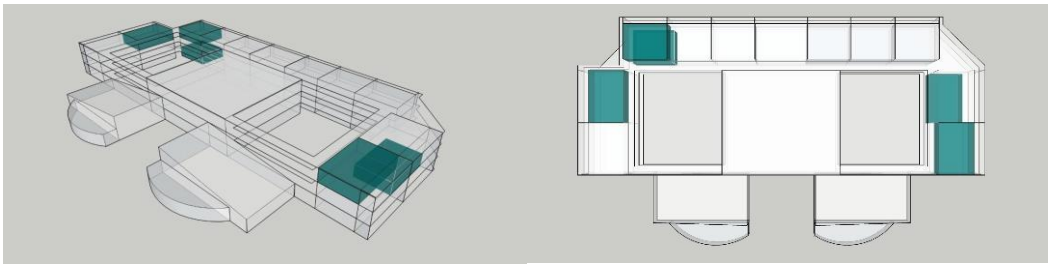

Source: Produced by the author

After selecting the classrooms, we measured them and noted the position and size of all openings. Since we chose to calibrate the classrooms using air temperature, we also set up data loggers (Onset HOBO Model U-12), which recorded the air temperature and relative humidity every five minutes. The measurements were taken in a time period without any internal gains, except for cleaning purposes.

The data loggers were set up in the classrooms and adjacent spaces (Figures 2.5 and 2.6) and labelled with the classroom number and a two-letter code referring to its position. Data loggers with code "*in"* were placed as close as possible to the center of the room, away from view, and carefully attached to one of the desks so as to not disturb airflow to the

Figure 2.4—Floor plan showing the second story and general building layout. Room 206 is outlined

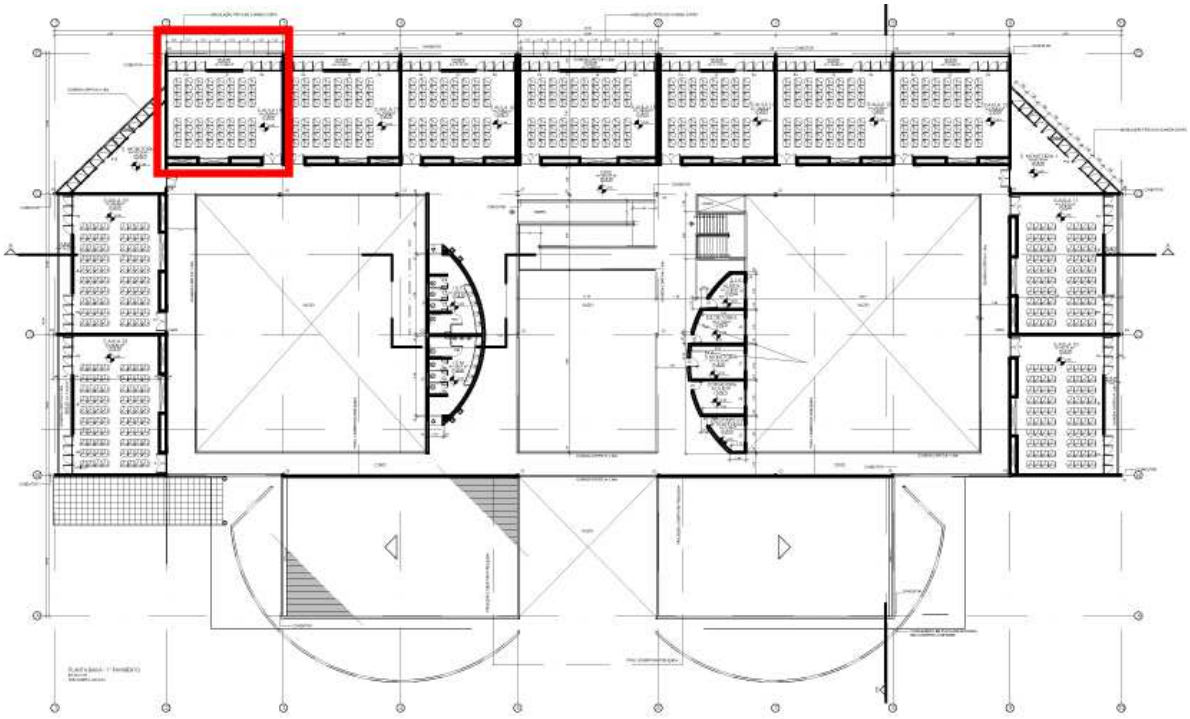

Source: UFV's Administration Office (PAD/UFV)

Figure 2.5—Left: thermal camera image; Right: Floor plan detail, showing the classroom and the adjacent areas: corridor (hatched orange) and balcony (hatched green). Data logger locations shown as blue dots, and thermal camera measurement points shown as blue arrows.

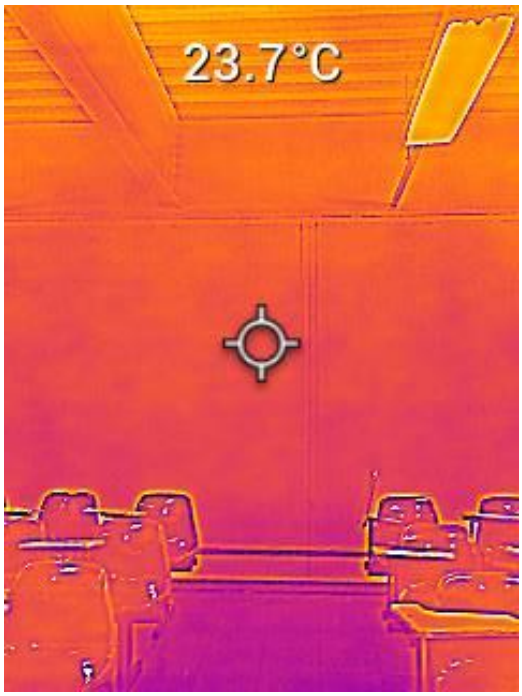

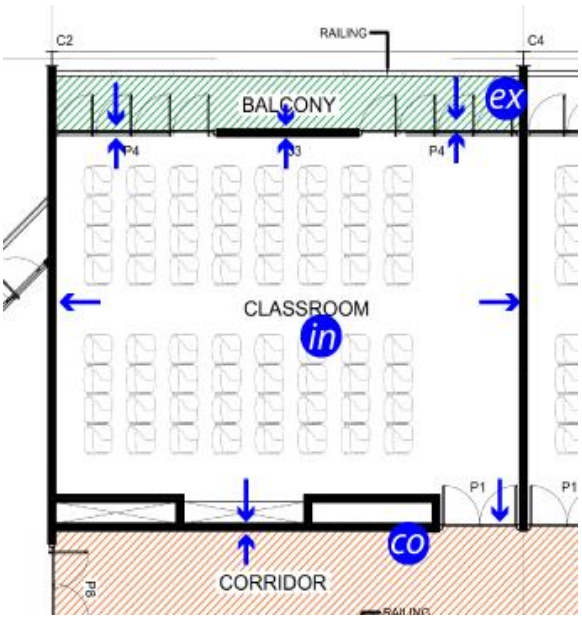

Sources: Left: Taken by the author. Right: UFV's Administration Office (PAD/UFV) Annotations by the Author

sensors. Dataloggers with code "*co"* were placed in the internal corridor of the building, inside a white ventilated plastic casing (10cm x 5cm approximately) which had been attached to the classroom wall. For the data loggers ending in "*ex",* on the balcony wall we used a similar plastic material casing, but this time coated with aluminum foil to avoid radiation gains from heating the air inside the case.

The data loggers recorded data for four days in mid-winter 2022 (August), and ten days in late summer 2023 (February).

While the data logging was in progress, we also measured the surface temperature of the floor, ceiling, walls, and doors in every classroom once every two hours with a FLIR TG-165X thermal camera. This helped check for errors in the model and target adjustments later in the experiment.

Table 2.2.1— Summary of measurement dates and data sources

Parameter	Equipment	Measurement Periods		Mode	Time Step
		Winter	Summer		
Inside Drybulb Air Temperature	Onset HOBO U-12 data logger	26/08/2022 08h00 to 29/08/2022 16h00	23/02/2023 to 06/03/2023*	auto.	5 min
Superficial Temperatures	FLIR TG-165X Thermal Camera	26/08/2022 from 08h00 to 16h00, and 29/08/2022 08h00 to 16h00	23/02/2023 from 08h00 to 16h00,24/02/2323 from 08h00 to 16h00, and 27/02/2023 from 08h00 to 16h00	manual	aprox. 2h
Outside Air Drybulb Temperature	Automatic Meteorological Station INMET A510	01/07/2022 to 31/03/2023	01/07/2022 to 31/03/2023	auto.	1h
Inside Relative Humidity	Onset HOBO U-12 data logger	26/08/2022 08h00 to 29/08/2022 16h00	23/02/2023 to 06/03/2023*	auto.	5 min
	Automatic Meteorological Station INMET A510	01/07/2022 to 31/03/2023	01/07/2022 to 31/03/2023	auto.	1h
Outside Relative Humidity	Onset HOBO U-12 data logger	26/08/2022 08h00 to 29/08/2022 16h00	23/02/2023 to 06/03/2023*	auto.	5 min
	Automatic Meteorological Station INMET A510	01/07/2022 to 31/03/2023	01/07/2022 to 31/03/2023	auto.	1h

2.5.3 Data Treatment.

Since the data loggers recorded the temperature and humidity once every five minutes, we averaged the values over one-hour intervals. This yielded hourly temperature values, which could be compared to the simulation outputs. In turn, we chose hourly simulated values for easy adherence to (ASHRAE, 2023). Once the measured air temperatures were treated compared to its respective simulated output. Surface temperatures were used as a way to verify the model.

Figure 2.6—Top: Interior corridors and courtyard, one week after measurements were taken Bottom: Classroom balconies on the southwestern façade.

Source: photographs taken by the author

2.5.3.1 Classroom characteristics

Each classroom is rectangular, with a ceiling height of 3,25m. Each classroom is equipped with fluorescent lighting, a projector and a computer, all of which remained off during data collection. The windows were opened on measurement days from 8h to 16h.

Table 2.2—Classroom dimensions and materials an asterisk (*) means the measurement was taken from the architectural plans.

	Long Dim.	Short Dim.	Thickness	Material
Ceiling	9m to 12m	7.87m	0.15m*	concrete slab, steel deck.
Walls				
Exterior	9m to 12m	3.25m	0.2m	Cellular concrete blocks, mortar, plaster, white paint
Interior	7.87m	3.25m	0.1m	Dry-wall, glass wool, air
Chimney			0.2m	Cellular concrete blocks, mortar, external face finished with plaster and white paint.
Floor				
Ground floor	9 to 12m	7.87m	0.20m*	concrete slab
Upper Levels	9 to 12m	7.87m	0.15m*	concrete slab, steel deck.
Openings				
Main door	2.10m	1.6m	0.03m	wood, air.
Balcony doors	2.2m	0.7m	0.01m	aluminium.
Windows	0.6m	0.55m	0.003m	aluminium, clear glass

Figure 2.7— The building is very close to weather station

Source: Google Maps, screenshot taken by the author.

2.5.4 Modelling

Model and Simulation Summary	
EnergyPlus Version	*22.1.0*
Solar Distribution Calculation Model	*FullInteriorAndExterior*
Undisturbed Ground Temperature Model	*Xing*
Ventilation Model	*AirflowNetwork*
Materials and Constructions	*Table 2.2*
Schedules	
Occupation	*always off*
Window opening	*always off*
Equipment:	*always off*
Lights:	*always off*
Run Period	*1/jan/2022 to 31/dec/2022*
Weather File	*TMY3 + Local data*[1]
Terrain	*Suburbs*
Orientation	*39.5°*
Site Location	*Viçosa*
Latitude	*-20.753889°*
Longitude	*-42.881944°*
Elevation	*648m*

[1] *Author-created file based on Guimarães e Carlo (2016) and in-situ measurements*

As with measurement, the simulation was run with no internal loads, with all openings closed at all times. The authors chose the FullInteriorAndExterior solar distribution model since no surfaces inside the classrooms were especially reflective. We chose a weather file by Guimarães e Carlo (2016) as a starting point for the final weather file. Initially, we adjusted the new weather file by substituting extant weather data for data from the nearby weather station (270m away). The intention was to ensure the model would receive the same outdoor temperatures and radiation values as the building for the analyzed period. Later, the authors observed that the weather station was recording temperatures significantly different from the ones picked up by the data loggers on the façades of the building. To investigate this discrepancy, we compared the average hourly dry-bulb temperatures from all five balcony data loggers to the hourly dry-bulb temperatures recorded by the weather station for the same period. We found the logged temperatures were, on average, 11.29% higher than the ones measured at the weather station. The authors knew the building was located next to a sizeable concrete parking lot and at a lower elevation than the weather station, and decided to take temperature and humidity data from one of the balcony data loggers (marked *ex*, for *"external",* as opposed to the ones next to the courtyard, marked *"co")* and substitute it for the corresponding data on the TMY3 weather file. The weather station still provided solar

radiation and wind data, and the dewpoints were calculated anew from local data. We chose data logger 106ex, located on the balcony of room 106, not only because it showed temperatures consistent with the mean between all other balcony data loggers but also because it was the most shielded from direct solar radiation, which improved trust in its measurements.

Table 2.2 Thermal Properties of the Materials and Constructions

Construction	**Reflectance (α) [%]**	**U-Factor with Film (Ut) [W/m2-K]**	**Thermal Capacity (Ct) [kJ/°Cm²]**
EXTERIOR WALL	0.47	2.487	385.25
EXTERIOR ROOF	0.75	0.586	1157,34
EXTERIOR FLOOR	0.30	1.534	1852
INTERIOR CEILING	0.11	1.577	1075,94
INTERIOR WALL	0.47	0.628	160,125
INTERIOR FLOOR	0.75	1.305	1075,94
CONARCONARG *(Chimney Walls)*	0.30	1.053	194
ARGCONARCON *(Chimney Walls)*	0.30	1.053	194
PORTAMETAL *(Balcony Metal Doors)*	-	0.398	-
EXTERIOR DOOR	-	2.860	-
INTERIOR WINDOW	-	5.894	-
EXTERIOR WINDOW	-	5.894	-

Source: produced by the author

The authors tested the effect of the Finite Differences method and Xing's method for undisturbed ground temperature calculations, with no real change between the two. The authors then chose to employ Finite Difference over Xing's model for its simplicity and

shorter runtime. Shading objects were modelled next to the building to simulate the nearby vegetation.

As for the model ventilation, we employed AirflowNetwork to model both wind-driven and buoyancy-driven ventilation, considering the lower chimney opening large enough for the *AirflowNetwork: HorizontalOpening* component. We are aware of the *ZoneThermalChimney* component, as discussed by Oliveira and Carlo (2018). However, it was deemed unfit for the simulation since it only calculates buoyancy-driven ventilation, which was determined to be a minority of chimney airflow. The authors do feel the need to emphasize that wind-driven ventilation did not significantly alter the model's accuracy regarding temperature (2% NMBE difference or 0.4°C in most cases) since all windows and doors remained shut during most of the simulation and measurement.

As simulation outputs, we requested the following variables for all zones (Classrooms and chimneys): ZoneMeanAirTemperature, AFN Zone Air Change Rate, and AFN Zone Ventilation Volume. We also requested Surface Inside Face Temperature and Surface Outside Face Temperature for all surfaces that had been measured: the four walls, ceiling, and floor of all zones (including chimneys).

2.5.5 Calibration

The calibration process followed a manual calibration procedure similar to those described in (LAMBERTS et al, 2010; O'DONOVAN et al, 2019, and SAKIYAMA et al 2021). The authors used the NMBE and CV(RMSE) to compare the simulated and measured temperatures on each classroom. After observing that these indices were outside acceptable limits, the authors iteratively altered the model at the uncertainty points and reran the simulation. The authors decided what to alter in the model based on the "direction" of NMBE (positive or negative, indicating under or over-prediction, respectively), the surface temperatures in the classroom(s) where the error occurred, the solar orientation of these surfaces, and their building components. Weather file data was checked eventually to cross-reference results. A hypothesis as to the origin of the error was then elaborated and tested by altering the model accordingly and re-running. If the NMBE and CVRMSE responded accordingly, the alteration was implemented. Otherwise, it was discarded. Figures 2.8 and 2.9 shows a comparison between the first valid model and the latest model.

2.6 Results and Discussion.

Figure 2.8 — Evolution of model error by version, winter data only.

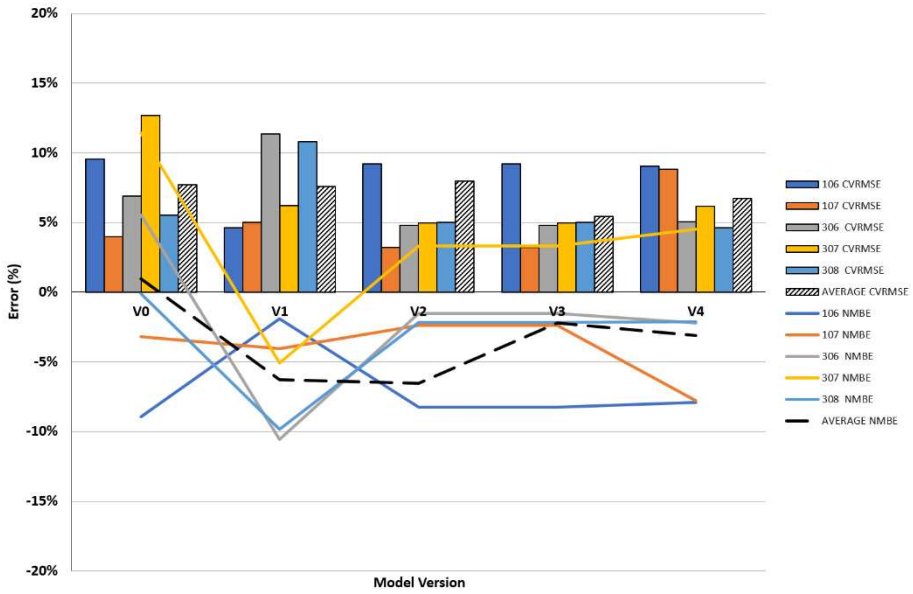

Figure 2.9 — Evolution of model error by version, summer data only

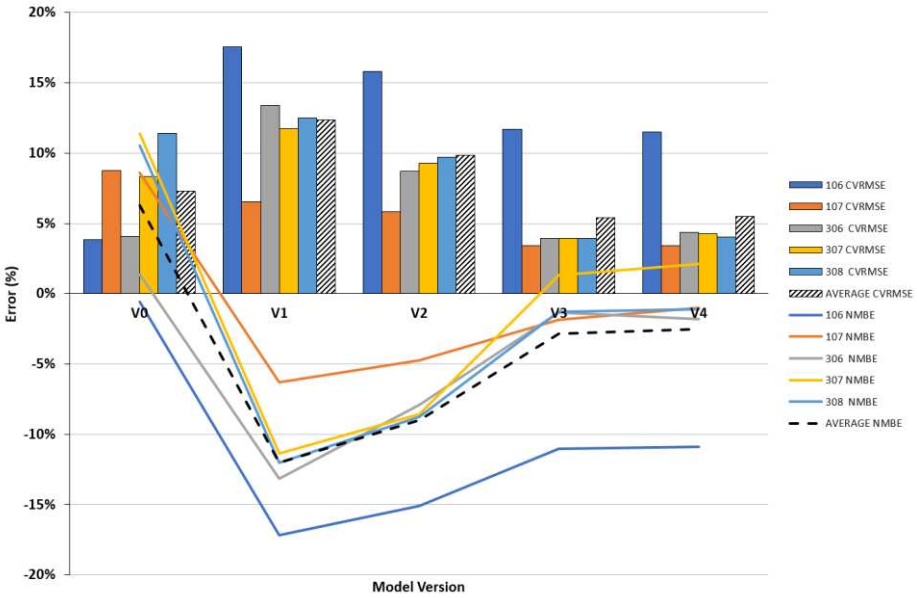

Source: produced by the author

As shown in Figures 2.8 and 2.9, the model was within calibration thresholds from the start, as NMBEs and CVRMSEs sat inside their thresholds (±10% and 30% respectively). The model that produced these results was later discovered to deeply incomplete, however, lacking ventilation modelling, many windows, and contained an incorrect conception of the thermal chimney design. Therefore, we decided to continue the modelling process. Nonetheless, version 0 illustrates this paper's main point: that CVRMSE and NMBE can be used for calibration processes beyond energy-use calibration, and a secondary one: that calibration without verification and validation does not assure model quality. Subsequent

versions were valid, and the calibration process started from version 1 to version 2, reaching a satisfactory threshold on version 4, beyond which computational costs mounted and modelling efforts would yield diminishing results.

Version 0's NMBE sits at 6.26% for the summer measurements and a meager 0.95% for the winter measurements. In simpler terms, the classrooms were, on average, 6.26% hotter in summer and 0.95% hotter in winter than the simulation predicted. While these NMBEs are well below the 10% threshold, the errors for each classroom vary significantly from one another which may (and do) indicate an untrustworthy model. Additionally, while CV(RMSE)s in V0 peak at 12.68%, with an average of 7.50% across all measurements (well below the 30% allowance), this variance does not reflect the actual temperature profile for the rooms, as we can see in the subsequent versions, owing to the incompleteness of model V0.

Versions 1 through 4, conversely, exhibit a consistent and coherent CV(RMSE) and NMBE profile for the classrooms. V4's summer NMBEs concentrate around the mean of -2.54%, with only room 106 as an outlier, at -10.90%. Winter NMBEs are less consistent, but the same pattern emerges, with room 307 having the highest error (+4,5%), followed by rooms 306, 308, and 107, and room 106 again being the lowest and most significant error (-7.90%). Unlike V0's, this error pattern reflects expectations regarding this building throughout the year. The overall average NMBE is -2.82% and overall average CV(RMSE) is 6.13%

Room 307, located on the top floor of the northeastern façade, receives disproportionately more solar radiation than all other rooms, causing it to be, on average 2.10% hotter than the simulation in summer and 4.50% hotter in winter. Furthermore, room 107, directly below, receives much less radiation in the winter months than in summer, causing it to change from 1,00% colder than the simulation in the summer to 7.80% colder in the winter. Rooms 306 and 308 face northwest and southeast, respectively. They exhibit an intermediary error that varies little between them, as expected since they are located next to each other.

Room 106 exhibits the most significant NMBEs and CV(RMSE)s of all rooms throughout the year. The simulation over-predicts the temperatures in that room by 7.90% in summer and 10.90% in winter, meaning the room is colder than predicted. Room 106 is on the southern corner of the southwestern façade's ground floor, next to a dense, tall vegetation mass. Its position means this room is largely shielded from direct solar radiation and is exposed to high humidity. Both factors force temperatures down throughout the year, missing predictions. The lack of solar radiation also causes the room to be more affected by thermal

losses to the soil, owing to the greater temperature difference between air and soil in summer, which increases the CV(RMSE). Room 106's error varies by 11.49% in summer and 9.04% during winter. In comparison, room 107, on the same floor but looking to the northwest, exhibits an error variation of 3.41% in summer when it receives the most radiation and 8.81% in winter when it receives the least.

Although the initial models were already mostly inside calibration thresholds, the authors managed to improve these models to further reduce the error in an effort to have the best model possible. The error spread in versions 1 and 4 have been shown in Figure (9).

Figure 2.10Comparison between simulated and measured temperatures, a) version 1; b) version 4

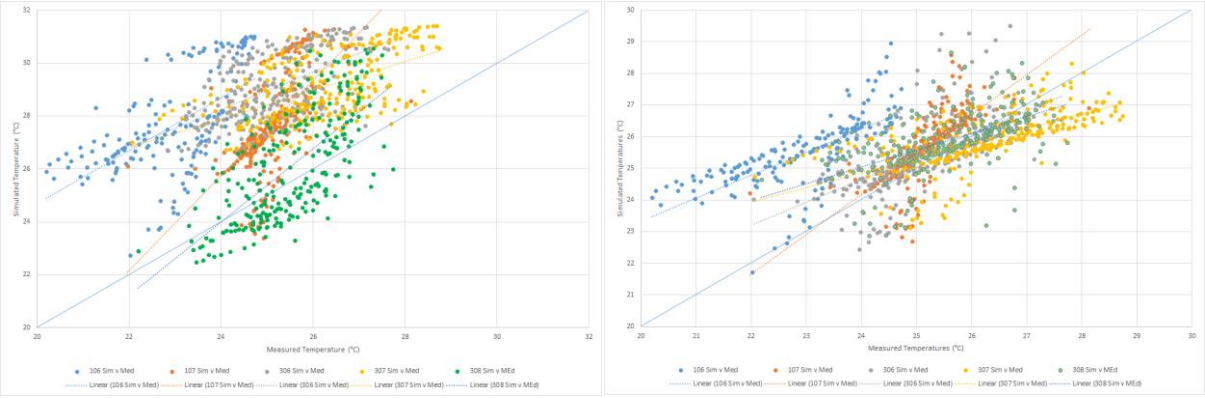

Source: produced by the author

Figure 2.10 demonstrates how a low CV(RMSE) results in a lower error: V4's significantly lower CV(RMSE) is accompanied by data points much closer to the y=x line. That means an R^2 much closer to 1, or in simpler terms, simulated results much more similar to measurements.

2.7 Conclusions

This work's main conclusions are that the current calibration standards posed by ASHRAE Guideline 14 are also suitable for calibrating natural ventilation simulations and, in fact, simulations of any nature beyond energy use simulations. We have also shown that the NMBE can be used to compare one model's error to another entirely different model's error, even if they deal with entirely different data since it measures the model's error relative to itself. So, for example, an educational building's model can be compared to a residential building's model with respect to their verisimilitude. Similarly, we have seen that CV(RMSE) can be used to show "trust" in the model's calibration, measuring whether the static NMBE number accurately represents the overall error. We have seen that by using these indices in tandem, researchers of many areas have a powerful tool to interpret the

results of their simulations. We can also conclude that these indices alone cannot judge a model's "plausibility." We should always see them in light of one another and the model's verification and validation whenever possible.

The *Modelling* section above also highlights the importance of quality weather data for simulations and the impact of the micro-climate on internal temperature measurements. Implementing corrections to the local weather file based on the on-site temperature and humidity measurements was integral to our modeling efforts. In the same vein, we could see the position of the rooms and their exposure to wind pressure, ground conditions and especially to solar radiation heavily influenced the accuracy of the model, the calibration process and data analysis. Nevertheless, the difference between the Finite Difference and the Xing ground models was deemed negligible.

Recording superficial temperatures in the measured rooms was very useful in determining what adjustments to make in the model. These data points guided our hypotheses and expedited the calibration process significantly, while also providing us with data to check our CVRMSE and NMBE findings.

2.8 Acknowledgements

This paper could not have been accomplished without the help and funding from FAPEMIG - Fundação de Amparo à Pesquisa do Estado de Minas Gerais, through funding our project "Uso de simulação e ferramentas computacionais no estudo de edifícios naturalmente ventilados", project number **APQ-00872-22.** We also thank CNPq - Conselho Nacional de Pesquisa, which fundamentally contributed to this paper, through funding our project "Tecnologias para adaptação de edificações às mudanças no clima", project registration number **60419479687**

2.9 Bibliography

APARICIO-FERNÁNDEZ, C. *et al.* Energy modelling and calibration of building simulations: A case study of a domestic building with natural ventilation. *Energies*, v. 12, 2019.

ASADI, S. *et al.* Building energy model calibration using automated optimization-based algorithm. *Energy and Buildings*, v. 198, p. 106–114, 2019. Disponível em: <https://doi.org/10.1016/j.enbuild.2019.06.001>.

ASHRAE. *Measurement of energy, demand, and water savings*. [S.l.]: ASHRAE, 2014. Disponível em: <www.ashrae.org>.

BLÁZQUEZ, T.; SUÁREZ, R.; J, S. J. Vista de Hacia una calibración de modelos energéticos: Caso de estudio del parque residencial español en clima mediterráneo. *Informes de la Construccion*, 2015. Disponível em: <https://informesdelaconstruccion.revistas.csic.es/index.php/informesdelaconstruccion/article/view/4607/5349>.

CHEN, Y. *et al.* Transfer learning with deep neural networks for model predictive control of HVAC and natural ventilation in smart buildings. *Journal of Cleaner Production*, v. 254, p. 119866, 2020.

CHONG, A.; GU, Y.; JIA, H. Calibrating building energy simulation models: A review of the basics to guide future work. *Energy and Buildings*, v. 253, p. 111533, 2021. Disponível em: <https://doi.org/10.1016/j.enbuild.2021.111533>.

DONOVAN, O.; PAUL; MURPHY, M. D. Predicting air temperatures in a naturally ventilated nearly zero energy building: Calibration, validation, analysis and approaches. *Applied Energy*, v. 250, p. 991–1010, 2019. Disponível em: <https://doi.org/10.1016/j.apenergy.2019.04.082>.

FABRIZIO, E.; MONETTI, V. Methodologies and advancements in the calibration of building energy models. *Energies*, v. 8, p. 2548–2574, 2015.

GOLDBERG, D. What every computer scientist should know about floating-point arithmetic. *ACM Computing Surveys (CSUR)*, v. 23, p. 5–48, 1991. Disponível em: <https://dl.acm.org/doi/10.1145/103162.103163>.

HENSEN, J. L. M.; LAMBERTS, R. Building performance simulation for design and operation: Expanded second edition. *Building Performance Simulation for Design and Operation: Expanded Second Edition*, p. 1–772, 2019.

HOU, D.; G, H. I.; WANG, L. Review on building energy model calibration by Bayesian inference. *Renewable and Sustainable Energy Reviews*, v. 143, p. 110930, 2021. Disponível em: <https://doi.org/10.1016/j.rser.2021.110930>.

KIUREGHIAN, ARMEN DER; DITLEVSEN, O. Aleatory or epistemic? Does it matter? *Structural Safety*, v. 31, p. 105–112, 2009.

LAMBERTS, R. *et al.* (Org.). *Casa eficiente: Simulação computacional do desempenho termo-energético*. [S.l.]: UFSC/LabEEE, 2010. v. 4. p. 1–53

LBL. *GenOpt - generic optimization program: Overview*. Disponível em: <https://simulationresearch.lbl.gov/GO/overview.html>. Acesso em: jan. 2024.

MANTESI, E. *et al.* The modelling gap: quantifying the discrepancy in the representation of thermal mass in building simulation. *Building and Environment*, v. 131, p. 74–98, 2017. Disponível em: </articles/journal_contribution/The_modelling_gap_quantifying_the_discrepancy_in_the_representation_of_thermal_mass_in_building_simulation/9443627/1>.

OLIVEIRA, M. M.; CARLO, J. C. Análise da qualidade da simulação do fluxo de ar de chaminés solares com o EnergyPlus. *PARC Pesquisa em Arquitetura e Construção*, v. 9, p. 86–96, 2018.

ORESKES, N.; SHRADER-FRECHETTE, K.; BELITZ, K. Verification, validation, and confirmation of numerical models in the earth sciences. *Science*, v. 263, p. 641–646, 1994. Disponível em: <https://www.science.org/doi/10.1126/science.263.5147.641>.

PICHERY, C. Sensitivity analysis. *Encyclopedia of Toxicology: Third Edition*, p. 236–237, 2014. Disponível em: <https://www.scribd.com/document/513788580/sensitivity-analysis>.

RUIZ, G. R.; BANDERA, C. F. Validation of calibrated energy models: Common errors. *Energies*, v. 10, 2017.

SAKIYAMA, N. R. M. *et al.* Natural ventilation potential from weather analyses and building simulation. *Energy and Buildings*, v. 231, p. 110596, 2021. Disponível em: <https://doi.org/10.1016/j.enbuild.2020.110596>.

TIAN, W. A review of sensitivity analysis methods in building energy analysis. *Renewable and Sustainable Energy Reviews*, v. 20, p. 411–419, 2013.

VIERLINGER, R. *Octopus | Food4Rhino*. Disponível em: <https://www.food4rhino.com/en/app/octopus>. Acesso em: jan. 2024.

WORTMANN, T. Opossum - introducing and evaluating a model-based optimization tool for grasshopper. 2022, [S.l.]: CAADRIA, 2022. p. 283–292. Disponível em: <https://www.icd.uni-stuttgart.de/research/research-tools/opossum/>.

2.10 Appendix: Simulation Model Characteristics by Version Number

The table starting on the next page appendix tracks the changes made to the model, from version 0 until version 4, which was considered calibrated. Entries in red represent a change from the original value, while versions highlighted yellow represent the first time that change occurred. Many more versions of the simulation model were crafted, but the only versions shown here were the ones that displayed an improvement in terms of calibration metrics in relation to their predecessor.

Class	Object	Field	V0	V1	V2	V3	V4
RunPeriod	1	Begin Month	1	1	1	1	1
		Begin Day of Month	1	1	1	1	1
		End Month	12	12	3	8	12
		End Day of Month	31	31	7	31	31
Site:GroundTemperature :Undisturbed		-	-	**Xing**	**FiniteDifference**	**Xing**	**Xing**
Material	4	**Name**	**Laje (SD) (Calc)**	**LajeSD_calc**	**LajeSD_calc**	**LajeSD_calc**	**LajeSD_calc**
		Roughness	MediumRough	Rough	Rough	Rough	Rough
		Thickness	0.398	0.1005	0.1005	**0.2**	**0.2**
		Conductivity	1.75	1.75	1.75	**0.85**	**0.85**
		Density	2300	2300	2300	**2400**	**2400**
		Specific Heat	368	1000	1000	**2000**	**2000**
		Thermal Absorptance	0.9	0.9	0.9	0.9	0.9
		Solar Absorptance	0.2	0.7	0.7	0.7	0.7
		Visible Absorptance	0.7	0.7	0.7	0.7	0.7
	12	**Name**	**Tijolo_Concreto**	**ConcCelAutoc**	**ConcCelAutoc**	**ConcCelAutoc**	**BlocoConcreto**
		Roughness	MediumRough	Rough	Rough	Rough	Rough
		Thickness	0.14	0.125	0.125	**0.15**	**0.15**
		Conductivity	1.75	0.17	0.17	**1.75**	**1.75**
		Density	2400	450	450	**2400**	**2400**
		Specific Heat	1000	1000	1000	1000	1000
		Thermal Absorptance	0.9	0.9	0.9	0.9	0.9

		Solar Absorptance	0.7	0.7	0.7	0.7	0.7
		Visible Absorptance	0.7	0.7	0.7	0.7	0.7
	17	**Name**	**Laje_chao**		**Laje_Terreo**	**LajeTerreo**	**LajeTerreo**
		Roughness	Smooth		Rough	Rough	Rough
		Thickness	0.1	0.08	0.08	**0.4**	**0.2**
		Conductivity	1.75	1.75	1.75	1.75	1.75
		Density	2300	2300	2300	**2200**	**2200**
		Specific Heat	1000	1000	1000	1000	1000
		Thermal Absorptance	0.9	0.9	0.9	0.9	0.9
		Solar Absorptance	0.7	0.7	0.7	0.7	0.7
		Visible Absorptance	0.7	0.7	0.7	0.7	0.7
Material:NoMass	1	**Name**	-	-	-	**LaVidro5cm**	**LaVidro5cm**
		Roughness				VeryRough	VeryRough
		Thermal Resistance				1.1111	1.1111
		Thermal Absorptance				0.9	0.9
		Solar Absorptance				0.7	0.7
		Visible Absorptance				0.7	0.7
	2	**Name**	-	-	-	**LaVidro2_5cm**	**LaVidro2_5cm**
		Roughness				VeryRough	VeryRough
		Thermal Resistance				0.55555	0.55555
		Thermal				0.9	0.9

		Absorptance					
		Solar Absorptance				0.7	0.7
		Visible Absorptance				0.7	0.7
Material:AirGap	6	Name	Ar2	Ar2	ArPortaMetal	**ArBlocoEq**	**ArBlocoEq**
		Thermal Resistance	0.43	0.43	0.14	0.654	0.654
		Name	Ar2	Ar2	ArPortaMad	ArPortaMetal	ArPortaMetal
		Thermal Resistance	0.43	0.43	0.16	0.14	0.14
		Name	-	-	ArParDW	ArPortaMad	ArPortaMad
		Thermal Resistance	-	-	0.17	0.16	0.16
		Name	-	-	ArForroBh	ArParDW	ArParDW
		Thermal Resistance	-	-	0.14	0.17	0.17
		Name	-	-	ArTelhado	ArForroBh	ArForroBh
		Thermal Resistance	-	-	0.21	0.14	0.14
		Name	-	-		ArTelhado	ArTelhado
		Thermal Resistance	-	-		0.21	0.21
Construction	4	**Name**	**Interior Wall**	**Interior Wall**	**Interior Wall**	**Interior Wall**	**Interior Wall**
		Outside Layer	Argamassa	GessoAcart	GessoAcart	GessoAcart	GessoAcart
		Layer 2	Tijolo	LaVidro_thin	LaVidro_thin	**LaVidro2_5cm**	**LaVidro2_5cm**
		Layer 3	Ar2	ArParDW	ArParDW	ArParDW	ArParDW
		Layer 4	Tijolo	LaVidro_thin	LaVidro_thin	**LaVidro2_5cm**	**LaVidro2_5cm**
		Layer 5	Argamassa	GessoAcart	GessoAcart	GessoAcart	GessoAcart
	5	**Name**	**Exterior Roof**	**Exterior Roof**	**Exterior Roof**	**Exterior Roof**	**Exterior Roof**

		Outside Layer	Telha Metalica Simples	AcoGalvSD	AcoGalvSD	AcoGalvSD	AcoGalvSD
		Layer 2	Ar3	LajeSD_calc	LajeSD_calc	**LaVidro5cm**	**LaVidro5cm**
		Layer 3	Forro	ContrapisoCob	LajeSD_calc	LajeSD_calc	LajeSD_calc
		Layer 4	-	ArTelhado	ContrapisoCob	ContrapisoCob	ContrapisoCob
		Layer 5	-	TelhaAcoGalvBranca	ArTelhado	ArTelhado	ArTelhado
		Layer 6	-	-	TelhaAcoGalvBranca	TelhaAcoGalvBranca	TelhaAcoGalvBranca
	29	**Name**	**PortaMetal**	**PortaMetal**	**PortaMetal**	**PortaMetal**	**PortaMetal**
		Outside Layer	Aluminio	AlumPortaCinza	AlumPortaCinza	AlumPortaCinza	AlumPortaCinza
		Layer 2	Ar2	ArPortaMetal	ArPortaMetal	LaVidro5cm	ArPortaMetal
		Layer 3	Aluminio	AlumPortaCinza	AlumPortaCinza	ArPortaMetal	AlumPortaCinza
		Layer 4	-	-	-	LaVidro5cm	-
		Layer 5	-	-	-	AlumPortaCinza	-
	31	**Name**	**Exterior Roof**	**Exterior Roof**	**Aco_LajeSD_ Contr_Ar_Telha**	**ArgConArCon**	**ArgConArCon**
		Outside Layer	Telha Metalica Simples	Telha Metalica Simples	AcoGalvSD	ArgaBlocoEq	ArgaBlocoEq
		Layer 2	Ar0	Ar1	LajeSD_calc	ConcBlocoEq	ConcBlocoEq
		Layer 3	Forro	Forro	ContrapisoCob	ArBlocoEq	ArBlocoEq
		Layer 4			ArTelhado	ConcBlocoEq	ConcBlocoEq
		Layer 5			TelhaAcoGalvBranca		
	32	**Name**	-	-		**ConArConArg**	**ConArConArg**
		Outside Layer				ConcBlocoEq	ConcBlocoEq
		Layer 2				ArBlocoEq	ArBlocoEq
		Layer 3				ConcBlocoEq	ConcBlocoEq
		Layer 4				ArgaBlocoEq	ArgaBlocoEq
	33	**Name**	-	-		**Contr_LajeSD_Aco**	**Contr_LajeSD_Aco**
		Outside Layer				ContrapisoCob	ContrapisoCob

		Layer 2				LajeSD_calc	LajeSD_calc
		Layer 3				AcoGalvSD	AcoGalvSD
	34	**Name**	-	-		**Aco_Contr_LajeSD**	**Aco_Contr_LajeSD**
		Outside Layer				AcoGalvSD	AcoGalvSD
		Layer 2				ContrapisoCob	ContrapisoCob
		Layer 3				LajeSD_calc	LajeSD_calc
	35	**Name**	-	-		**Telha**	**Telha**
		Outside Layer				TelhaAcoGalvBranca	TelhaAcoGalvBranca
AirflowNetwork: MultizoneZone:Zone	1	**Zone Name**	-	**Ch111**	**Ch01**	**Ch00**	**Ch00**
		Ventilation Control Mode	-	Constant	NoVent	NoVent	Constant
		Venting Availability Schedule Name	-	AlwaysOn	-	-	Always On
	2	**Zone Name**	-	**Ch211**	**Ch02**	**Ch01**	**Ch01**
		Ventilation Control Mode	-	Constant	NoVent	NoVent	Constant
		Venting Availability Schedule Name	-	AlwaysOn	-	-	Always On
	3	**Zone Name**	-	**Ch311**	**Ch03**	**Ch02**	**Ch02**
		Ventilation Control Mode	-	Constant	NoVent	NoVent	Constant
		Venting Availability Schedule Name	-	AlwaysOn	-	-	Always On
	4	**Zone Name**	-	**Ch109**	**Ch04**	**Ch03**	**Ch03**
		Ventilation	-	Constant	NoVent	NoVent	Constant

		Control Mode					
		Venting Availability Schedule Name	-	AlwaysOn	-	-	Always On
	5	**Zone Name**	-	**Ch209**	**Ch05**	**Ch04**	**Ch04**
		Ventilation Control Mode	-	Constant	Constant	Constant	Constant
		Venting Availability Schedule Name	-	AlwaysOn	Always On	Always On	Always On
	6	**Zone Name**	-	**Ch309**	**Ch06**	**Ch05**	**Ch05**
		Ventilation Control Mode	-	Constant	NoVent	NoVent	Constant
		Venting Availability Schedule Name	-	AlwaysOn	-	-	Always On
	7	**Zone Name**	-	**Ch107**	**Ch07**	**Ch06**	**Ch06**
		Ventilation Control Mode	-	Constant	Constant	Constant	Constant
		Venting Availability Schedule Name	-	AlwaysOn	Always On	Always On	Always On
	8	**Zone Name**	-	**Ch207**	**Ch08**	**Ch07**	**Ch07**
		Ventilation Control Mode	-	Constant	NoVent	NoVent	Constant
		Venting Availability Schedule	-	AlwaysOn	-	-	Always On

		Name					
	9	**Zone Name**	-	**Ch307**	**Ch09**	**Ch08**	**Ch08**
		Ventilation Control Mode	-	Constant	Constant	Constant	Constant
		Venting Availability Schedule Name	-	AlwaysOn	Always On	Always On	Always On
	10	**Zone Name**	-	**Ch105**	**Ch10**	**Ch09**	**Ch09**
		Ventilation Control Mode	-	Constant	NoVent	NoVent	Constant
		Venting Availability Schedule Name	-	AlwaysOn	-	-	Always On
	11	**Zone Name**	-	**Ch205**	**Ch11**	**Ch10**	**Ch10**
		Ventilation Control Mode	-	Constant	Constant	Constant	Constant
		Venting Availability Schedule Name	-	AlwaysOn	Always On	Always On	Always On
	12	**Zone Name**	-	**Ch305**	**z101**	**z100**	**z100**
		Ventilation Control Mode	-	Constant	Constant	Constant	Constant
		Venting Availability Schedule Name	-	AlwaysOn	**Aulas**	**Always Off**	Aulas
	13	**Zone Name**	-	**Ch103**	**z102**	**z101**	**z101**
		Ventilation Control Mode	-	Constant	Constant	Constant	Constant

		Venting Availability Schedule Name	-	AlwaysOn	**Aulas**	**Always Off**	Aulas
	14	**Zone Name**	-	**Ch203**	**z103**	**z102**	**z102**
		Ventilation Control Mode	-	Constant	Constant	Constant	Constant
		Venting Availability Schedule Name	-	AlwaysOn	**Aulas**	**Always Off**	Aulas
	15	**Zone Name**	-	**Ch303**	**z104**	**z103**	**z103**
		Ventilation Control Mode	-	Constant	Constant	Constant	Constant
		Venting Availability Schedule Name	-	AlwaysOn	**Aulas**	**Always Off**	Aulas
	16	**Zone Name**	-	**Ch101**	**z105**	**z104**	**z104**
		Ventilation Control Mode	-	Constant	Constant	Constant	Constant
		Venting Availability Schedule Name	-	AlwaysOn	**Aulas**	**Always Off**	Aulas
	17	**Zone Name**	-	**Ch201**	**z106**	**z105**	**z105**
		Ventilation Control Mode	-	Constant	Constant	Constant	Constant
		Venting Availability Schedule Name	-	AlwaysOn	**Aulas**	**Always Off**	Aulas

	18	**Zone Name**	-	**Ch301**	**z107**	**z106**	**z106**
		Ventilation Control Mode	-	Constant	Constant	Constant	Constant
		Venting Availability Schedule Name	-	AlwaysOn	Aulas	Aulas	Aulas
	19	**Zone Name**	-	**Ch102**	**z108**	**z107**	**z107**
		Ventilation Control Mode	-	Constant	Constant	Constant	Constant
		Venting Availability Schedule Name	-	AlwaysOn	Aulas	Aulas	Aulas
	20	**Zone Name**	-	**Ch202**	**z108_comp**	**z108_comp**	**z108_comp**
		Ventilation Control Mode	-	Constant	Constant	Constant	Constant
		Venting Availability Schedule Name	-	AlwaysOn	**Aulas**	**Always Off**	Aulas
	21	**Zone Name**	-	**Ch302**	**z110**	**z109**	**z109**
		Ventilation Control Mode	-	Constant	Constant	Constant	Constant
		Venting Availability Schedule Name	-	AlwaysOn	**Aulas**	**Always Off**	Aulas
	22	**Zone Name**	-	**Ch104**	**z110_cantina**	**z110_cantina**	**z110_cantina**
		Ventilation Control Mode	-	Constant	Constant	Constant	Constant
		Venting	-	AlwaysOn	**Aulas**	**Always Off**	Aulas

		Availability Schedule Name					
	23	**Zone Name**	-	**Ch204**	**z201**	**z200**	**z200**
		Ventilation Control Mode	-	Constant	Constant	Constant	Constant
		Venting Availability Schedule Name	-	AlwaysOn	**Aulas**	**Always Off**	Aulas
	24	**Zone Name**	-	**Ch304**	**z202**	**z201**	**z201**
		Ventilation Control Mode	-	Constant	Constant	Constant	Constant
		Venting Availability Schedule Name	-	AlwaysOn	**Aulas**	**Always Off**	Aulas
	25	**Zone Name**	-	**Ch106**	**z203**	**z202**	**z202**
		Ventilation Control Mode	-	Constant	Constant	Constant	Constant
		Venting Availability Schedule Name	-	AlwaysOn	**Aulas**	**Always Off**	Aulas
	26	**Zone Name**	-	**Ch206**	**z204**	**z203**	**z203**
		Ventilation Control Mode	-	Constant	Constant	Constant	Constant
		Venting Availability Schedule Name	-	AlwaysOn	**Aulas**	**Always Off**	Aulas
	27	**Zone Name**	-	**Ch306**	**z205**	**z204**	**z204**

		Ventilation Control Mode	-	Constant	Constant	Constant	Constant
		Venting Availability Schedule Name	-	AlwaysOn	**Aulas**	**Always Off**	Aulas
	28	**Zone Name**	-	**Ch108**	**z206**	**z205**	**z205**
		Ventilation Control Mode	-	Constant	Constant	Constant	Constant
		Venting Availability Schedule Name	-	AlwaysOn	**Aulas**	**Always Off**	Aulas
	29	**Zone Name**	-	**Ch208**	**z207**	**z206**	**z206**
		Ventilation Control Mode	-	Constant	Constant	Constant	Constant
		Venting Availability Schedule Name	-	AlwaysOn	**Aulas**	**Always Off**	Aulas
	30	**Zone Name**	-	**Ch308**	**z208**	**z207**	**z207**
		Ventilation Control Mode	-	Constant	Constant	Constant	Constant
		Venting Availability Schedule Name	-	AlwaysOn	**Aulas**	**Always Off**	Aulas
	31	**Zone Name**	-	**Ch110**	**z209**	**z208**	**z208**
		Ventilation Control Mode	-	Constant	Constant	Constant	Constant
		Venting Availability	-	AlwaysOn	**Aulas**	**Always Off**	Aulas

		Schedule Name					
	32	**Zone Name**	-	**Ch210**	**z210**	**z209**	**z209**
		Ventilation Control Mode	-	Constant	Constant	Constant	Constant
		Venting Availability Schedule Name	-	AlwaysOn	**Aulas**	**Always Off**	Aulas
	33	**Zone Name**	-	-	**z211**	**z210**	**z210**
		Ventilation Control Mode			Constant	Constant	Constant
		Venting Availability Schedule Name			**Aulas**	**Always Off**	Aulas
	34	**Zone Name**	-	-	**z301**	**z300**	**z300**
		Ventilation Control Mode			Constant	Constant	Constant
		Venting Availability Schedule Name			**Aulas**	**Always Off**	Aulas
	35	**Zone Name**	-	-	**z302**	**z301**	**z301**
		Ventilation Control Mode			Constant	Constant	Constant
		Venting Availability Schedule Name			**Aulas**	**Always Off**	Aulas
	36	**Zone Name**	-	-	**z303**	**z302**	**z302**
		Ventilation			Constant	Constant	Constant

		Control Mode					
		Venting Availability Schedule Name			**Aulas**	**Always Off**	Aulas
	37	**Zone Name**	-	-	**z304**	**z303**	**z303**
		Ventilation Control Mode			Constant	Constant	Constant
		Venting Availability Schedule Name			**Aulas**	**Always Off**	Aulas
	38	**Zone Name**	-	-	**z305**	**z304**	**z304**
		Ventilation Control Mode			Constant	Constant	Constant
		Venting Availability Schedule Name			**Aulas**	**Always Off**	Aulas
	39	**Zone Name**	-	-	**z306**	**z305**	**z305**
		Ventilation Control Mode			Constant	Constant	Constant
		Venting Availability Schedule Name			**Aulas**	**Always Off**	Aulas
	40	**Zone Name**	-	-	**z307**	**z306**	**z306**
		Ventilation Control Mode			Constant	Constant	Constant
		Venting Availability Schedule			Aulas	Aulas	Aulas

		Name					
	41	**Zone Name**	-	-	**z308**	**z307**	**z307**
		Ventilation Control Mode			Constant	Constant	Constant
		Venting Availability Schedule Name			Aulas	Aulas	Aulas
	42	**Zone Name**	-	-	**z309**	**z308**	**z308**
		Ventilation Control Mode			Constant	Constant	Constant
		Venting Availability Schedule Name			Aulas	Aulas	Aulas
	43	**Zone Name**	-	-	**z311**	**z310**	**z310**
		Ventilation Control Mode			Constant	Constant	Constant
		Venting Availability Schedule Name			**Aulas**	**Always Off**	Aulas

3 Obtaining the Air Exchange Profile of a Tropical Naturally Ventilated Building through Calibrated Simulation

3.1 Abstract

This paper studies indoor air quality (IAQ) and natural ventilation in educational buildings within tropical climates, using a lecture hall at a university in southeastern Brazil as case study. Employing calibrated simulations through EnergyPlus, it scrutinizes air changes per hour (ACH) as a pivotal IAQ metric within PVB's classrooms, examining various occupancy rates (10%, 50%, and 90%) to evaluate their impact on ventilation patterns and indoor air quality. The literature review emphasizes IAQ's paramount importance for occupants' health, well-being, and academic performance in naturally ventilated educational buildings, highlighting proper ventilation's role in creating a healthy learning environment. The paper details methodologies using calibrated simulation models to replicate real-world conditions and assess air exchange rates. Results disclose distinctive ventilation profiles among classrooms, indicating variations in air exchange rates influenced by occupancy levels and room orientation. Higher occupancy corresponds to increased air exchange rates, implying a potential self-regulation mechanism in response to elevated indoor temperatures. Higher numbers of air renovations were observed in classrooms on the ground with taller thermal chimneys, when compared to classrooms on the top floor with shorter thermal chimneys. This research provides valuable insights into the indoor environmental conditions considering natural ventilation in educational buildings in tropical climates. The findings underscore the importance of considering occupancy levels and architectural features in designing educational buildings within tropical climates.

Keywords: Indoor air quality, natural ventilation, air changes per hour, occupancy rates, calibrated simulation.

3.2 Introduction

Indoor air quality (IAQ) is a paramount concern in educational buildings, as it plays a pivotal role in shaping the learning environment. The importance of IAQ extends far beyond the realm of comfort; it directly impacts students' and educators' health, well-being, and academic performance (ISMAIL et al., 2022; HOZ-TORRES et al., 2023). Inadequate IAQ can lead to various health issues, including respiratory ailments, allergies, and reduced cognitive function, which can substantially impede the educational process (KUMAR et al., 2022).

This research paper explores the interplay between indoor air quality and natural ventilation in the context of educational buildings in tropical climates. The central objective of this study is to obtain a comprehensive profile of the air changes per hour (ACH) within the classrooms of a lecture hall – known as *"Pavilhão de Aulas II" or "PVB"* – located on a university campus in a humid subtropical climate (PEEL ET AL., 2007). The ACH metric serves as a critical indicator for assessing IAQ, and its calculation is indispensable in understanding the risk of airborne disease transmission within confined spaces (LUNATI and MUCIGNAT, 2022; LAU et al., 2022; ROJAS, SALCEDO and SAHONERO, 2022). By measuring and analyzing ACH, we aim to provide valuable insights into these classrooms' indoor environmental conditions, especially their implications for airborne disease control.

This paper is structured as follows: first, the authors present a literature review concerning IAQ in naturally ventilated educational buildings. Next, we detail the methodology employed in our study, outlining the simulation tools and data collection procedures. Subsequently, we present the results of our ACH measurements, accompanied by relevant data visualizations and statistical analyses. The results and discussion section critically interprets these findings, elucidating their significance for educational building design. Finally, the conclusion summarizes our key insights and underscores the role of this research in enhancing IAQ standards in tropical educational buildings.

3.3 Literature Review

Several studies have highlighted the impact of indoor air pollutants on occupants' health and comfort (ISMAIL et al., 2022; KAPOOR et al., 2022; TAO et al., 2022; RODRIGUES AND FELICIANO, 2019; BUONANNO et al., 2022). These studies have found that pollutants such as carbon dioxide, formaldehyde, particulate matter, bacteria, and fungi can contribute to occupants' sick building syndrome, respiratory symptoms, and other health complaints. This shows that Indoor air quality in naturally ventilated educational buildings is an essential factor for the health and well-being of occupants. The ventilation system plays a

crucial role in maintaining good indoor air quality, and naturally ventilated buildings need to ensure proper airflow and ventilation rates to reduce the concentration of pollutants. We reviewed two recent studies (RODRIGUES AND FELICIANO, 2019; BUONANNO ET AL., 2022) that showed how opening windows for a few minutes during class periods or breaks can significantly improve indoor air quality and provide a healthier environment for occupants. These findings emphasize the need for proper ventilation and control of indoor air pollutants in naturally ventilated educational buildings to create a healthy and conducive learning environment.

Many studies assess a room's IAQ indirectly by measuring biological factors or particulate matter in a classroom, likely based on Steztenbach et al. (2004). (LESTINEN ET AL., 2021; GARG AND GOEL, 2019). However, other studies, including Henriques et al. (2021), Rodrigues and Feliciano (2019), Tao et al. (2022), Buonanno et al. (2022), and others, turn to mathematical equations that have been in use for decades (ASHRAE, 2009) to calculate the behavior of a room's airflow directly.

Tao et al. (2022) use a mathematical model, valid ated through CFD simulations, to describe airflow in a room equipped with a Naturally Ventilated Double Skin Façade (NVDSF), a ventilation device akin to a Solar Chimney or Trombe Wall. The paper analyses ACH (air changes per hour) and MAA (mean age of air) metrics to assess ventilation and air quality. It uses CO_2 as a pollutant to calculate ventilation efficiency . As a further example, Rodrigues and Feliciano (2019) assessed classroom ventilation by experimentally measuring CO_2 concentrations and then using those as a variable in an Eulerian box model. This model describes CO_2 concentration over time as a function of external CO_2 concentration, internal CO_2 production, room volume, and outbound airflow. The outbound airflow, in turn, was calculated using simple pressure-driven and buoyancy-driven airflow equations present in the ASHRAE Handbook of Fundamentals (2009). The authors then used this model to predict CO_2 concentrations over time with different open and closed door and window configurations.

The two works pointed out previously evidence the need to understand of the equations governing air changes per hour, airflow (Q) and the mechanics of CFD. According to Lamberts et al. (2013), one simple way of calculating the airflow (Q) passing through a room is to use equations (1) to (4), as follows:

$$Q = 0{,}6 \cdot A_j \cdot V \cdot \sqrt{\Delta Cp} \qquad \textit{(eq. 1a)}$$

$$Q = 0{,}025 \cdot A \cdot V \qquad \textit{(eq. 1b)}$$

$$\frac{V}{Vm} = kz^{a} \qquad \textit{(eq. 2)}$$

$$\frac{1}{A_j{}^2} = \frac{1}{(\Sigma\, A_{inlet})^2} + \frac{1}{(\Sigma\, A_{outlet})^2} + \frac{1}{(\Sigma\, A_{internal\ doors})^2} \qquad \textit{(eq. 3)}$$

$$ACH = \frac{Q}{v} \cdot 3600 \qquad \textit{(eq. 4)}$$

Where:

Q is the airflow (m³/s)

Aj is the effective ventilation area of the openings (m²)

V is the average wind speed around the building, at the height of the opening (m/s)

ΔCp is the wind pressure coefficient on the façade

Vm is the average wind speed measured at a weather station (m/s)

k, and a are the roughness coefficients of the terrain

v is the room volume

One can understand that applying these equations iteratively for each room under analysis is a somewhat long and laborious process. Some modern softwares automate this process and offer alternative ways to model airflow

Softwares like EnergyPlus can tackle the air flow problem using network models, which interpret the floor plan of the building as a "network," where the rooms and façades are "nodes," and the openings that connect them are "links," which offer resistance to the passage of wind. Allard & Ghiaus (2005) propose that starting from the pressure coefficient on the façades (which is assumed to be known), one can calculate the airflow between all the rooms by applying mass balance equations to all the "nodes" of the network (i.e., internal rooms). This model is based on the Mass Balance premise, i.e., that the total mass of air present in the room remains constant, so the amount of air entering, in kilograms, is equal to the amount leaving. The Airflow Network module of the EnergyPlus software (DOE, 2019) uses this model to simulate ventilation in buildings, employing equations (5) and (6). $Q_w = C_w A_{opening} F_{schedule} V \qquad (eq.5)$ $C_w = 0.55 - \frac{|Effective\ Angle - Wind\ Direction|}{180} \times 0.25 \qquad (eq.6)$ Where

Qw is the Volumetric wind-driven air flow rate, in cubic meters

Cw is the adimensional opening effectiveness

$A_{opening}$ is the opening area in square meters

$F_{Schedule}$ is the opening fraction, according to the defined schedule

V is the local wind speed in meters per second

CFD software, or Computational Fluid Dynamics, takes advantage of the high speed of computer information processing to simulate fluid interactions in motion using finite volume methods. In essence, this type of software divides the space (called the "Domain") into a certain number of cells of known volume and applies mass balance equations, energy balance, Navier-Stokes and Euler integrals (equations derived from the principle of conservation of momentum) to these cells. Given the complexity of the process and its large number of operations, the latter growing exponentially the larger the mesh definition (i.e., number of cells in the domain), high-powered computers, and well-programmed software are of paramount importance for the real application of this method. Several recent papers discuss their application not only in engineering problems but also in predicting the dispersion of contaminants through space, such as SARS-CoV-2 (BHAGAT, 2020; ZIVELONGHI, 2021; FOSTER & KINZEL, 2020).

The methods presented by Tao et al. (2022) and Rodrigues and Feliciano (2019) showcase one of the main methods of assessing airflow in indoor environments today: Calibrated simulation. We chose to use air renewal as a metric that contributes to IAQ in classrooms using the network model because employing CFD software would be too time-intensive and computationally expensive for the purposes of this work, which includes simulating the hourly conditions of 30 classrooms for an entire year. Additionally, ACH will fit in nicely with future work, in which we shall use it to calculate the risk of infection by COVID and other diseases in a classroom. (ROJAS, SALCEDO and SAHONERO, 2022; HENRIQUES et al., 2021)

One can see there is a gap in literature regarding the study of tropical classrooms, and no studies mention the increase in ventilation caused by ventilation chimneys such as the ones in PVB. We posit the higher temperature in these classrooms results in better ventilation.

3.4 Goal

This paper aims to construct a ventilation profile of the “PVB” lecture hall by analyzing the air exchange rates of its classrooms through Building Energy Simulation.

3.5 Method

As stated previously, this paper centers on a specific lecture hall in southeastern Brazil. The building, known as “PVB”, is a three-story, 30-classroom, square figure eight-shaped facility with classroom façades facing northwest, southeast, and southwest. (Figure 3.1). The building is on the far end of the relatively flat, vegetated university campus. Peel et al. (2007) classifies the local climate as “humid subtropical” (Cwa).

Figure 3.1 Second-story floor plan of PVB.

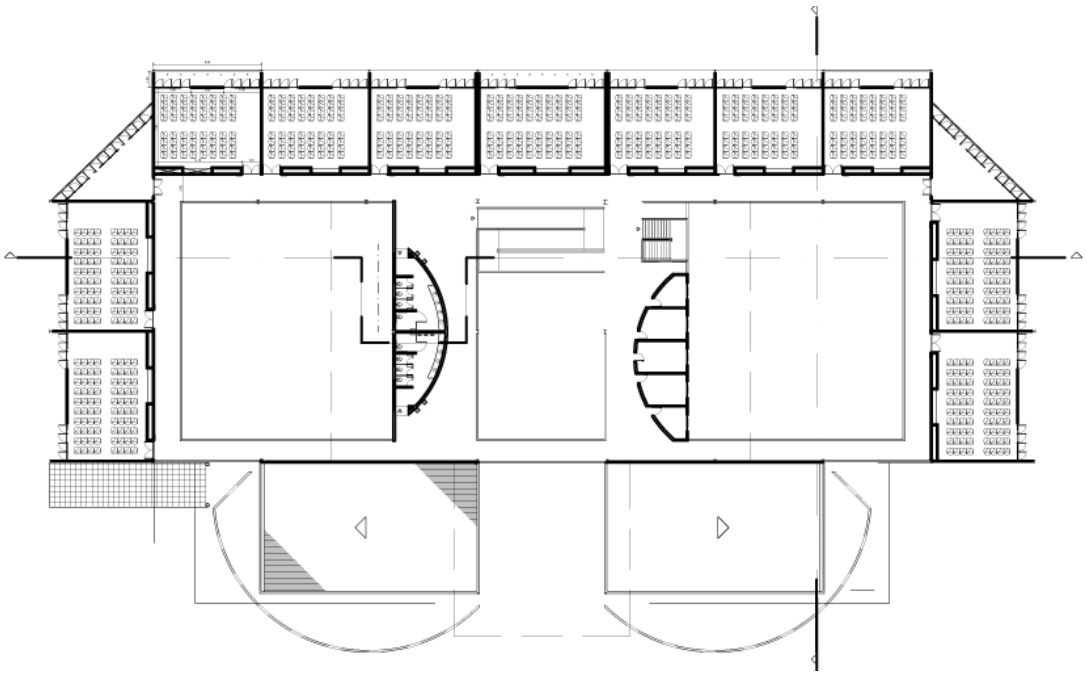

Source: UFV Administrations Office (PAD/UFV)

Figure 3.2 Internal Spaces. a) galleries and courtyard, with a ventilation chimney outlet on top. b) private balconies. c) classroom interior

Source: Photographs taken by the author

through its façades, with external walls out of 14cm x 19cm x 39 cm cellular concrete blocks covered in 2,5cm thick plaster on both sides and internal 15cm-thick insulated dry-walls covered in projected plaster. Each of its classrooms can be accessed through double semi-solid wooden doors from galleries that overlook the open-air courtyards. Each classroom also has its own private balcony, accessible through one of two ensembles of four 70cm x 200cm cm metal doors at the front and back of the room. The classrooms have a row of 60cm x 55 cm maxim-air steel-framed windows that run the length of the balcony wall, and across from that, a thermal chimney intake opening on the ceiling, which provides vital cross-ventilation. Figure 3.1 shows a floor plan of the second story of PVB, and Figure 3.2 shows the gallery, courtyard, balcony, and classroom interior.

EnergyPlus is a widely used, powerful building energy simulation software developed by the U.S. Department of Energy (USDOE, 2015). It is designed to model the energy performance of buildings and HVAC systems in intricate detail. In the context of this study, EnergyPlus serves as the foundational tool for simulating the thermal and environmental conditions within the educational building, allowing us to replicate real-world scenarios accurately. It considers various parameters, including weather data, building materials, occupancy, and HVAC systems, to compute various building performance metrics. Importantly, EnergyPlus enables us to calculate air exchanges (ACH) by simulating the classrooms' natural ventilation and airflow patterns. It provides a robust platform for assessing indoor air quality and energy efficiency, making it well-suited for our research on IAQ in educational settings.

The simulation model was built in EnergyPlus 22.1 and calibrated with data gathered on site to an NMBE of -2.82% and a CV(RMSE) of 6.13%.It consisted of 55 thermal zones (classrooms, thermal chimneys, and adjacent spaces) and 645 surfaces among walls, roofs, and glazing. The authors gave special attention to the modeling of the fenestrations. We modeled each classroom as a single zone with five[1] openings: one for the main door, one for the row of windows above the balcony wall, two for the balcony door groups, and one for the thermal chimney opening. Table 3.1shows their ventilation areas.

[1] Except for zones 301 and 303, which exhibit slightly altered geometries. See figure (4)

Table 3.1 Gross area of openings in the model. Observe some zones have more than one opening of the same type. These have been listed as a sum of the individual opening areas

	Chimney	**Main Doors**	**Balcony Doors**	**Total Windows**	**Zone Volume**
Zones 100, 200, and 300	1.69m²	3.6m²	7.24m² + 7.24m²	6.35m²	327.18m³
Zones 101-106	1.41m²	3.6m²	7.24m² + 7.24m²	5.39m²	272.8m³
Zones 107 - 109	1.84m²	3.6m²	7.24m² + 7.24m²	7.1m²	328.34m³
Zones 201-206	1.41m²	3.6m²	7.24m² + 7.24m²	5.39m²	268.23m³
Zones 207-210	1.84m²	3.6m²	7.24m² + 7.24m²	6.54m²	321.87 m³
Zone 301	1.31m²	3.6m²	7.24m² + 7.24m² + 7.24m	5.34m² + 2.4m²	384.36m³
Zone 303	1.31m²	3.6m²	7.24m² + 7.24m² + 7.24m	5.42m² + 3.02m²	405.2m³
Zones 302, 304 and 306	1.31m²	3.6m²	7.24m² + 7.24m²	5.39m²	262.87m³
Zones 305, 307 and 310	1.84m²	3.6m²	7.24m² + 7.24m²	5.39m²	315.20m³

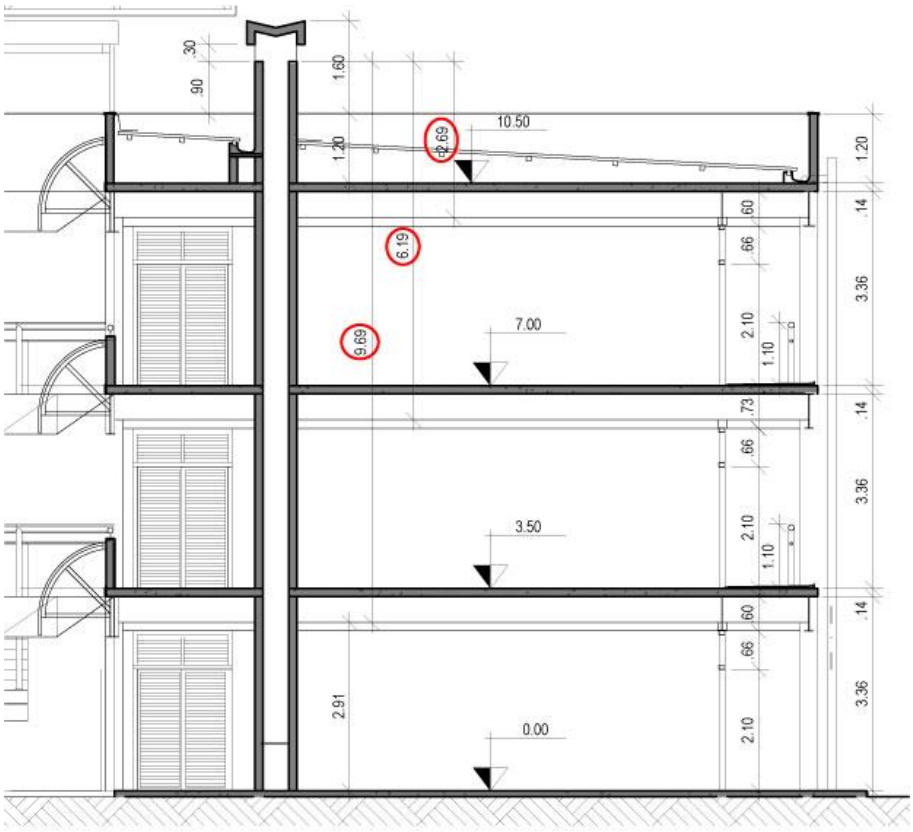

Source: UFV's Administrations Office (PAD/UFV) Empahsis added by the author

We simulated the ventilation patterns throughout the building with the calibrated model to evaluate airflow rates and indoor air quality in each classroom under varying conditions, chief among which was the occupancy rate of the room. To this end, we calculated the buoyancy-driven air exchange rates and the wind pressure-driven air exchange rates in two separate simulations in EnergyPlus, with the AirflowNetwork and ZoneThermalChimney modules. For the wind-driven ventilation, we obtained the façade wind pressure coefficients (Cp) by running CFD simulations of the building in OpenFOAM. For the buoyancy-driven ventilation, the EnergyPlus algorithm uses equations (7) an (8), which calculates the increase in air renovation based on the air temperatures of the thermal chimney and the classrooms, hour by hour.

$$Q = CdA_o\sqrt{\frac{2(\frac{T_{f0}-T_r}{T_r})gL}{(1+{A_r}^2)}} \qquad (eq\ 7)$$

$$A_r = A_o/A_i \qquad (eq\ 8)$$

Where

Q is the increase in airflow (m³/s)

Cd is the coefficient of discharge

A_0 is the cross sectional area of the chimney outlet (m²)

A_i is the cross sectional area of the chimney inlet (m²)

T_{fo} is the outlet air temperature of the thermal chimney (K)

T_r is the inlet air temperature, the same as the temperature of the room (K)

g is the constant of gravity (m/s²)

L is the length of the thermal chimney (m)

The wind-driven and buoyancy cases were evaluated for each individual hour of the year to determine the most appropriate value for each hour, using equation (9). All of the building's operating hours favoured wind-driven ventilation.

$$Q = Qb \Leftarrow \frac{V_z}{\sqrt{\Delta t}} < 0.26 \cdot \sqrt{\frac{A_b}{A_w}} \cdot \sqrt{\frac{H}{\Delta C_p}} \qquad (eq\ 9)$$

$$else$$

$$Q = Qw$$

Where:

Q is the ventilation value to be used (m³/s)

Qb is the buoyancy-driven ventilation value (m³/s)

Qw is the wind-driven ventilation value (m³)

Δt is the temperature difference between inside and outside air (K)

Ab is inlet area when buoyancy-driven airflow is considered (m²)

Aw is the inlet area when wind-driven airflow is considered (m²)

H is the chimney height (m)

To assess the impact of ventilation on indoor air quality, we requested hourly air renovations (ACH) and hourly indoor air temperatures for all classrooms, totaling 8760 for each room, for each of three scenarios based on the number of seats: 10% of seats filled, 50% of seats filled, or 90% of seats filled.

Each room's data set was then compiled into various graphs, which allowed us to identify the ventilation profiles in each room and evidenced the most common air exchange rates in each scenario.

3.6 Results and Discussion

Figure 3.4 displays the air renovations for each classroom, weighted by its frequency of occurrence, for each occupation case. We see a rise in occupancy follows a rise in air

renovations, a relationship that can also be seen in figure 3.4 and in table 3.2. This difference can be explained by the classroom's temperature rise when more people are present (around an average difference of 1.90 °C between 10% occupied classrooms and 90% occupied

Figure 3.4 - Frequency-weighted average of the air renovations in each classroom, by occupancy

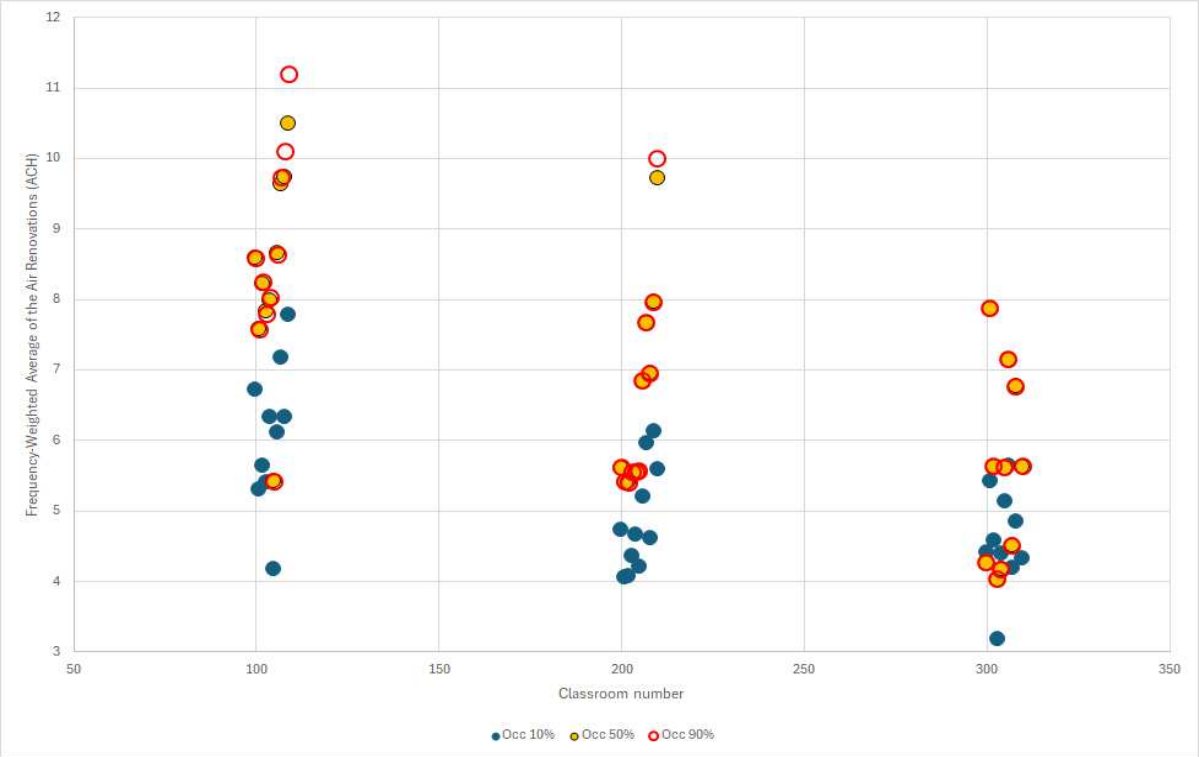

classrooms. See Figure 3.5). This difference is also a promising indicator that, to a certain extent, the indoor air quality of naturally ventilated, chimney-equipped buildings may self-regulate in response to higher occupancy levels. Figure 3.4 also shows that the bottom floors are more responsive to rising occupation than the top ones, as the air renovations are more spread out in the former than in the latter.

Figure 3.4 also confirms the well-established relationship between a chimney's height and its efficiency, as the data show that groundfloor classrooms experience more renovations per hour. They also provide the higher air renovation differences between classrooms with low and high occupancy (10% and 90%).

Tables 3.2 to 3.4 expands on this data condensing each classroom's air renovation histogram (see figures 3.7 and 3.8) to a single number of air renovations. Rooms 303, 301, and 105 stand out by their high frequency of low renovations per hour. Room 301 exhibits less than one renovation per hour for 62% of the time when it is 10% occupied and 61% of the time when it is 90% occupied. Room 303 exhibits a better profile, spending 45% to 33%

of its operational hours on 2 to 3 renovations per hour, at 10% and 90% occupancy, respectively.

Table 3.2 - Average air exchange rates (ach) weighted by frequency, and façade orientations of top floor classrooms (openings 7m to 10m above ground level)

	300	***301***	***302***	***303***	***304***	***305***	***306***	***307***	***308***	***310***
Facing	*219° (SW)*	*219° (SW)*	*219° (SW)*	*219° (SW)*	*219° (SW)*	*309° (NW)*	*219° (SW)*	*309° (NW)*	*129° (SE)*	*129° (SE)*
10%	*4,40*	*5,41*	*4,58*	*3,18*	*4,38*	*5,12*	*5,64*	*4,18*	*4,85*	*4,32*
50%	*4,26*	*7,86*	*5,62*	*4,02*	*4,16*	*5,60*	*7,14*	*4,50*	*6,76*	*5,62*
90%	*4,26*	*7,86*	*5,62*	*4,02*	*4,16*	*5,60*	*7,14*	*4,50*	*6,76*	*5,62*

Table 3.3 Average air exchange rates (ach) weighted by frequency, and façade orientations of first floor classrooms (openings 3.5m to 6.5m above ground level)

	200	***201***	***202***	***203***	***204***	***205***	***206***	***207***	***208***	***209***	***210***
Facing	*219° (SW)*	*219° (SW)*	*219° (SW)*	*219° (SW)*	*219° (SW)*	*309° (NW)*	*219° (SW)*	*309° (NW)*	*129° (SE)*	*309° (NW)*	*219° (SW)*
10%	*4,73*	*4,05*	*4,07*	*4,35*	*4,66*	*4,20*	*5,20*	*5,95*	*4,61*	*6,13*	*5,58*
50%	*5,60*	*5,40*	*5,39*	*5,54*	*5,54*	*5,55*	*6,83*	*7,66*	*6,94*	*7,96*	*9,71*
90%	*5,60*	*5,40*	*5,39*	*5,54*	*5,54*	*5,55*	*6,83*	*7,67*	*6,94*	*7,95*	*9,99*

Table 3.4Average air exchange rates (ach) weighted by frequency, and façade orientations of ground floor classrooms (openings 0m to 3m above ground level)

	100	**101**	**102**	**103**	**104**	**105**	**106**	**107**	**108**	**109**
Facing	*219° (SW)*	*219° (SW)*	*219° (SW)*	*219° (SW)*	*219° (SW)*	*309° (NW)*	*219° (SW)*	*309° (NW)*	*129° (SE)*	*129° (SE)*
10%	6,71	5,29	5,63	5,39	6,32	4,17	6,10	7,17	6,33	7,77
50%	8,58	7,57	8,21	7,83	7,98	5,41	8,65	9,63	9,72	10,48
90%	8,58	7,56	8,23	7,79	8,02	5,41	8,63	9,72	10,09	11,19

In room 105, operational hours with 1 to 2 renovations per hour rose from 32% to 34% when occupancy changed from 10% to 90%, while hours with less than 1 renovation diminished from 22% to 17% and higher renovation values became more frequent. While this frequency shift can be partially explained by the diminutive wind pressure coefficients acting on the façades of these classrooms, especially for room 105 which exhibits the fewest air

renovations of its floor, the increased volume of classrooms 301 and 303 also dramatically affects their ventilation behavior (see Figure 3.10). Furthermore, we can demonstrate that despite rooms 301 and 303 exhibiting higher temperatures (figures 3.4 and 3.5), their short chimney heights ultimately contribute to them being less ventilated.

Figure 3.5 Difference between each room's yearly average temperatures during useful hours when 10% occupied, 50% occupied, and 90% occupied.

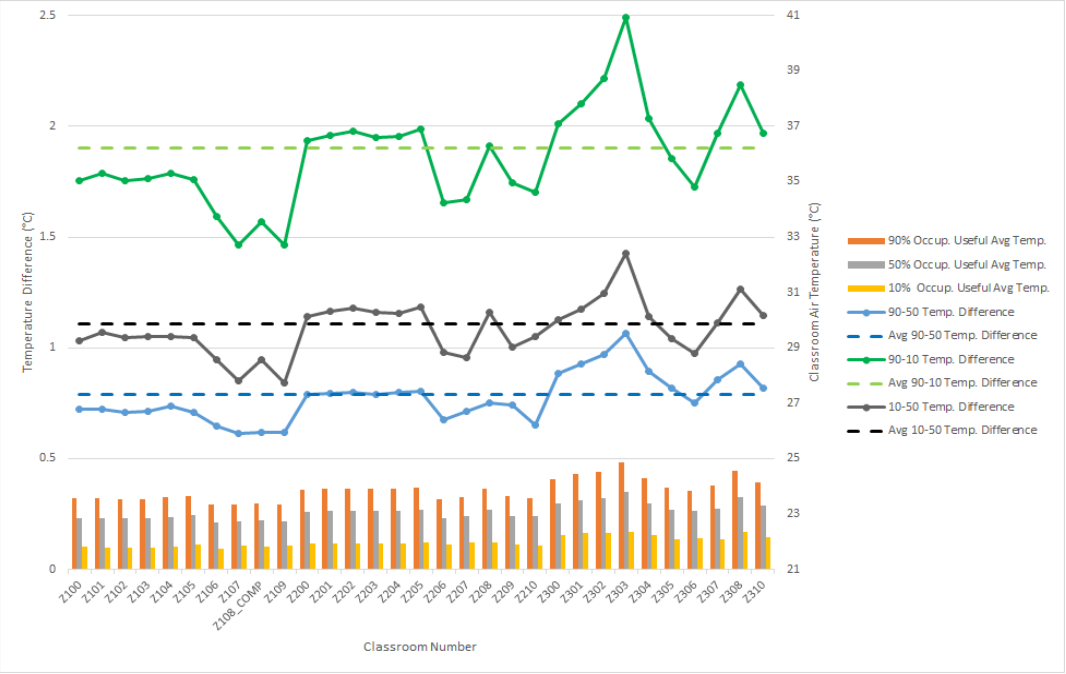

Figure 3.5: Frequency of Occurrence of Number of Air Renovations per Hour (ach) for selected rooms and all occupancy rates

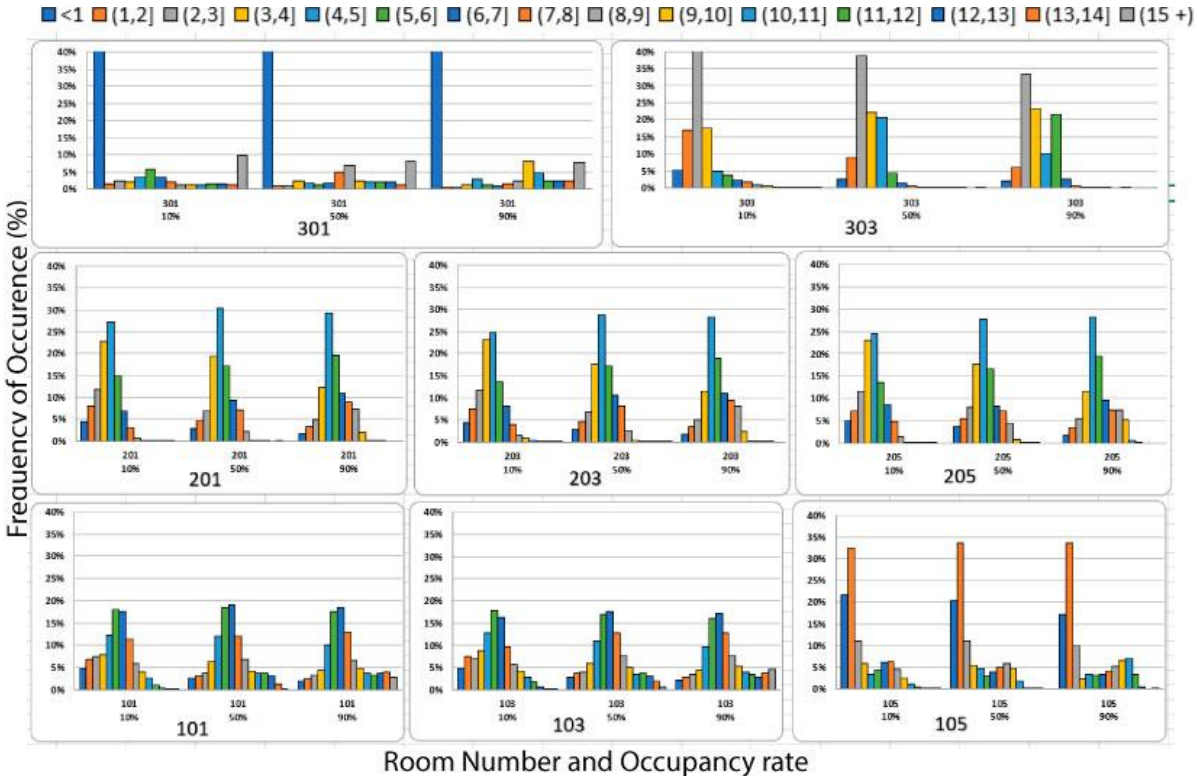

Source: produced by the author

The classrooms on the top floor tend to be warmer (Figure 3.4) due to their proximity to the roof, but the data shows that, for PVB at least, the height of the chimney has a stronger correlation with air renewal than the temperature gradient. Figure (3.7) further shows this relationship. It is important to underline the fact that, for the same room (and therefore same chimney height), different occupations result in different air change rates, which means that the chimneys are responding to the temperature gradient, albeit less significantly.

One can also notice that classrooms facing west (107, 207, 305, 109, 209, and 307) see more renovations than their eastern counterparts (108, 208, 308, 210, and 310) and significantly more than the south-facing middle section (100 to 102, 200 to 202, 300 and 302.) The westernmost classroom on the ground floor, room 105, exhibited the least yearly average renovations of that floor (4.17 to 5.41 renovations for 10% and 50%, and 90% respectively) and the second lowest of all classrooms (the lowest being room 302, at 3.18 renovations when 10% and 50% occupied, to 4.02 renovations when 90% occupied) . This low number coincides with the wind direction on the weather file, which puts this classroom on the leeward side of the building most of the time (figure 3.8).

Figure 3.7 Correlation between yearly averaged air temperatures and corresponding number of air renovations. left: Whole building air renovations. Right: air renovations by floor

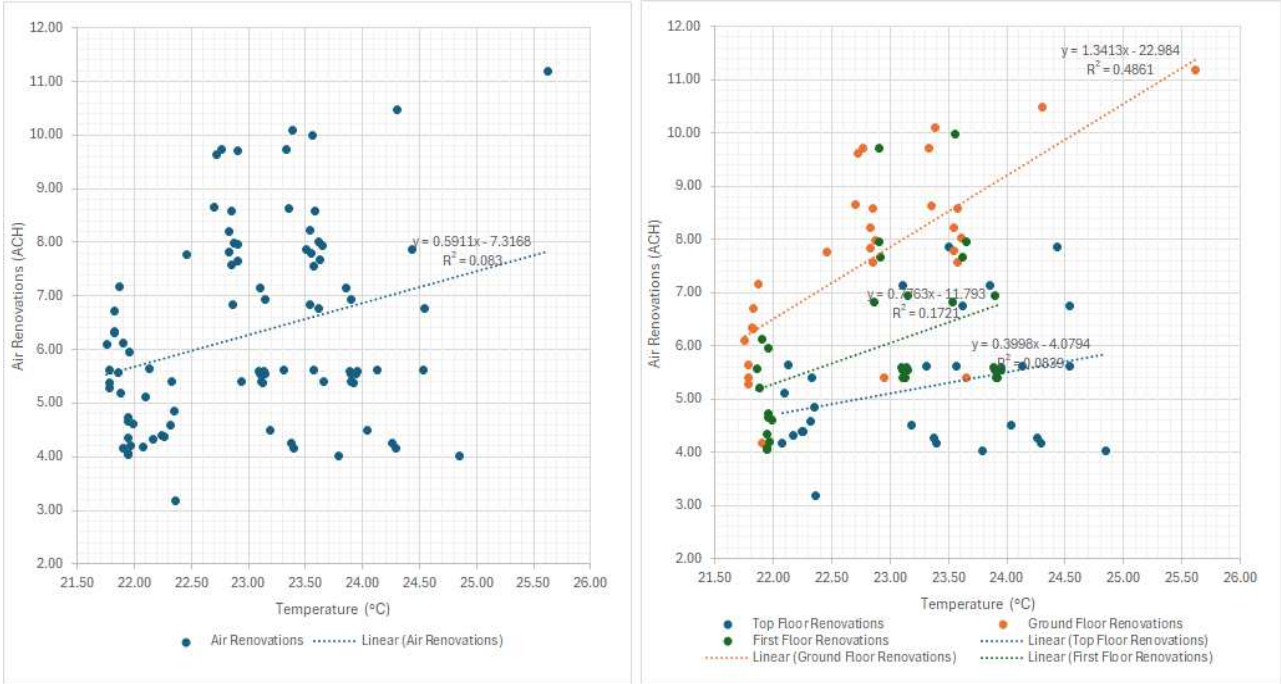

Source: produced by the author

Figure 3.8 - Wind direction and speed frequency according to the weather file in use

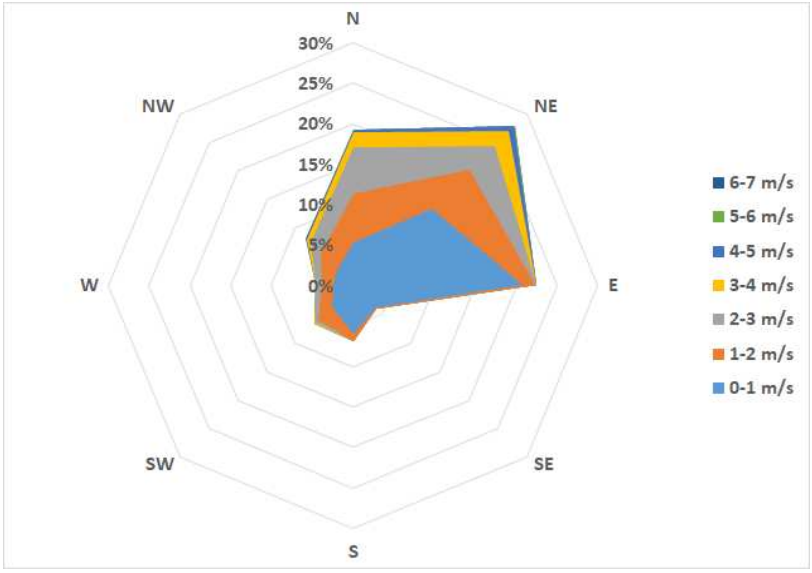

Source: produced by the author

Figure 3.9 - Classroom typologies in PVB. Rooms 301 and 303 result from dividing a typical room (like room 305) and adding its parts to its neighbors

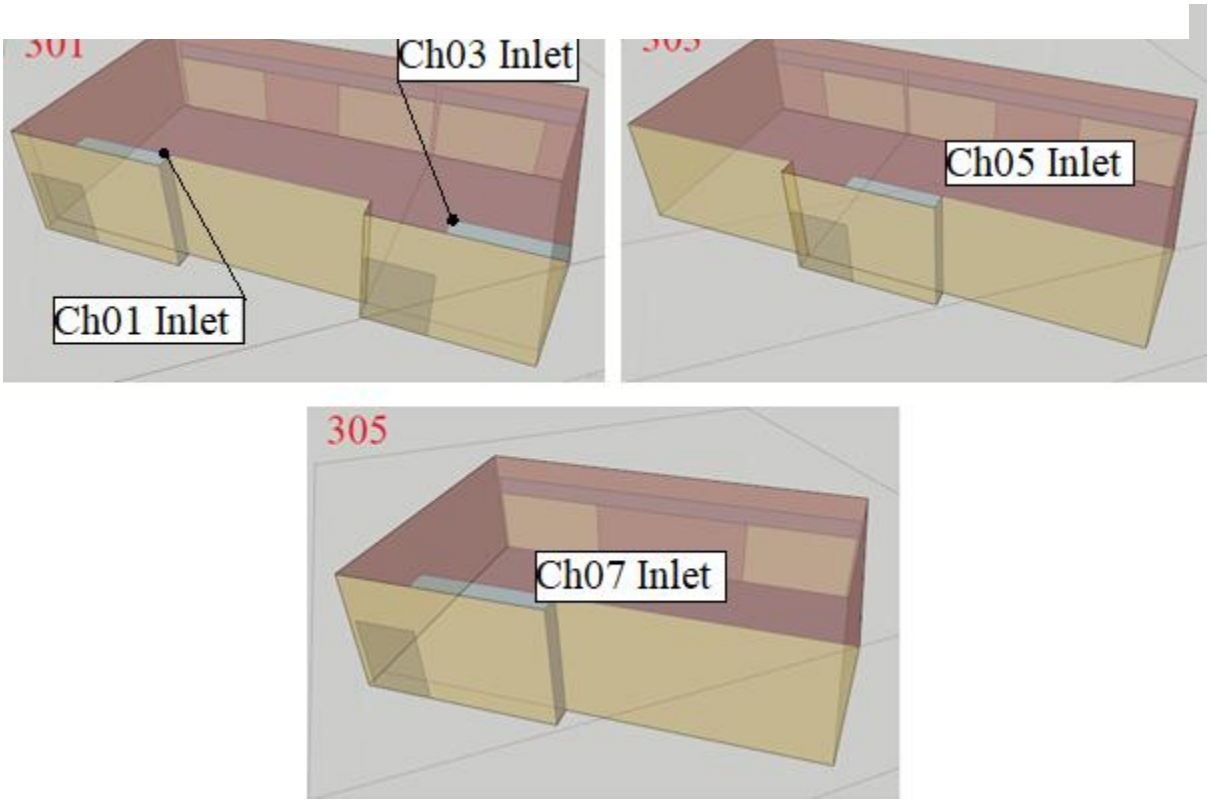

Source: produced by the author

As shown in Figure 3.16, room 301 is connected to two thermal chimneys, Ch01 and Ch03, while room 303 only connects to Ch05. Despite having double the number of thermal

chimneys than other rooms, room 301 has a higher frequency of less than one renovation per hour, which points to the relative inefficiency of these elements on the top floors of the building due to their short height. (2.69m from inlet to outlet) That correlation is further emphasized by the aforementioned higher average air renovations exhibited by the ground-floor classrooms.

All classrooms exhibited a weighted average of 3 renovations per hour or higher, peaking at 11.19 renovations per hour in room 109 (a room with a 9.69m tall chimney on a windward corner of the building). On the other hand, the air exchanges varied less between the middle (50% occupied) and top (90% occupied) occupation cases than between 50% and 10%, or 90% and 10%. Once again, this follows the trend of classroom temperatures, which varied by 59% less between the middle and top occupations than between the bottom and middle occupations. This relationship seems to suggest causation by way of simple thermodynamics (WHITE, 2011)

The authors feel the need to underline the impact of the thermal chimneys on the overall air renovations in this building must not be understated, since ultimately the warmer, short chimney-equipped top floor classrooms displayed less renovations than the cooler, longer chimney-equipped ground floor classrooms. This leads to the conclusion that a more pronounced temperature gradient was, and possibly is, less impactful to air renovations in thermal chimney-equipped rooms than a pronounced pressure gradient. In other words, chimney height is possibly more important than air temperature for air renewal in these classrooms.

3.7 Conclusions

This paper aimed to obtain a ventilation profile of PVB's classrooms, allowing for a better understanding of the airflow throughout the educational spaces of this lecture hall. The initial suspicion that the warmer classrooms would display better ventilation was partially refuted since the relationship between ventilation and classroom position was shown to be more complex than that. The data seems to indicate that, specifically for PVB, the pressure differential between chimney openings accounts for more air renovations than the temperature gradient alone, especially seeing the increased air renovations on the northwestern and southeasthern façades of the building, and on the rooms with longer chimneys.

This paper has shown that, in general terms, PVB is a well-ventilated building. It has also shown that a higher occupancy rate frequently results in more air exchanges per hour, up

to a certain limit, pointing to possible self-regulation in indoor air quality. Thermal chimneys have been shown to increase air renovation in the building proportionally to their height (i.e. inlet to outlet height difference). Additionally, classroom window height appears to be less influential in determining air changes per hour.

Further studies shall also better explore the relationship between classroom occupancy and air exchange rates, delving further into the mechanics of such an interaction as well as statistical analysis of the parameters involved - more specifically, a sensitivity analysis shall indicate the precise mathematical interplay between the occupancy of a classroom and the increase or decrease in air exchange rates.

3.8 Acknowledgements

This paper could not have been accomplished without the help and funding from FAPEMIG - Fundação de Amparo à Pesquisa do Estado de Minas Gerais, through funding our project "Uso de simulação e ferramentas computacionais no estudo de edifícios naturalmente ventilados", project number **APQ-00872-22.** We also thank CNPq - Conselho Nacional de Pesquisa, which fundamentally contributed to this paper, through funding our project "Tecnologias para adaptação de edificações às mudanças no clima", project registration number **60419479687**

3.9 Bibliography

ALESSANDRO ZIVELONGHI; LAI, M. Mitigating aerosol infection risk in school buildings: the role of natural ventilation, volume, occupancy and CO2 monitoring. *Building and Environment*, v. 204, n. May, p. 108139, 2021. Disponível em: <https://doi.org/10.1016/j.buildenv.2021.108139>.

ALLARD, F.; CRISTIAN GHIAUS (Org.). *Natural ventilation in the urban environment: Assessment and design*. [S.l.]: Earthscan, 2005. p. 238

ASHRAE handbook of fundamentals. [S.l: s.n.], 2009.

ASHRAE. *2021 ashrae handbook*. [S.l: s.n.], 2021. p. 29.1–29.9

BHAGAT, R. K. *et al.* Effects of ventilation on the indoor spread of COVID-19. *Journal of Fluid Mechanics*, v. 903, 2020.

BUONANNO, G. *et al.* Increasing ventilation reduces SARS-CoV-2 airborne transmission in schools: A retrospective cohort study in Italy's Marche region. *Frontiers in public health*, v. 10, dez. 2022. Disponível em: <https://pubmed.ncbi.nlm.nih.gov/36568748/>.

HOZ-TORRES, MARIA DE, L. *et al.* Predictive model of clothing insulation in naturally ventilated educational buildings. *Buildings 2023, Vol. 13, Page 1002*, v. 13, n. 4, p. 1002, abr. 2023. Disponível em: <https://www.mdpi.com/2075-5309/13/4/1002/htm%20https://www.mdpi.com/2075-5309/13/4/1002>.

FOSTER, A.; KINZEL, M. Estimating COVID-19 exposure in a classroom setting: A comparison between mathematical and numerical models. *Physics of Fluids*, v. 33, n. 2, 2021.

HENRIQUES, A. *et al.* Modelling airborne transmission of SARS-CoV-2 using CARA: Risk assessment for enclosed spaces. *medRxiv*, p. 2021.10.14.21264988, out. 2021. Disponível em: <https://www.medrxiv.org/content/10.1101/2021.10.14.21264988v1%20https://www.medrxiv.org/content/10.1101/2021.10.14.21264988v1.abstract>.

GARG, D.; GOEL, A. Comparison of indoor air quality for air-conditioned and naturally ventilated office spaces in urban area. *Lecture Notes in Civil Engineering*, v. 60, p. 1–8, 2020. Disponível em: <https://link.springer.com/chapter/10.1007/978-981-15-1334-3_1>.

KUMAR, P.; RAWAT, N.; TIWARI, A. Micro-characteristics of a naturally ventilated classroom air quality under varying air purifier placements. *Environmental research*, v. 217, jan. 2023. Disponível em: <https://pubmed.ncbi.nlm.nih.gov/36414109/>.

LAMBERTS, R.; DUTRA, L.; FERNANDO. *Eficiencia energética na arquitetura*. 3rd. ed. [S.l.]: Eletrobras, 2013. p. 365

LAU, Z. *et al.* Predicting the spatio-temporal infection risk in indoor spaces using an efficient airborne transmission model. *Proceedings. Mathematical, physical, and engineering sciences*, v. 478, n. 2259, 2022. Disponível em: <https://pubmed.ncbi.nlm.nih.gov/35310953/>.

LUNATI, I.; MUCIGNAT, C. Infection risk in cable cars and other enclosed spaces. *Indoor Air*, v. 32, n. 8, p. e13094, ago. 2022. Disponível em: <https://onlinelibrary.wiley.com/doi/full/10.1111/ina.13094%20https://onlinelibrary.wiley.com/doi/abs/10.1111/ina.13094%20https://onlinelibrary.wiley.com/doi/10.1111/ina.13094>.

OLIVEIRA, M. M.; CARLO, J. C. Análise da qualidade da simulação do fluxo de ar de chaminés solares com o EnergyPlus. *PARC Pesquisa em Arquitetura e Construção*, v. 9, n. 2, p. 86–96, jun. 2018.

NISHANT RAJ KAPOOR *et al.* A systematic review on indoor environmental quality in naturally ventilated school classrooms: A way forward. *Advances in Civil Engineering*, v. 2021, 2021.

PEEL, M. C.; FINLAYSON, B. L.; MCMAHON, T. A. Updated world map of the Köppen-Geiger climate classification. *Hydrology and Earth System Sciences*, v. 11, n. 5, p. 1633–1644, 2007.

RODRIGUES, F.; FELICIANO, M. Improving indoor air quality of naturally ventilated classrooms in the northeast of portugal. *Environmental Engineering and Management Journal*, v. 18, n. 7, p. 1423–1437, jul. 2019. Disponível em: <https://www.researchgate.net/publication/339735410_IMPROVING_INDOOR_AIR_QUALITY_OF_NATURALLY_VENTILATED_CLASSROOMS_IN_THE_NORTHEAST_OF_PORTUGAL>.

ROJAS, W.; SALCEDO, E.; SAHONERO, G. ADRAS: Airborne disease risk assessment system for closed environments. *Communications in Computer and Information Science*, v. 1837 CCIS, p. 96–112, 2023. Disponível em: <https://link.springer.com/chapter/10.1007/978-3-031-35445-8_8>.

SAMI LESTINEN *et al.* Effects of night ventilation on indoor air quality in educational Buildings—A field study. *Applied Sciences 2021, Vol. 11, Page 4056*, v. 11, n. 9, p. 4056, abr. 2021. Disponível em: <https://www.mdpi.com/2076-3417/11/9/4056/htm%20https://www.mdpi.com/2076-3417/11/9/4056>.

SYAZWAN AIZAT ISMAIL *et al.* Indoor air quality level influence sick building syndrome among occupants in educational buildings. *International Journal of Public Health Science (IJPHS)*, v. 11, n. 2, p. 503–517, jun. 2022. Disponível em: <https://ijphs.iaescore.com/index.php/IJPHS/article/view/21125>.

TAO, Y. *et al.* Predicting airflow in naturally ventilated double-skin facades: theoretical analysis and modelling. *Renewable Energy*, v. 179, p. 1940–1954, dez. 2021.

USDOE. *Input output reference*. *The Encyclopedic Reference to EnergyPlus Input and Output*. [S.l: s.n.], 2019.

White, F. M.. Fluid mechanics (7a ed.). McGraw-Hill, 2011.

4 Creating a Safe Use Matrix for a Naturally Ventilated Educational Building in Tropical Climate

4.1 Abstract

This study presents a comprehensive analysis of naturally ventilated classrooms within a university's lecture hall in a tropical climate, focusing on the dynamics of airborne disease transmission. Examining three major pathogens—COVID-19, Tuberculosis, and Measles—the research integrates calibrated Building Energy Simulation models to determine air change rates (ACH) and a literature review for Effective quanta release values (ERq). The GN-Riley model incorporates these data to assess the risk of airborne disease transmission. Findings reveal that PVB`s lecture halls can effectively mitigate airborne infection risks, enabling safe utilization of classrooms for limited durations or at reduced occupancies. Intriguingly, despite enhanced ventilation, densely occupied classrooms may pose elevated infection risks due to narrower admissible risk thresholds. The study emphasizes that pathogen concentrations stabilize over time, influenced by mathematical modeling and continuous removal of infective particles. Risks, however, steadily increase with prolonged exposure to infected air. Comparative analyses underscore varying infectivity among diseases, emphasizing the crucial role of vaccination and prevention measures. A unique contribution lies in addressing naturally-ventilated tropical classrooms, which differently from temperate climates, seem to pose low infection risk without the aid of mechanical ventilation.

Keywords: COVID-19, Tuberculosis, Measles, Quanta, EnergyPlus

4.2 Introduction

The relationship between the spread of airborne diseases and natural ventilation of indoor environments is firmly established in academia (MACIEL apud VITRUVIUS, 2006; NIGHTINGALE, 1863). The recent COVID-19 pandemic further reinforces this relationship.

COVID-19 is but a recent example of a viral respiratory syndrome, transmitted mainly through airborne droplets of saliva and phlegm (ZHANG et al, 2020; MORAWSKA et al, 2020). Humans have been dealing with similar diseases for centuries, such as measles (RILEY et al, 1978) and tuberculosis (NIGHTINGALE, 1863; RILEY, 1957). Infectious droplets can remain suspended in environments with little or no natural ventilation for considerable periods of time (MORAWSKA et al, 2009; XIE et al, 2007), being able to infect people tens of meters away (LU et al, 2020) if not expelled into the external environment. In addition, singing or speaking loudly expels large amounts of phlegm and saliva (GUPTA, LIN & CHEN 2010), which increases the chances of an infected speaker infecting healthy listeners in an environment with few air changes per hour. Understandably, there are concerns about the spread of airborne infections in indoor environments, especially in indoor environments such as classrooms.

This article quantifies the risk of airborne disease transmission in the classrooms of a naturally ventilated educational building in a university in a tropical climate, each equipped with a thermal chimney. This paper suggests safe usage protocols for these and similar classrooms. It becomes evident that the total estimation of risk relies heavily on understanding the behavior of air in the room.

4.3 Goal

To create a maximum safe occupancy/duration matrix of PVB’s classrooms based on the infection risk of 3 major airborne diseases: COVID-19, Tuberculosis and Measles.

4.4 Method

Our research design follows a multi-faceted approach. To begin, we obtained the air change rates for each classroom for every hour throughout the year (ACH), using a calibrated Building Energy Simulation model, which enabled us to accurately simulate the dynamic airflow behavior and thermal characteristics within these spaces. Additionally, to estimate the potential for disease transmission within these environments, we conducted a thorough literature review to acquire the "Infectivity" (Effective Rate of Emmision of “quanta”, or ERq) values associated with three major airborne diseases: COVID-19, Measles, and Tuberculosis. These values were subsequently incorporated into the GN-Riley model (ZIVELONGHI et al., 2021), a widely accepted framework for assessing the risk of airborne

disease transmission. The ensuing sections of this paper will delve into the specific steps and intricacies of each of these methodological components, shedding light on the relationship between natural ventilation, indoor air quality, and the potential for airborne infections in the context of tropical educational indoor environments.

The process of obtaining air change rates (ACH) from a calibrated model started with creating a computational simulation model that replicated the architectural and environmental characteristics of the educational building under study. This model integrated room dimensions, thermal properties of building materials, climate data, and occupancy patterns. Following model creation, a manual calibration process was undertaken to ensure the accuracy of our simulated ACH values. First, the model was simulated to predict indoor environmental conditions, and these results were subsequently verified against real-world data. The coefficient of variation of the root mean square error (CVRMSE) and the normalized mean bias error (NMBE) were used as performance metrics to verify this. If the results fell outside acceptable tolerances, the model was adjusted, and the process was repeated until a satisfactory calibration level was achieved. With a well-calibrated simulation model in place, we proceeded to simulate the ventilation patterns throughout the building. This involved running the model for each hour of the year, resulting in 8760 data points (i.e., hourly air renovation rates) per classroom. To properly fit the data to our infection model, we took the weighted average of the hourly renovations (ACH), relative to their prevalence (% of time). Table 4.1 displays a ventilation summary of the building.

It was subsequently necessary to obtain “Infectivity” rates (Emission Rate of quanta, or ERq) for measles, Tuberculosis (TB), and COVID-19. The Wells-Riley model of infection, which quantifies the risk of airborne disease transmission, underpins this process. This model, which was later updated by Gammaitoni and Nucci (1997), Zivelonghi et al (2021) and Buonanno et al. (2020), accounts for parameters such as the quanta generation rate, ventilation (i.e. quanta removal) rate, and exposure time, allowing for a precise estimation of infection risk.

Both the original Wells-Riley model and the updated GN-Riley model approach infection as a physical transport problem rather than a physiological susceptibility issue. In essence, the primary focus is on tracking the physical trajectory of infectious particles rather than assessing the likelihood of a specific individual or group contracting the disease. It operates on several key assumptions, with the central concept being that of "Quanta." A Quanta, as originally defined by William F. Wells (1933), represents a sufficient dose of infectious particles to infect a susceptible individual. By abstracting the precise viral or

bacterial load needed for infection, the model can ignore individual susceptibility instead of focusing on the probability of an individual encountering one or more "doses," regardless of their size. The model also assumes that these doses instantaneously and uniformly disperse into the room upon release, justifying the use of thermal and mass-balance algorithms instead of flow pathway-specific computational fluid dynamics (CFD) software. Additionally, it assumes a constant rate of introduction and removal of the infective agent from the room. This level of simplification is acknowledged to come at the expense of accuracy (FOSTER and KINZEL, 2021; GAMMAITONI and NUCCI, 1997), prompting recent interpretations of the model to consider factors such as the time required for pathogen dispersion within the room, viral inactivation, and the settling of airborne particles onto surfaces when room air remains undisturbed.(GAMMAITONI & NUCCI, 1997; ZIVELONGHI et al., 2021).

Table 4.1 - Average air exchange rates (ach) weighted by frequency, and façade orientations of top floor classrooms (openings 7m to 10m above ground level)

	300	***301***	***302***	***303***	***304***	***305***	***306***	***307***	***308***	***310***
Facing	*219° (SW)*	*219° (SW)*	*219° (SW)*	*219° (SW)*	*219° (SW)*	*309° (NW)*	*219° (SW)*	*309° (NW)*	*129° (SE)*	*129° (SE)*
10%	*4,40*	*5,41*	*4,58*	*3,18*	*4,38*	*5,12*	*5,64*	*4,18*	*4,85*	*4,32*
50%	*4,26*	*7,86*	*5,62*	*4,02*	*4,16*	*5,60*	*7,14*	*4,50*	*6,76*	*5,62*
90%	*4,26*	*7,86*	*5,62*	*4,02*	*4,16*	*5,60*	*7,14*	*4,50*	*6,76*	*5,62*

Table 4.2 - Average air exchange rates (ach) weighted by frequency, and façade orientations of first floor classrooms (openings 3.5m to 6.5m above ground level)

	200	***201***	***202***	***203***	***204***	***205***	***206***	***207***	***208***	***209***	***210***
Facing	*219° (SW)*	*219° (SW)*	*219° (SW)*	*219° (SW)*	*219° (SW)*	*309° (NW)*	*219° (SW)*	*309° (NW)*	*129° (SE)*	*309° (NW)*	*219° (SW)*
10%	*4,73*	*4,05*	*4,07*	*4,35*	*4,66*	*4,20*	*5,20*	*5,95*	*4,61*	*6,13*	*5,58*
50%	*5,60*	*5,40*	*5,39*	*5,54*	*5,54*	*5,55*	*6,83*	*7,66*	*6,94*	*7,96*	*9,71*
90%	*5,60*	*5,40*	*5,39*	*5,54*	*5,54*	*5,55*	*6,83*	*7,67*	*6,94*	*7,95*	*9,99*

Table 4.3 - Average air exchange rates (ach) weighted by frequency, and façade orientations of ground floor classrooms (openings 0m to 3m above ground level)

	100	**101**	**102**	**103**	**104**	**105**	**106**	**107**	**108**	**109**
Facing	*219° (SW)*	*219° (SW)*	*219° (SW)*	*219° (SW)*	*219° (SW)*	*309° (NW)*	*219° (SW)*	*309° (NW)*	*129° (SE)*	*129° (SE)*
10%	6,71	5,29	5,63	5,39	6,32	4,17	6,10	7,17	6,33	7,77
50%	8,58	7,57	8,21	7,83	7,98	5,41	8,65	9,63	9,72	10,48
90%	8,58	7,56	8,23	7,79	8,02	5,41	8,63	9,72	10,09	11,19

The original equation was initially introduced by Riley in 1978 (RILEY et al., 1978). Subsequently, it underwent improvements by Gammaitoni and Nucci in 1997 (GAMMAITONI and NUCCI, 1997). These enhancements to the equation led to its further development, and the resulting model was articulated as equations (1) and (2) in the work of Buonanno et al. (BUONANNO, STABILE, & MORAWSKA, 2020). These iterations and contributions by various researchers have contributed to a more comprehensive and refined understanding of the model's functionality.

$$R = 1 - e^{-IR \int_0^T n(t)dt} \qquad \textit{eq. (1)}$$

$$n(t) = \frac{ER_q \cdot I}{IVRR \cdot V} + \left(n_0 + \frac{ER_q \cdot I}{IVRR}\right) \cdot \frac{e^{-IVRR \cdot t}}{V} \qquad \textit{eq. (2)}$$

Where:

- R is the risk of infection (%)
- e is Euler's Number
- IR is the Inhalation Rate of the exposed subject (a function of the subject's metabolism)
- T is the total time of contact with infected air, in hours
- n(t) is the quanta (units of infection) concentration in the air
- ERq is the disease's quanta emission rate
- I is the number of infected people
- IVRR is the Infective Virus Removal Rate, that is, the rate at which viruses depose onto surfaces, get ventilated out, or die without infecting a host. The classroom's air renovations in this paper account for >99% of this number. (Yang and Marr, 2011)
- V is the volume of the room
- n_0 is the initial quanta in the room

It becomes evident from equations (1) and (2) that the risk of infection from airborne diseases is directly linked to several key factors. These include the duration of exposure to infected air, the number of infected individuals, the unique characteristics of the disease in question, and the rate of air changes per hour within the room. It is important to note that certain factors, such as the quanta emission rate, the number of infected individuals, and the average pulmonary volume of an individual (assumed by Gammaitoni et al. as 0.01m³/min (GAMMAITONI & NUCCI, 1997)), may be beyond control or not readily ascertainable in advance. However, the variables that can be managed and regulated are exposure time and

room ventilation. These two variables form the primary focus of this study, as they represent the elements that can be effectively controlled to mitigate the risk of airborne infection in indoor environments.

A comprehensive literature review was conducted to gather the necessary ERq values for measles, Tuberculosis (TB), and COVID-19 in indoor settings. Measles, known for its high infectivity (RILEY ET AL. 1978), offers a foundational reference point in the context of the Wells-Riley model, as it has been well-documented. Tuberculosis was the second deadliest infectious disease even in the wake of the recent COVID-19 pandemic (TAYLOR et al, 2016, WHO 2023), making it an essential benchmark for assessing indoor infection risk. The inclusion of COVID-19 is imperative due to its recent emergence and global prevalence. Furthermore, all three diseases share the traits of being airborne and highly contagious (BUONANNO, STABILE and MORAWSKA, 2020), making them pertinent choices for this study. Additionally, the diversity in microbial types—viral for measles and COVID-19, bacterial for TB—ensures a comprehensive evaluation of infectious disease scenarios. Table 4.4 displays the values and their sources.

Table 4.4 - Quanta generation values compatible with an infected teacher (light exercise, speaking)

Disease	**ERq (q/h)**	**Source**
COVID-19 (original strain)	4.9	Buonanno, Stabile and Morawska. 2020
COVID-19 (Delta variant)	69.2	Bertone 2022.
COVID-19 (Omicron variant)	94	Huang, Jones and He. 2022
Tuberculosis	12.7	Nardell, Keegan et al. 1991
Measles	570	Riley, Murphy et al. 1978

As with Zivelonghi et al. (2021), we have worked with a zero-infection threshold. That means if a classroom is currently being occupied by 75 people, one of whom is infected (and therefore not susceptible), permanence in that classroom will be considered safe while the risk remains below 1/74 or 1.35%. Table 4.5 shows the number of people in all classrooms in each occupation case. The theoretical maximum number of occupants in a classroom was determined by counting the available individual seats in each classroom, dividing them by the total area of the classroom, and taking the weighted average of these values across all classrooms. We inserted this into the EnergyPlus Model as an occupation density of 1.15m²/person. For cases that pose an infection risk above the zero-infection threshold, we

have calculated the reduced maximum number of occupants so that the risk remains below the threshold when all other variables remain the same (air exchange rate, number of infection sources, ERq, etc.). This was achieved by taking the reciprocal of the risk at each time. (equation 3)

$$R(t)_{max} = \frac{1}{Occ} \Rightarrow Occ_{max} = \frac{1}{R(t)} \qquad (eq\ 3)$$

Table 4.5 - Number of people in each occupation case. The maximum occupation was defined as a minimum of 1.15m² of floor area per person, by taking the average number of chairs per square meters in all classrooms, as determined by the architectural plan

Zone Name	Volume (m³)	10% Occupied	50% Occupied	90% Occupied
Z100	327,19	8	42	75
Z101	272,8	7	35	63
Z102	272,8	7	35	63
Z103	272,8	7	35	63
Z104	272,8	7	35	63
Z105	272,8	7	35	63
Z106	272,8	7	35	63
Z107	328,34	8	42	75
Z108	269,52	7	34	62
Z109	327,64	8	42	75
Z200	321,21	8	41	74
Z201	268,23	7	34	62
Z202	267,83	7	34	61
Z203	267,95	7	34	61
Z204	268,19	7	34	62
Z205	267,95	7	34	61
Z206	267,4	7	34	61
Z207	321,87	8	41	74
Z208	322,66	8	41	74
Z209	321,05	8	41	74
Z210	321,86	8	41	74
Z300	315,5	8	40	72
Z301	384,36	10	49	88
Z302	263,12	7	34	60
Z303	405,2	10	52	93
Z304	263,47	7	34	60
Z305	315,25	8	40	72
Z306	262,03	7	33	60
Z307	314,46	8	40	72
Z308	316,84	8	40	73
Z310	315,88	8	40	72

4.5 Results and Discussion

Figure 4.1 shows the airborne viral load in the classrooms under study, evidencing a pattern that repeats itself across all diseases and occupation rates in this paper, appearing also in previous works (Gammaitoni and Nucci, 1997; Buonanno et al. 2020). In all cases, the pathogen load in the air stabilizes over time, especially after 100 minutes. Differences in pathogen concentration between classrooms can be explained by differing air exchange rates, as seen in Table (1). Equation (2) shows the IVRR (infective virus removal rate) works as a percentage, removing a proportion of the infectious particles produced, as opposed to an absolute number of them, causing this stabilization. Furthermore, the mathematical model in use considers that eventually, infectious particles exit the room at the same rate as they're being produced, and so for as long as there is at least one infected person in the room (I>0), there will be infectious particles in the air. This aids us in calculating the infection risk later, as we must consider the infected person to be speaking constantly, i.e., like a teacher.

Figure 4.1- COVID-19 pathogen concentration in each classroom over time, at 10% occupied (Quanta/ m³)

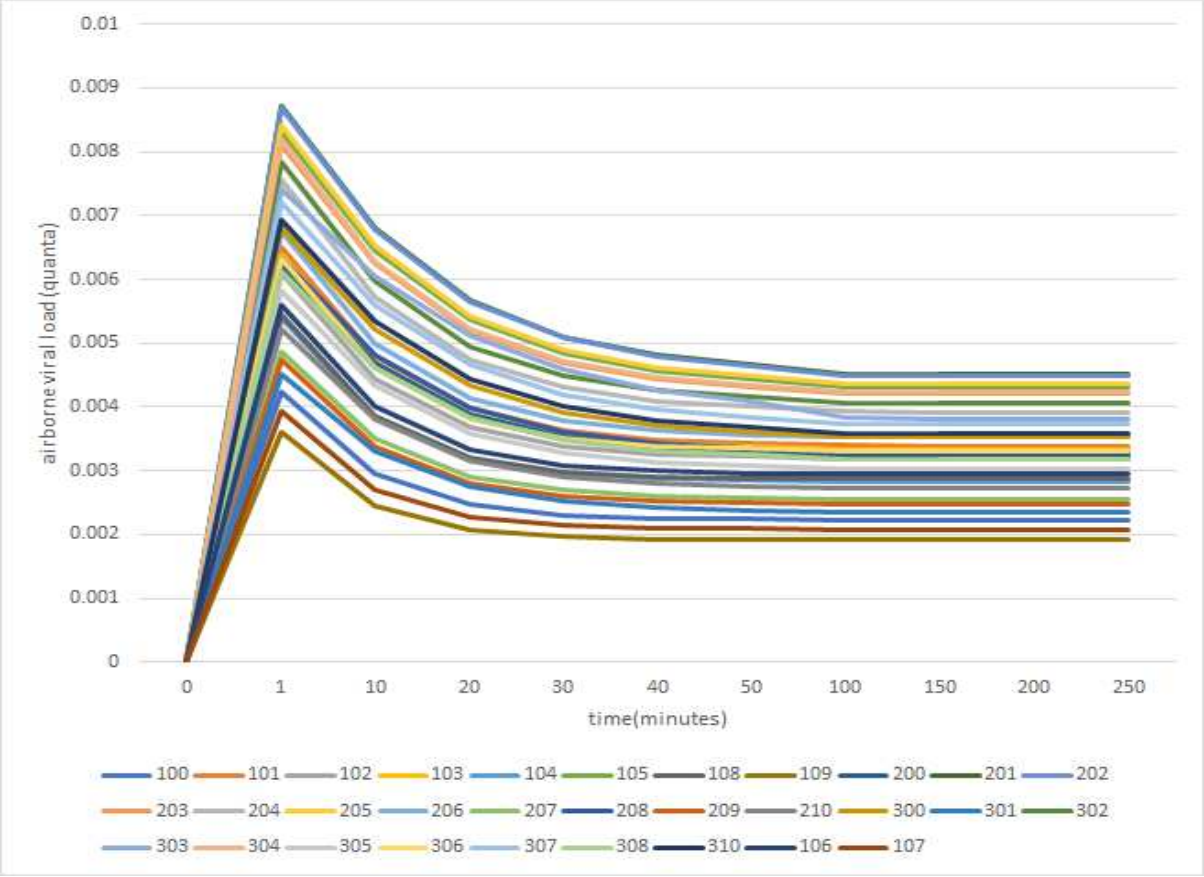

Source: produced by the author

Figures 4.2 to 4.4 show that infection risk rises over time, akin to a logarithmic growth curve. This pattern is again similar to what has been found in other works (BUONANNO et al, 2022, ZIVELONGHI et al, 2020), and indicates the obvious: that risk continues to

increase even if the pathogen load has already stabilized (i.e.: after minute 50). Beyond that, lies some less obvious but more interesting insight. Firstly, one could note that the original Wuhan strain of the COVID-19 pathogen studied by Buonanno et al (2020) offers less risk than the Tuberculosis outbreak described in Nardell et al (1991), and that both cases would, statistically, yield no new infections even after the most drastic case (least ventilated classroom at 90% occupation), as the risk never rises above the zero-infection threshold. We must remind the reader that these simulations do not factor in masks or social distancing, which further underline the value of this conclusion. This observation also relates to the importance of the ERq value of both diseases, since a higher ERq value consists in a wider risk spread at longer occupation times.

Another observation to be made is that Measles exhibited the highest risk across all cases (51.71% risk in a 90% full room 304, that is, 60 people, who have been there for 250 minutes) even at short exposure times in very well-ventilated rooms. (a 4.46% risk in a 90% full room 109, at 50 minutes). The contrast between the infection risk across pathogens can be explained by their vastly different infective particle production rates (ERq), but it is important to note that the variants of SARS-CoV-2 may exhibit ERq values closer or even superior to those of measles (HUANG ET AL. 2022, MIKSZEWSKI ET AL 2022, AGANOVIC ET AL 2022). Oddly, this may lead to the conclusion that both the original Wuhan strain of COVID-19 and Tuberculosis could theoretically be contained without the need of masks, but it also does underline the importance of disease control measures for the later variants.

Overall, the absolute risk of infection decreased as more people occupied the room (Figures 4.2 to 4.5), in consonance with the overall increased air exchange rates observed in such a situation (Table 1). Once again, Room 304 remained as an outlier, actually increasing from 49.76% to 51.71% infection risk, since its average air exchange rate decreased. One interesting consequence of the small change in individual risk (smaller than 0,01% on average) between the middle and top occupation cases is that, despite posing essentially the same individual infection risk, fuller classrooms can be considered less safe, since the individual risk is closer to the zero-infection threshold. To illustrate: the zero-infection threshold is 2.5% for room 109 at 50% occupation. In the same scenario, the tuberculosis risk at 250 minutes of exposure is 0.50% and the COVID-19 infection risk is 0.19% For 90% occupation, that threshold drops to 1.35%. Much closer to the now 0.47% Tuberculosis risk and 0.18% COVID-19 risk at 250 minutes of exposure time. It is therefore less safe.

Figure 4.3 - COVID-19 Infection risk ranges across all classrooms for 0-250 minutes of exposure at 10%, 50% and 90% occupations.

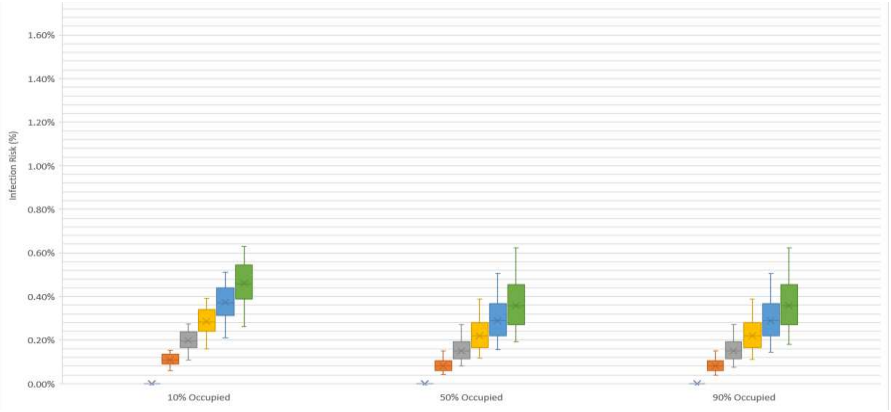

Figure 4.4 - Tuberculosis infection risk ranges across all classrooms for 0-250 minutes of exposure at 10%, 50% and 90% occupations.

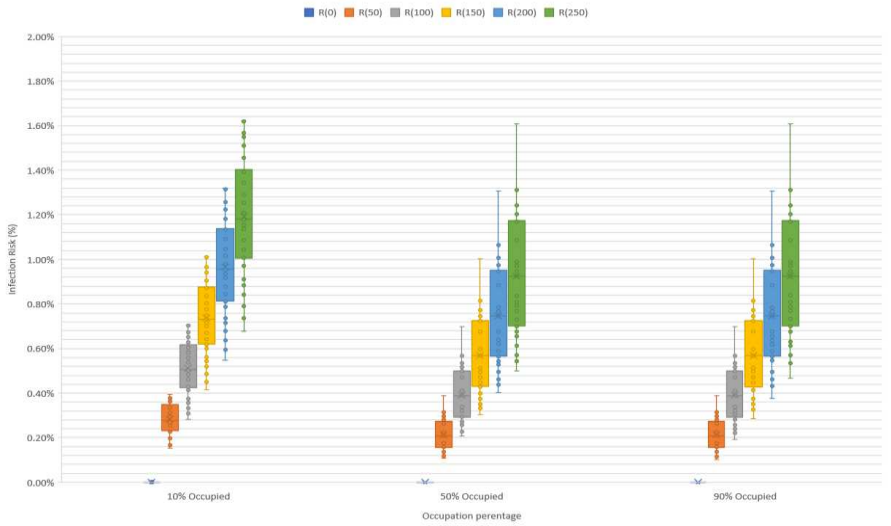

Figure 4.2 - Measles infection risk ranges across all classrooms for 0-250 minutes of exposure at 10%, 50% and 90% occupations.

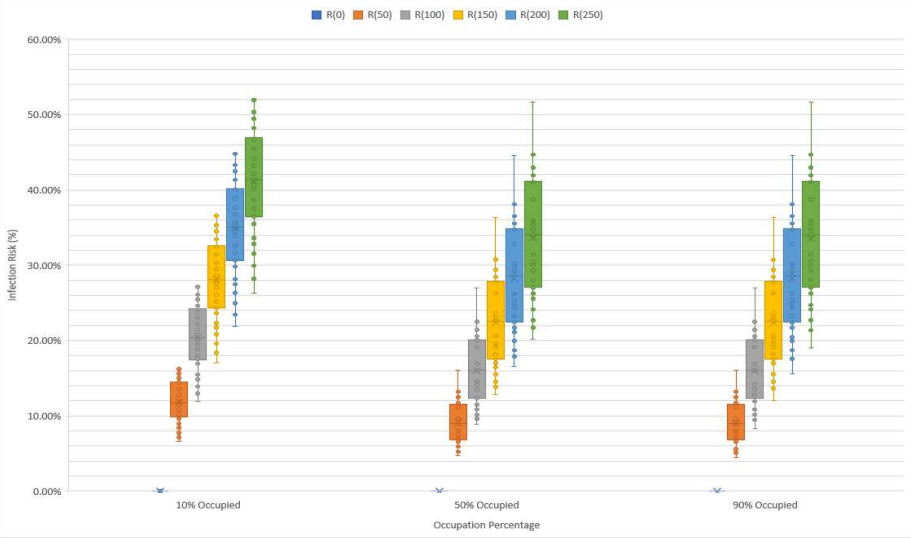

Figure 4.5 - Measles (left), Tuberculosis (middle), and COVID-19 (right) infection risk over time for each classroom, at 10% occupation (top), 50% occupation (middle) and 90% occupation (bottom) and Note once again the scale change for Measles.

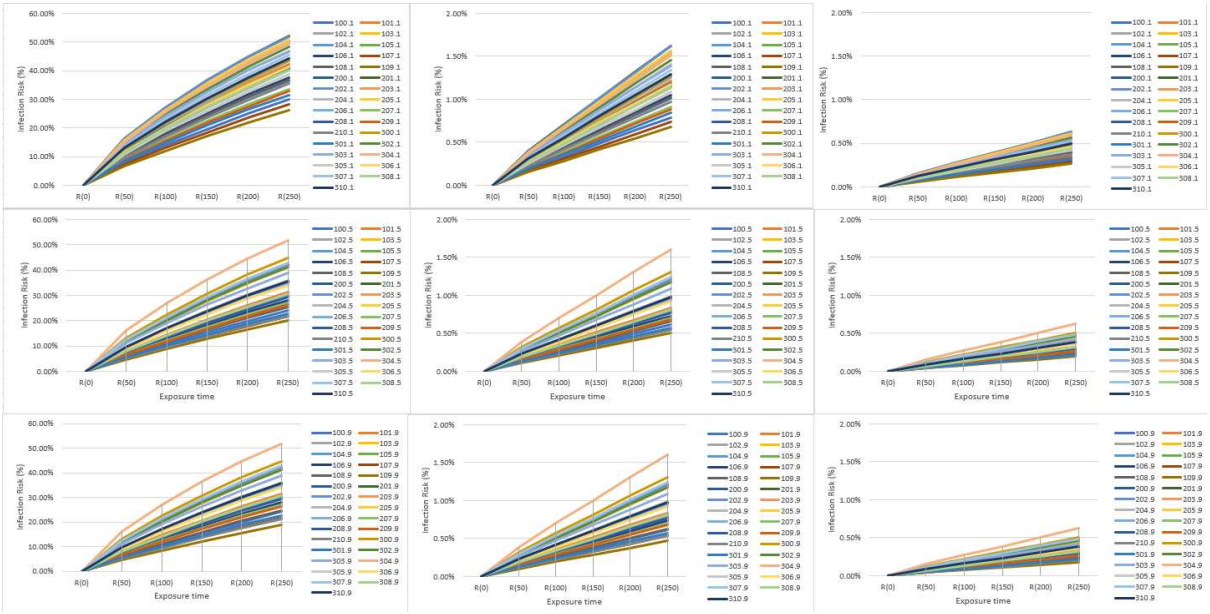

Source: produced by the author

As for maximum occupancy, only measles exhibited infection risk above the zero-infection threshold, so it is not justifiable to suggest reduced occupancy rates for any classrooms to avoid tuberculosis or original strain COVID-19 infections (Figure 4.6). For measles, on the other hand, all classrooms would have to operate under drastically reduced occupation, effectively making in-person classes impossible.

In the face results that seemed to contradict the sheer number of deaths and infections caused by the recent coronavirus pandemic, we turned to the study of more recent variants of COVID-19 to seek an explanation. Figures (4.6) shows that the increased quanta production of the Delta and Omicron variants indeed warrants a reduction in occupancy in the classrooms of the building under study, for longer exposure times. The data suggest that, even for more infectious versions of COVID-19, almost half (13 out of 30) of this lecture hall's classrooms could be utilized at up to half capacity for lessons of up to 200 minutes. Beyond that, short lessons (up to 50min) seem to be safe even at 90% classroom capacity for most classrooms in PVB (Figure (4.6)). This could indicate that, based on Zivelonghi (2021), ventilation breaks between lessons could be sufficient to eliminate new infections in these classrooms.

Figure 4.6 - Adjusted maximum number of occupants per classroom and exposure time, so that no new infections arise. An "n/a" indicates no adjustment is needed, and the full percentage can be occupied safely. 90% occupation.

		COVID					Delta					Omicron					Measles					Tuberculosis				
	90% occup	50 min	100min	150min	200min	250 min	50 min	100min	150min	200min	250 min	50 min	100min	150min	200min	250 min	50 min	100min	150min	200min	250 min	50 min	100min	150min	200min	250 min
100	75	n/a	n/a	n/a	n/a	n/a	n/a	72	49	38	30	n/a	53	36	28	22	17	9	6	5	4	n/a	n/a	n/a	n/a	n/a
101	63	n/a	n/a	n/a	n/a	n/a	n/a	53	36	28	22	n/a	39	27	20	17	12	7	5	4	3	n/a	n/a	n/a	n/a	n/a
102	63	n/a	n/a	n/a	n/a	n/a	n/a	58	39	30	24	n/a	43	29	22	18	14	7	5	4	3	n/a	n/a	n/a	n/a	n/a
103	63	n/a	n/a	n/a	n/a	n/a	n/a	54	37	28	23	n/a	40	28	21	17	13	7	5	4	3	n/a	n/a	n/a	n/a	n/a
104	63	n/a	n/a	n/a	n/a	n/a	n/a	56	38	29	24	n/a	41	28	22	18	13	7	5	4	3	n/a	n/a	n/a	n/a	n/a
105	63	n/a	n/a	n/a	n/a	n/a	n/a	37	26	20	16	49	27	19	15	12	9	5	4	3	2	n/a	n/a	n/a	n/a	n/a
106	63	n/a	n/a	n/a	n/a	n/a	n/a	61	41	32	25	n/a	45	31	23	19	14	8	5	4	4	n/a	n/a	n/a	n/a	n/a
107	75	n/a	n/a	n/a	n/a	n/a	n/a	56	43	34	n/a	61	42	32	26	19	10	7	6	5	n/a	n/a	n/a	n/a	n/a	
108	62	n/a	n/a	n/a	n/a	n/a	n/a	48	37	29	n/a	52	36	27	22	17	9	6	5	4	n/a	n/a	n/a	n/a	n/a	
109	75	n/a	n/a	n/a	n/a	n/a	n/a	65	49	40	n/a	70	48	36	29	22	12	8	6	5	n/a	n/a	n/a	n/a	n/a	
200	74	n/a	n/a	n/a	n/a	n/a	45	31	24	19	60	33	23	18	14	10	6	4	3	3	n/a	n/a	n/a	n/a	n/a	
201	62	n/a	n/a	n/a	n/a	n/a	36	25	19	16	49	27	19	14	12	8	5	4	3	2	n/a	n/a	n/a	n/a	n/a	
202	61	n/a	n/a	n/a	n/a	n/a	36	25	19	16	48	27	19	14	12	8	5	4	3	2	n/a	n/a	n/a	n/a	n/a	
203	61	n/a	n/a	n/a	n/a	n/a	37	26	20	16	50	27	19	15	12	9	5	4	3	2	n/a	n/a	n/a	n/a	n/a	
204	62	n/a	n/a	n/a	n/a	n/a	37	26	20	16	50	28	19	15	12	9	5	4	3	2	n/a	n/a	n/a	n/a	n/a	
205	61	n/a	n/a	n/a	n/a	n/a	37	26	20	16	50	28	19	15	12	9	5	4	3	2	n/a	n/a	n/a	n/a	n/a	
206	61	n/a	n/a	n/a	n/a	n/a	46	32	24	20	n/a	34	24	18	15	11	6	4	3	3	n/a	n/a	n/a	n/a	n/a	
207	74	n/a	n/a	n/a	n/a	n/a	63	43	33	27	n/a	47	32	24	20	15	8	6	4	4	n/a	n/a	n/a	n/a	n/a	
208	74	n/a	n/a	n/a	n/a	n/a	57	39	30	24	n/a	42	29	22	18	13	7	5	4	3	n/a	n/a	n/a	n/a	n/a	
209	74	n/a	n/a	n/a	n/a	n/a	65	45	34	28	n/a	48	33	25	20	15	8	6	5	4	n/a	n/a	n/a	n/a	n/a	
210	74	n/a	n/a	n/a	n/a	n/a	n/a	57	43	35	n/a	61	42	32	26	20	11	7	6	5	n/a	n/a	n/a	n/a	n/a	
300	72	n/a	n/a	n/a	n/a	59	33	23	18	14	43	24	17	13	11	8	4	3	3	2	n/a	n/a	n/a	n/a	n/a	
301	88	n/a	n/a	n/a	n/a	n/a	77	53	40	33	n/a	57	39	30	24	18	10	7	5	4	n/a	n/a	n/a	n/a	n/a	
302	60	n/a	n/a	n/a	n/a	n/a	37	26	20	16	50	27	19	15	12	9	5	4	3	2	n/a	n/a	n/a	n/a	n/a	
303	93	n/a	n/a	n/a	n/a	70	39	28	21	17	52	29	20	16	n/a	9	5	4	3	3	n/a	n/a	n/a	n/a	92	
304	60	n/a	n/a	n/a	n/a	48	27	19	14	12	35	20	14	11	9	6	4	3	2	2	n/a	n/a	n/a	n/a	n/a	
305	72	n/a	n/a	n/a	n/a	n/a	44	31	23	19	59	33	23	17	14	10	6	4	3	3	n/a	n/a	n/a	n/a	n/a	
306	60	n/a	n/a	n/a	n/a	n/a	48	33	25	20	n/a	35	24	19	15	11	6	4	4	3	n/a	n/a	n/a	n/a	n/a	
307	72	n/a	n/a	n/a	n/a	62	35	24	19	15	46	26	18	14	11	8	5	3	3	2	n/a	n/a	n/a	n/a	n/a	
308	73	n/a	n/a	n/a	n/a	n/a	54	37	28	23	n/a	40	28	21	17	13	7	5	4	3	n/a	n/a	n/a	n/a	n/a	
310	72	n/a	n/a	n/a	n/a	n/a	44	31	24	19	60	33	23	17	14	10	6	4	3	3	n/a	n/a	n/a	n/a	n/a	

Source: produced by the author

Figure 4.7 - Adjusted maximum number of occupants per classroom and exposure time, so that no new infections arise. An "n/a" indicates no adjustment is needed, and the full percentage can be occupied safely. 10% occupation

		COVID					Delta					Omicron					Measles					Tuberculosis				
	10% occupied	50 min	100min	150min	200min	250 min	50 min	100min	150min	200min	250 min	50 min	100min	150min	200min	250 min	50 min	100min	150min	200min	250 min	50 min	100min	150min	200min	250
100	8	n/a	n/a	n/a	n/a	n/a	n/a	n/a	n/a	n/a	n/a	n/a	n/a	n/a	n/a	n/a	n/a	7	5	4	3	n/a	n/a	n/a	n/a	n/a
101	7	n/a	n/a	n/a	n/a	n/a	n/a	n/a	n/a	n/a	n/a	n/a	n/a	n/a	n/a	n/a	n/a	5	3	3	2	n/a	n/a	n/a	n/a	n/a
102	7	n/a	n/a	n/a	n/a	n/a	n/a	n/a	n/a	n/a	n/a	n/a	n/a	n/a	n/a	n/a	n/a	5	4	3	2	n/a	n/a	n/a	n/a	n/a
103	7	n/a	n/a	n/a	n/a	n/a	n/a	n/a	n/a	n/a	n/a	n/a	n/a	n/a	n/a	n/a	n/a	5	4	3	2	n/a	n/a	n/a	n/a	n/a
104	7	n/a	n/a	n/a	n/a	n/a	n/a	n/a	n/a	n/a	n/a	n/a	n/a	n/a	n/a	n/a	n/a	6	4	3	3	n/a	n/a	n/a	n/a	n/a
105	7	n/a	n/a	n/a	n/a	n/a	n/a	n/a	n/a	n/a	n/a	n/a	n/a	n/a	n/a	n/a	6	4	3	2	2	n/a	n/a	n/a	n/a	n/a
106	7	n/a	n/a	n/a	n/a	n/a	n/a	n/a	n/a	n/a	n/a	n/a	n/a	n/a	n/a	n/a	n/a	6	4	3	3	n/a	n/a	n/a	n/a	n/a
107	8	n/a	n/a	n/a	n/a	n/a	n/a	n/a	n/a	n/a	n/a	n/a	n/a	n/a	n/a	n/a	n/a	8	5	4	4	n/a	n/a	n/a	n/a	n/a
108	7	n/a	n/a	n/a	n/a	n/a	n/a	n/a	n/a	n/a	n/a	n/a	n/a	n/a	n/a	n/a	n/a	6	4	3	3	n/a	n/a	n/a	n/a	n/a
109	8	n/a	n/a	n/a	n/a	n/a	n/a	n/a	n/a	n/a	n/a	n/a	n/a	n/a	n/a	n/a	n/a	8	6	5	4	n/a	n/a	n/a	n/a	n/a
200	8	n/a	n/a	n/a	n/a	n/a	n/a	n/a	n/a	n/a	n/a	n/a	n/a	n/a	n/a	n/a	n/a	5	4	3	2	n/a	n/a	n/a	n/a	n/a
201	7	n/a	n/a	n/a	n/a	n/a	n/a	n/a	n/a	n/a	n/a	n/a	n/a	n/a	n/a	n/a	6	4	3	2	2	n/a	n/a	n/a	n/a	n/a
202	7	n/a	n/a	n/a	n/a	n/a	n/a	n/a	n/a	n/a	n/a	n/a	n/a	n/a	n/a	n/a	6	4	3	2	2	n/a	n/a	n/a	n/a	n/a
203	7	n/a	n/a	n/a	n/a	n/a	n/a	n/a	n/a	n/a	n/a	n/a	n/a	n/a	n/a	n/a	7	4	3	2	2	n/a	n/a	n/a	n/a	n/a
204	7	n/a	n/a	n/a	n/a	n/a	n/a	n/a	n/a	n/a	n/a	n/a	n/a	n/a	n/a	n/a	n/a	4	3	2	2	n/a	n/a	n/a	n/a	n/a
205	7	n/a	n/a	n/a	n/a	n/a	n/a	n/a	n/a	n/a	n/a	n/a	n/a	n/a	n/a	n/a	6	4	3	2	2	n/a	n/a	n/a	n/a	n/a
206	7	n/a	n/a	n/a	n/a	n/a	n/a	n/a	n/a	n/a	n/a	n/a	n/a	n/a	n/a	n/a	n/a	5	3	3	2	n/a	n/a	n/a	n/a	n/a
207	8	n/a	n/a	n/a	n/a	n/a	n/a	n/a	n/a	n/a	n/a	n/a	n/a	n/a	n/a	n/a	n/a	6	4	4	3	n/a	n/a	n/a	n/a	n/a
208	8	n/a	n/a	n/a	n/a	n/a	n/a	n/a	n/a	n/a	n/a	n/a	n/a	n/a	n/a	n/a	n/a	5	4	3	2	n/a	n/a	n/a	n/a	n/a
209	8	n/a	n/a	n/a	n/a	n/a	n/a	n/a	n/a	n/a	n/a	n/a	n/a	n/a	n/a	n/a	n/a	6	5	4	3	n/a	n/a	n/a	n/a	n/a
210	8	n/a	n/a	n/a	n/a	n/a	n/a	n/a	n/a	n/a	n/a	n/a	n/a	n/a	n/a	n/a	n/a	6	4	3	3	n/a	n/a	n/a	n/a	n/a
300	8	n/a	n/a	n/a	n/a	n/a	n/a	n/a	n/a	n/a	n/a	n/a	n/a	n/a	n/a	n/a	8	5	3	3	2	n/a	n/a	n/a	n/a	n/a
301	10	n/a	n/a	n/a	n/a	n/a	n/a	n/a	n/a	n/a	n/a	n/a	n/a	n/a	n/a	n/a	n/a	7	5	4	3	n/a	n/a	n/a	n/a	n/a
302	7	n/a	n/a	n/a	n/a	n/a	n/a	n/a	n/a	n/a	n/a	n/a	n/a	n/a	n/a	n/a	n/a	4	3	2	2	n/a	n/a	n/a	n/a	n/a
303	10	n/a	n/a	n/a	n/a	n/a	n/a	n/a	n/a	n/a	n/a	n/a	n/a	n/a	n/a	n/a	7	4	3	2	2	n/a	n/a	n/a	n/a	n/a
304	7	n/a	n/a	n/a	n/a	n/a	n/a	n/a	n/a	n/a	n/a	n/a	n/a	n/a	n/a	n/a	7	4	3	2	2	n/a	n/a	n/a	n/a	n/a
305	8	n/a	n/a	n/a	n/a	n/a	n/a	n/a	n/a	n/a	n/a	n/a	n/a	n/a	n/a	n/a	n/a	5	4	3	3	n/a	n/a	n/a	n/a	n/a
306	7	n/a	n/a	n/a	n/a	n/a	n/a	n/a	n/a	n/a	n/a	n/a	n/a	n/a	n/a	n/a	n/a	5	4	3	2	n/a	n/a	n/a	n/a	n/a
307	8	n/a	n/a	n/a	n/a	n/a	n/a	n/a	n/a	n/a	n/a	n/a	n/a	n/a	n/a	n/a	7	4	3	3	2	n/a	n/a	n/a	n/a	n/a
308	8	n/a	n/a	n/a	n/a	n/a	n/a	n/a	n/a	n/a	n/a	n/a	n/a	n/a	n/a	n/a	n/a	5	4	3	2	n/a	n/a	n/a	n/a	n/a
310	8	n/a	n/a	n/a	n/a	n/a	n/a	n/a	n/a	n/a	n/a	n/a	n/a	n/a	n/a	n/a	8	5	3	3	2	n/a	n/a	n/a	n/a	n/a

Source: produced by the author

4.6 Conclusions

This paper aimed to produce a safe usage matrix for the classrooms of a naturally-ventilated lecture hall (PVB) in a tropical climate. Following this matrix was intended to

mitigate the risk of infection by three major airborne diseases: COVID-19, Tuberculosis, and Measles, without considering the effect of disease control measures such as masks or vaccines, and was thus useful to better understand the role of natural ventilation in disease control. It has been shown that, based on infective particle production rates (ERq) and the classroom's air exchange rates, lecture halls like PVB can be well-ventilated enough to reduce airborne infection risk to near zero. That is to say, the data seems to agree that, for classrooms exhibiting air renovation ranges from 3,18 ACH to 11,19 ACH, the risk of infection by the airborne disease under study can be considered low. Beyond that, many of this lecture hall`s classrooms can be utilized for a limited amount of time or at a reduced occupancy with statistically no new infections. We have also shown that more densely occupied classrooms often pose a greater infection risk despite offering better ventilation due to the increased number of susceptible occupants.

We have shown that, on average, for PVB as for other cases in literature, the pathogen concentration in the classroom stabilizes over time as a consequence of both the mathematical modelling of the problem and the constant release and removal of infective particles to and from the air by a talking infection source and the room's ventilation. Despite this, the risk rises steadily over time since continued exposure to infected air increases the risk of coming in contact with an infective dose. The paper also shows that, according to Buonanno et al. (2020), the original strain of COVD-19 was less infectious than Tuberculosis, which underlines the importance of vaccination and other forms of disease prevention, especially in light of the elevated number of deaths both diseases cause even today.

Among the contributions of this paper is studying the effect of airborne disease specifically in naturally-ventilated tropical classrooms, which seems to be lacking in literature. While similar studies have indicated that natural ventilation alone was not sufficient to mitigate infection risk in temperate classrooms, we have shown that, in some cases, tropical classrooms do not have this problem, especially when equipped with ventilation devices such as a thermal chimney.

It is important to underline this paper does not advocate against mask use or vaccinations as prevention measures. On the contrary, the findings underline the importance of these measures on reducing infections, once we compare the expected number of infections to the actual number of cases today. This paper is intended only as a study of indoor air quality.

The averaged quanta production rate for an infected individual performing a specific activity, coupled with the weighted average of all air renovation values in a year for each room are satisfactory enough to calculate the generally expected risk of infection in the classrooms of a lecture hall such as PVB, but in no way it is an absolute assurance of safety or danger, especially since both parameters - quanta production and ventilation- are known to vary quite widely and quite rapidly (BUONANNO ET AL., 2020; LAMBERTS ET AL., 2010). Furthermore, a low risk of infection does not mean there is no risk. This study does not account for the pattern of airflow inside classrooms, or the stratification of air which has been shown to create lower and higher concentration regions of infectious particles in classrooms (BHAGAT ET AL. 2020, FOSTER AND KINZEL. 2020).

Further studies shall focus on calculating the same infection metrics (risk over time, maximum safe occupancy rate for a set time and maximum safe duration a for a set occupancy) in other building typologies and comparing the effect of different architectural elements and configurations on disease. It shall also construct an infection landscape for classrooms such as these, revealing potential "dead zones" of air circulation and higher particle density.

4.7 Acknowledgements

This paper could not have been accomplished without the help and funding from FAPEMIG - Fundação de Amparo à Pesquisa do Estado de Minas Gerais, through funding our project "Uso de simulação e ferramentas computacionais no estudo de edifícios naturalmente ventilados", project number **APQ-00872-22.** We also thank CNPq - Conselho Nacional de Pesquisa, which fundamentally contributed to this paper, through funding our project "Tecnologias para adaptação de edificações às mudanças no clima", project registration number **60419479687**

4.8 Bibliography

ALESSANDRO ZIVELONGHI; LAI, M. Mitigating aerosol infection risk in school buildings: the role of natural ventilation, volume, occupancy and CO2 monitoring. *Building and Environment*, v. 204, n. May, p. 108139, 2021. Disponível em: <https://doi.org/10.1016/j.buildenv.2021.108139>.

AMAR AGANOVIC *et al.* New dose-response model and SARS-CoV-2 quanta emission rates for calculating the long-range airborne infection risk. *Building and Environment*, v. 228, p. 109924, jan. 2023.

BERTONE, M. *et al.* Assessment of SARS-CoV-2 airborne infection transmission risk in public buses. *Geoscience frontiers*, v. 13, n. 6, nov. 2022. Disponível em: <https://pubmed.ncbi.nlm.nih.gov/37521135/>.

BUONANNO, G. *et al.* Increasing ventilation reduces SARS-CoV-2 airborne transmission in schools: A retrospective cohort study in Italy's Marche region. *Frontiers in public health*, v. 10, dez. 2022. Disponível em: <https://pubmed.ncbi.nlm.nih.gov/36568748/>.

BUONANNO, G.; L. MORAWSKA; STABILE, L. Quantitative assessment of the risk of airborne transmission of SARS-CoV-2 infection: Prospective and retrospective applications. *Environment International*, v. 145, n. September, p. 106112, 2020. Disponível em: <https://doi.org/10.1016/j.envint.2020.106112>.

BUONANNO, G.; STABILE, L.; L MORAWSKA. Estimation of airborne viral emission: Quanta emission rate of SARS-CoV-2 for infection risk assessment. *Environment International*, n. 141, p. 105794, 2020. Disponível em: <https://doi.org/10.1016/j.envint.2020.105794%20Received>.

C.E, R.; RILEY. AIRBORNE SPREAD OF MEASLES IN A SUBURBAN ELEMENTARY SCHOOL. *American Journal of Epidemiology*, v. 107, n. 5, p. 421–432, 1978.

DAI, H.; ZHAO, B. Association between the infection probability of COVID-19 and ventilation rates: An update for SARS-CoV-2 variants. *Building Simulation*, v. 16, n. 1, p. 3–12, jan. 2023. Disponível em: <https://link.springer.com/article/10.1007/s12273-022-0952-6>.

FOSTER, A.; KINZEL, M. Estimating COVID-19 exposure in a classroom setting: A comparison between mathematical and numerical models. *Physics of Fluids*, v. 33, n. 2, 2021.

GUPTA, J. K.; CHAO HSIN LIN; CHEN, Q. Characterizing exhaled airflow from breathing and talking. *Indoor Air*, v. 20, n. 1, p. 31–39, fev. 2010. Disponível em: <https://onlinelibrary.wiley.com/doi/full/10.1111/j.1600-0668.2009.00623.x%20https://onlinelibrary.wiley.com/doi/abs/10.1111/j.1600-0668.2009.00623.x%20https://onlinelibrary.wiley.com/doi/10.1111/j.1600-0668.2009.00623.x>.

HUANG, J. *et al.* Airborne transmission of the Delta variant of SARS-CoV-2 in an auditorium. *Building and Environment*, v. 219, p. 109212, jul. 2022.

L. MORAWSKA *et al.* Size distribution and sites of origin of droplets expelled from the human respiratory tract during expiratory activities. *Journal of Aerosol Science*, v. 40, n. 3, p. 256–269, 2009.

L.GAMMAITONI; M.C.NUCCI. Using a mathematical model to evaluate the efficacy of TB control measures. *Emerg. Infect. Dis.*, v. 3, n. 3, p. 335–342, 1997.

LU, J. *et al.* COVID-19 outbreak associated with air conditioning in restaurant, guangzhou, china, 2020 - volume 26, number 7—July 2020 - emerging infectious diseases journal - CDC. *Emerging Infectious Diseases*, v. 26, n. 7, p. 1628–1631, jul. 2020. Disponível em: <https://wwwnc.cdc.gov/eid/article/26/7/20-0764_article>.

MIKSZEWSKI, A. *et al.* The airborne contagiousness of respiratory viruses: A comparative analysis and implications for mitigation. *Geoscience Frontiers*, v. 13, n. 6, p. 101285, nov. 2022.

MORAWSKA, L.; MILTON, D. K. It is time to address airborne transmission of coronavirus disease 2019 (COVID-19). *Clinical Infectious Diseases*, v. 71, n. 9, p. 2311–2313, 2020.

NARDELL, E. A. *et al.* Airborne infection: Theoretical limits of protection achievable by building ventilation. *https://doi.org/10.1164/ajrccm/144.2.302*, v. 144, n. 2, p. 302–306, dez. 2012.

NIGHTINGALE, F. *Notes on hospitals*. 3rd. ed. [S.l.]: Longman, Green, Longman, Roberts and Gre, 1863. p. 187Disponível em: <https://books.google.com/books?hl=en&lr=&id=n5FtEAAAQBAJ&oi=fnd&pg=PA1&dq=good+governance&ots=6UIHTdayhH&sig=sO-wYh6SQrgpIFukLwvBQeCPru8>.

RILEY, R. L. Aerial dissemination of pulmonary tuberculosis. *American review of tuberculosis*, v. 76, n. 6, p. 931–941, 1957.

VITRUVIUS. *Vitruvio: Tratado de arquitectura*. [S.l.]: IST Press c2006, [S.d.]. p. 454

WELLS, W. F. ON AIR-BORNE INFECTION.* STUDY II. DROPLETS AND DROPLET NUCLEI. under the title, "Viability of Bacteria in. *t Stokes' Mathematical and Physical*

Papers, v. 1, n. 01, p. 60, 1933. Disponível em: <https://academic.oup.com/aje/article/20/3/611/280025>.

WORLD HEALTH ORGANIZATION. *Global tuberculosis report 2023*. *World Health Organization*. [S.l: s.n.], 2023.

XIE, X. *et al.* How far droplets can move in indoor environments - revisiting the Wells evaporation-falling curve. *Indoor Air*, v. 17, n. 3, p. 211–225, 2007.

YANG, W.; MARR, L. C. Dynamics of airborne influenza a viruses indoors and dependence on humidity. *PLOS ONE*, v. 6, n. 6, p. e21481, 2011. Disponível em: <https://journals.plos.org/plosone/article?id=10.1371/journal.pone.0021481>.

ZHANG, R. *et al.* Identifying airborne transmission as the dominant route for the spread of COVID-19. *Proceedings of the National Academy of Sciences of the United States of America*, v. 117, n. 26, p. 14857–14863, 2020.

5 Conclusions

This Master's dissertation has explored three main subjects. Chapter 2 delves into the calibration of naturally ventilated (NV) building energy models, Chapter 3 investigates the ventilation potential of Pavilhão de Aulas II (PVB), and Chapter 4 calculates airborne infection risk in that building. These chapters discuss the Coefficient of Variation of Root Mean Square Error (CV(RMSE)) and the Normalized Mean Bias Error (NMBE) as effective indicators for calibrating Natural Ventilation (NV) simulations, assess the differences in number of air renovations between PVB's classrooms, investigate the building ventilation's relationship to the buildings' architectural and usage parameters, and quantify the risk of contamination by measles, Tuberculosis (TB), and COVID-19 in classrooms with air renovation rates similar to PVB's.

The NMBE, in particular, emerges as a valuable metric for comparing different types of simulations, as it measures model error relative to itself. By employing these calibration techniques, the study was able to enhance the accuracy and reliability of NV simulations.

The assessment of nearby weather station data revealed a discrepancy from its data from the microclimate of "Pavilhão de Aulas II" ("Lecture Hall II" or PVB). Subsequently, with a calibrated model, the study delved into the analysis of PVB ventilation. Considering that the Cps had minor impact in ACH compared to chimney height, the ground floor classrooms experienced more air renovations regardless of the higher thermal loads on the top floor. Furthermore, the study observed that ventilation exhibited some correlation with classroom occupancy. Chimney height emerged as a more influential factor on ventilation for these classrooms compared to thermal gradient and wind pressure.

With a comprehensive understanding of ventilation patterns, the research extended its focus to safety evaluation. The assessment of infection risk indicated that under normal use conditions, the risk remained below the established zero-infection threshold for the original Wuhan strain of COVID-19 and Tuberculosis. However, the risk of measles transmission was found to be significantly above the threshold, underscoring the importance of vaccines in mitigating airborne disease risks.

Remarkably, the study revealed that despite improved ventilation, an increase in occupancy resulted in higher risk, as it narrowed the admissible threshold. This insight emphasizes the need for a holistic approach to safety in building design and occupancy management.

A noteworthy observation was made in tropical classrooms, where a higher temperature gradient appeared to render them less susceptible to airborne diseases. This finding highlights the potential role of environmental factors in shaping the transmission dynamics of diseases in different settings.

It is essential to note that the paper intentionally refrained from evaluating the specific pathways of air inside classrooms, instead employing CFD only for outdoor airflow. Further studies shall evaluate the unique landscape of the room, in terms of airborne pollutant concentrations, utilizing CFD software. The conclusions drawn from the present work are applicable to the classroom typology and use case studied and should not be extrapolated to commercial or residential scenarios without careful consideration. Further studies should investigate the applicability of the methods present here to commercial or residential scenarios, evaluating the construction codes of various locations to determine the infection risk in a space that is strictly up to code, and suggesting updates if applicable. Additionally, this work limits itself to the statistical indices of CV(RMSE) and NMBE. Further studies shall broaden the focus, with special interest in running sensitivity analyses on ventilation variables to quantify and further demonstrate the influence of factors such as occupation on the natural ventilation potential in classrooms.

The author considers all the main research goals of this dissertation to have been reached. Chapter 2 reviews calibration methods for BES models discusses the applicability of CV(RMSE) and NMBE for calibrating NV simulations, and presents a calibrated model of PVB. Chapter 3 uses this model to quantify and analyze the airflow in the classrooms this building, and Chapter 4 builds on the previous chapter's findings to obtain permanence and occupancy safe limits of PVB's classrooms. The findings underscore the importance of considering multiple variables in building design and ventilation strategies to optimize safety, especially in the context of infectious disease control.

6 Appendix: Airborne Viral Load Over Time and Infection Risk Over Time for Tuberculosis, Measles and COVID-19, in classrooms that are 10%, 50% and 90% occupied.

Note: all graphs produced by the author

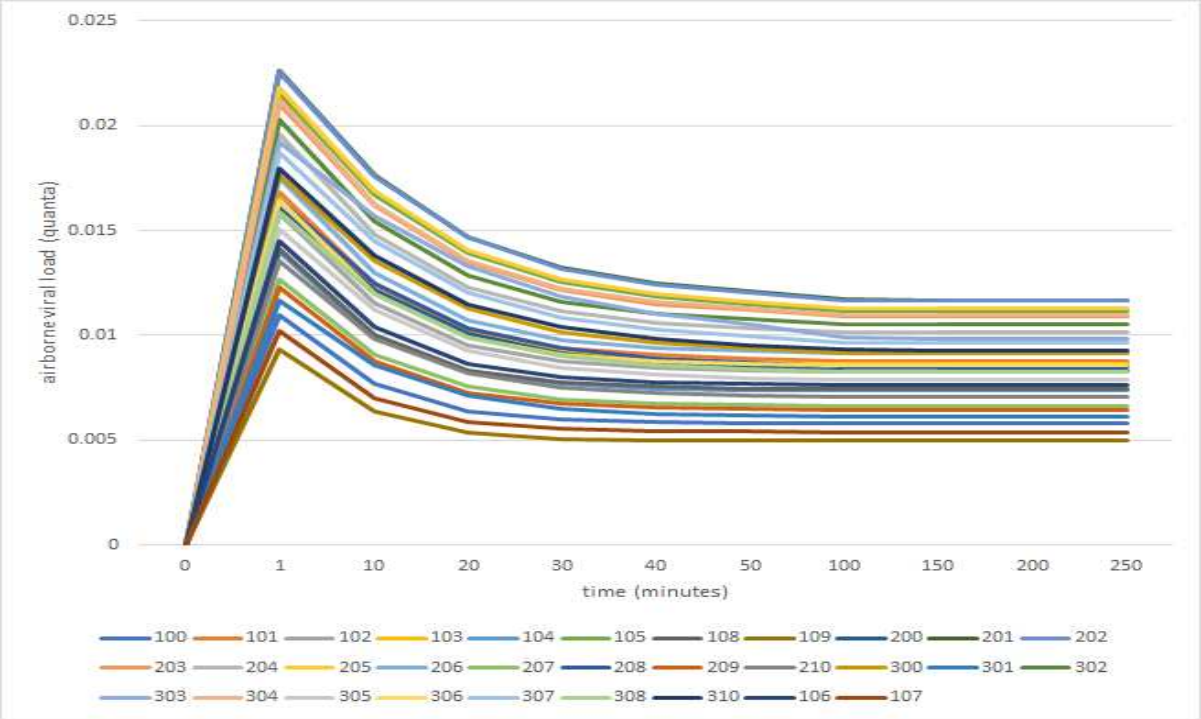

Tuberculosis at 10% occupation.

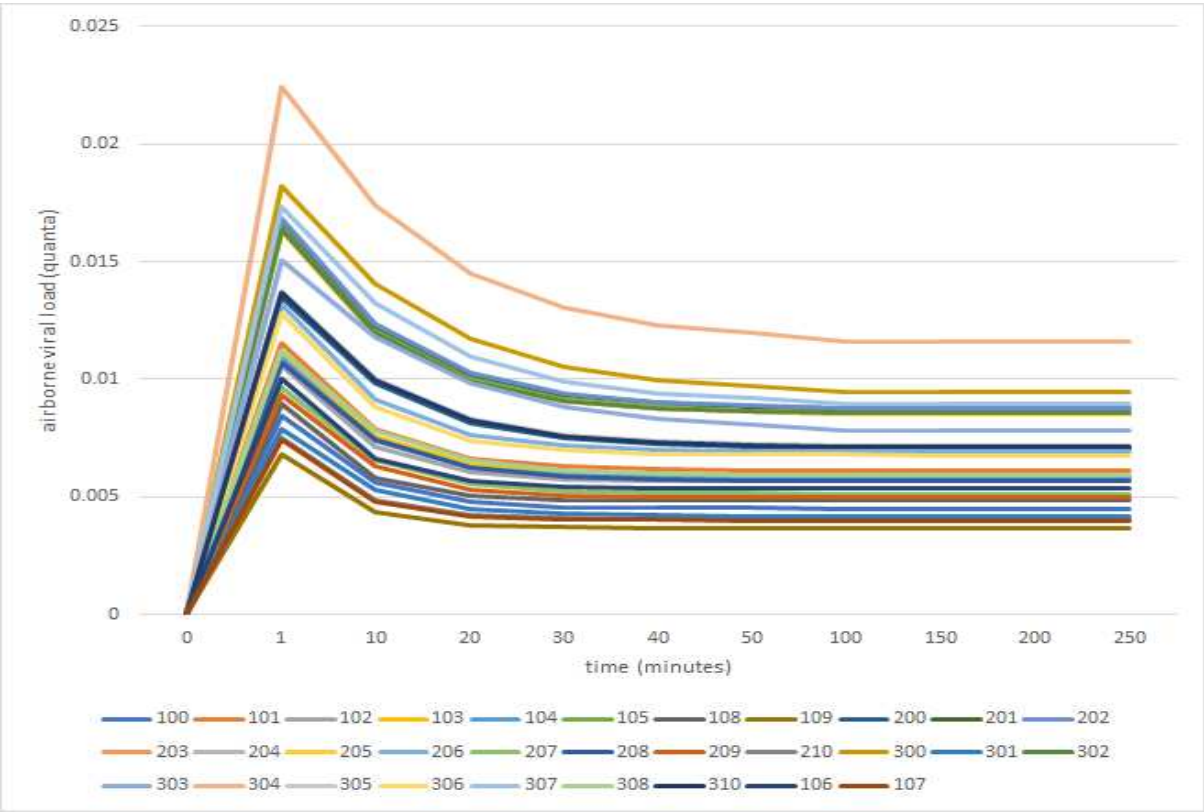

Tuberculosis at 50% occupation.

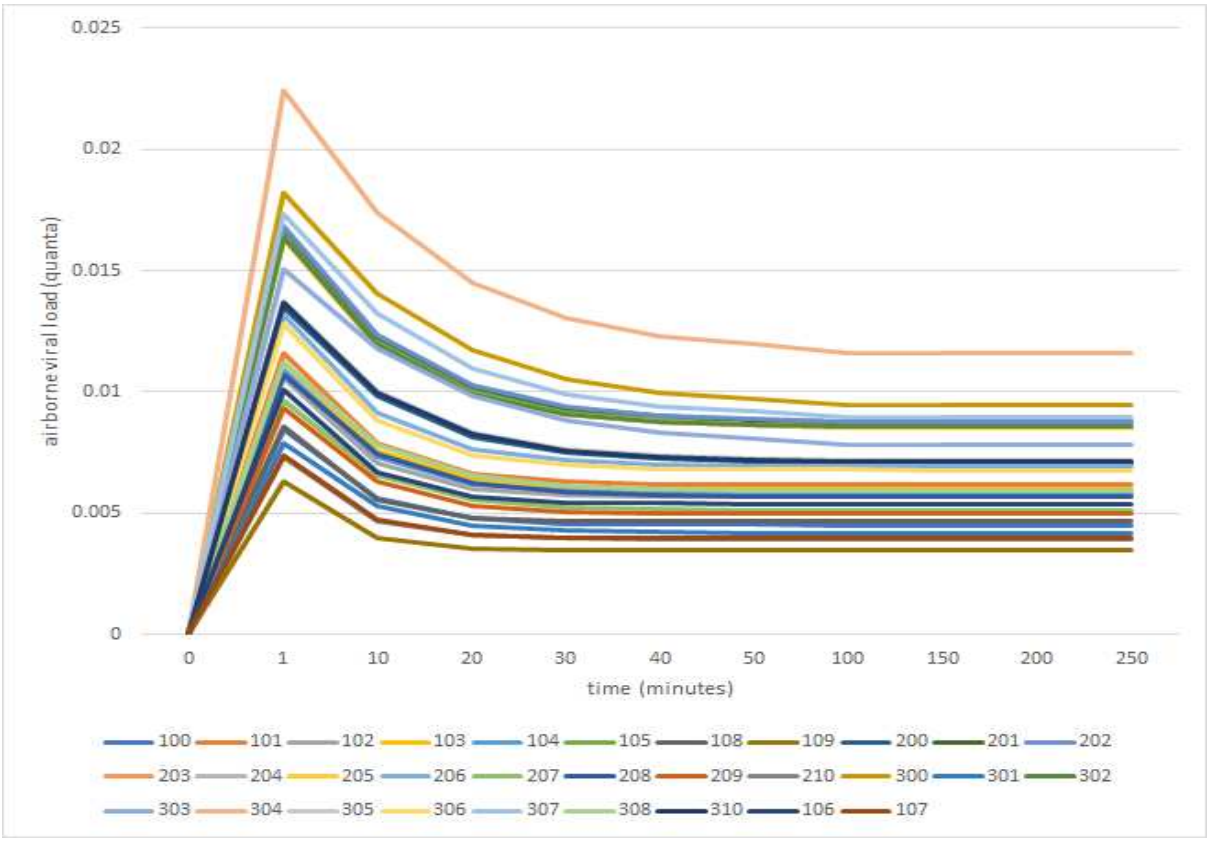

Tuberculosis at 90% occupation.

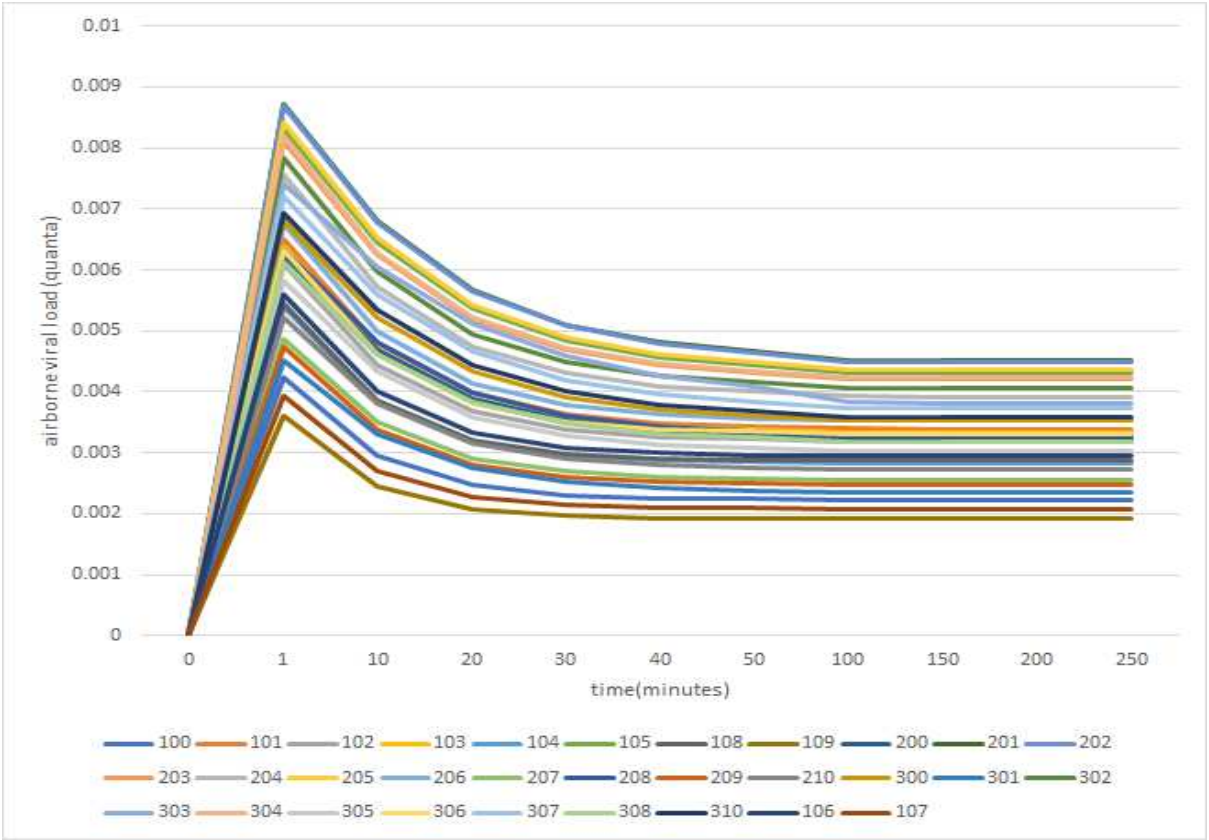

Covid at 10% occupation

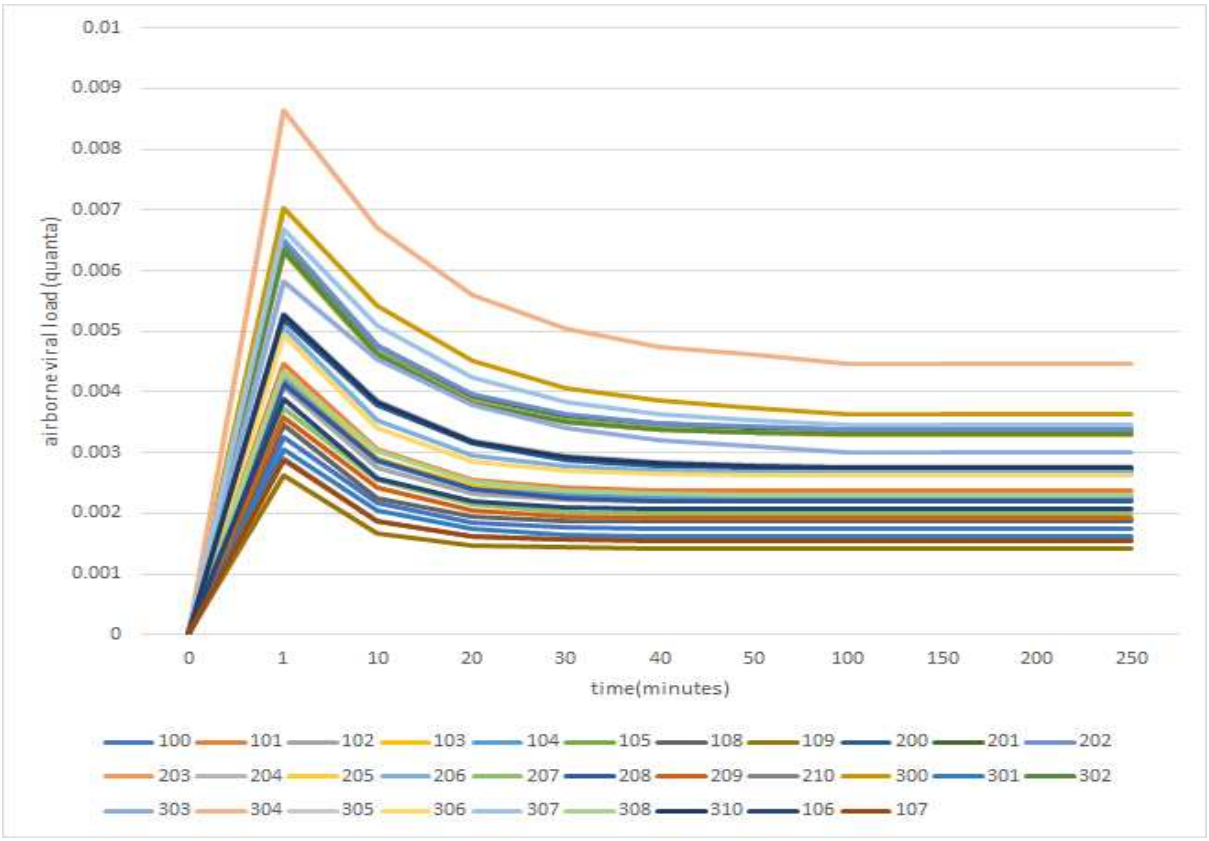

Covid at 50% occupation

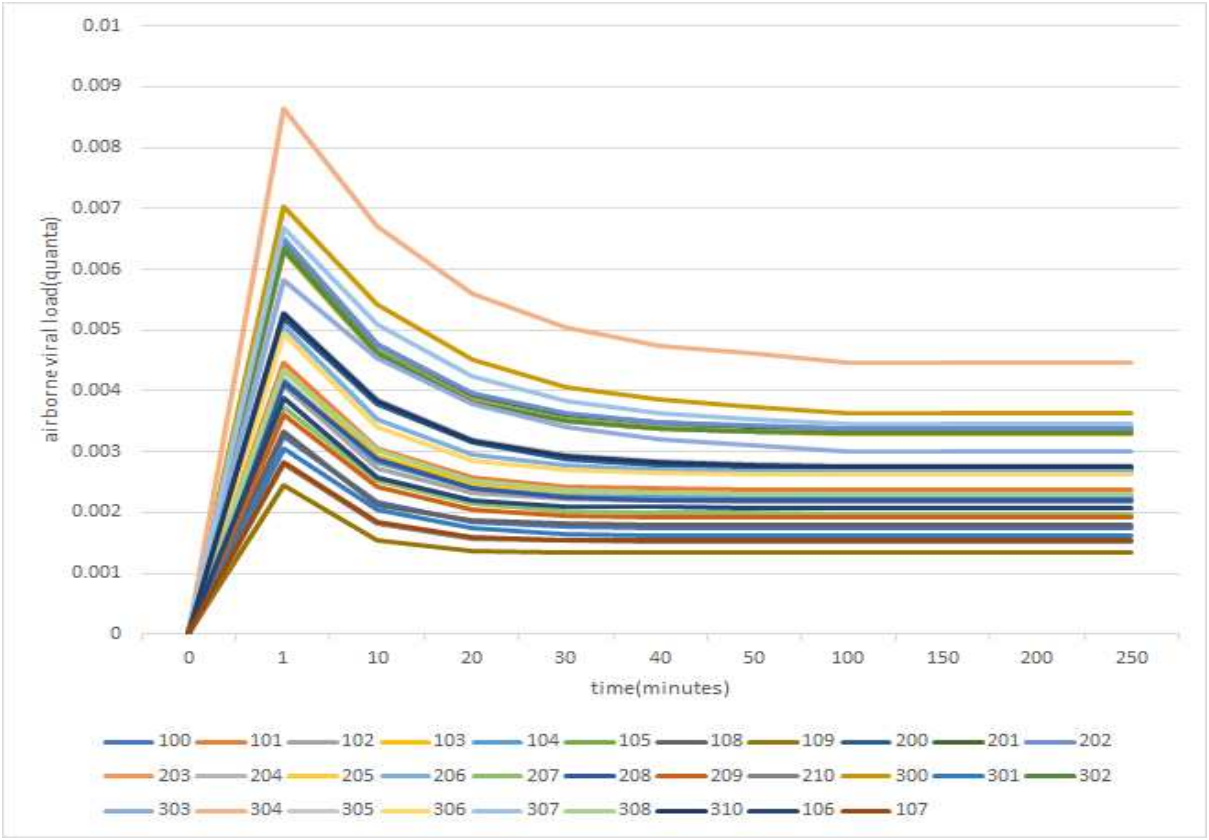

Covid at 90% occupation

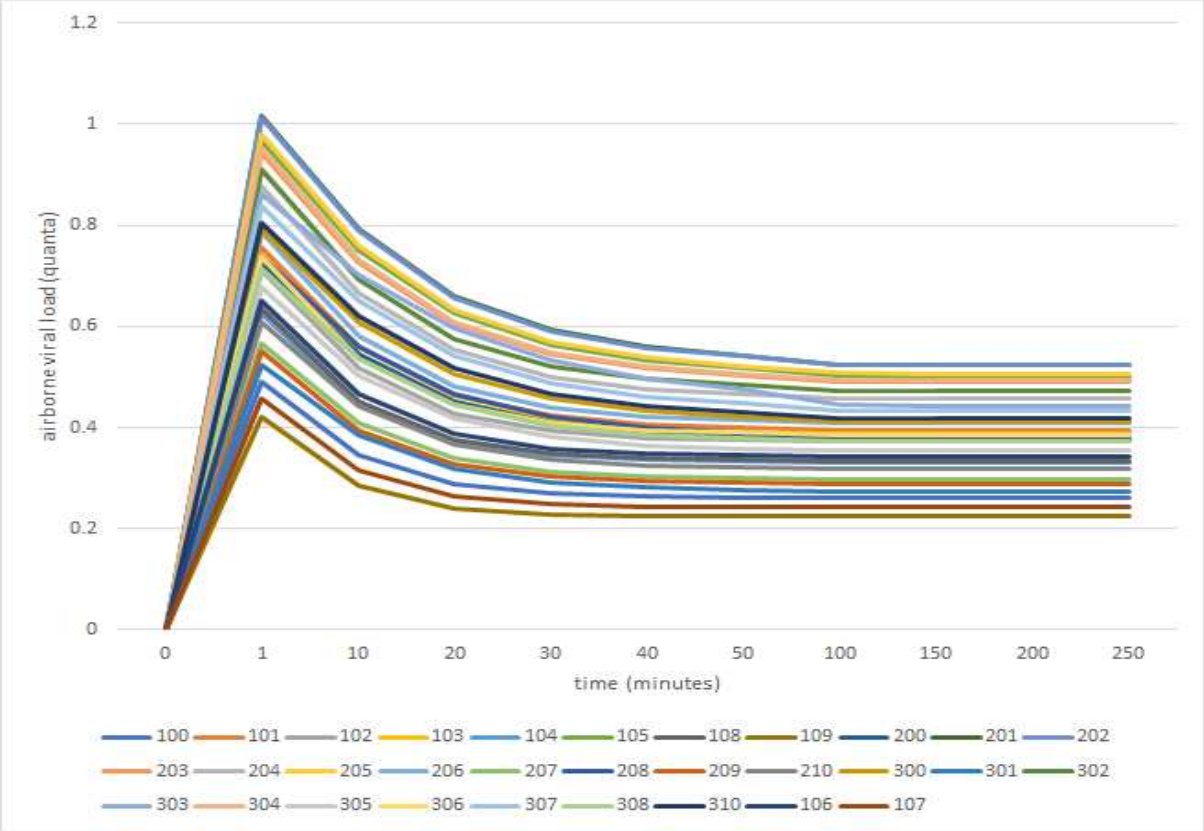

Measles at 10% occupation

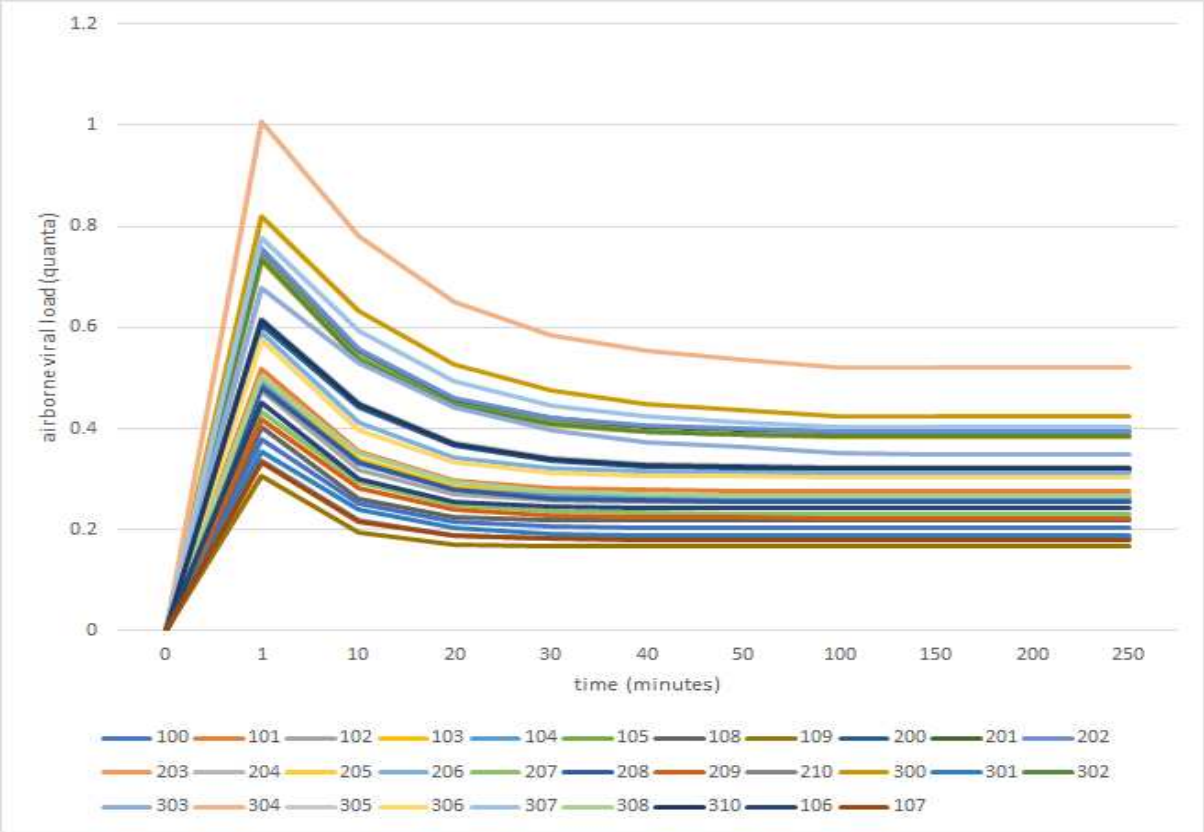

Measles at 50% occupation

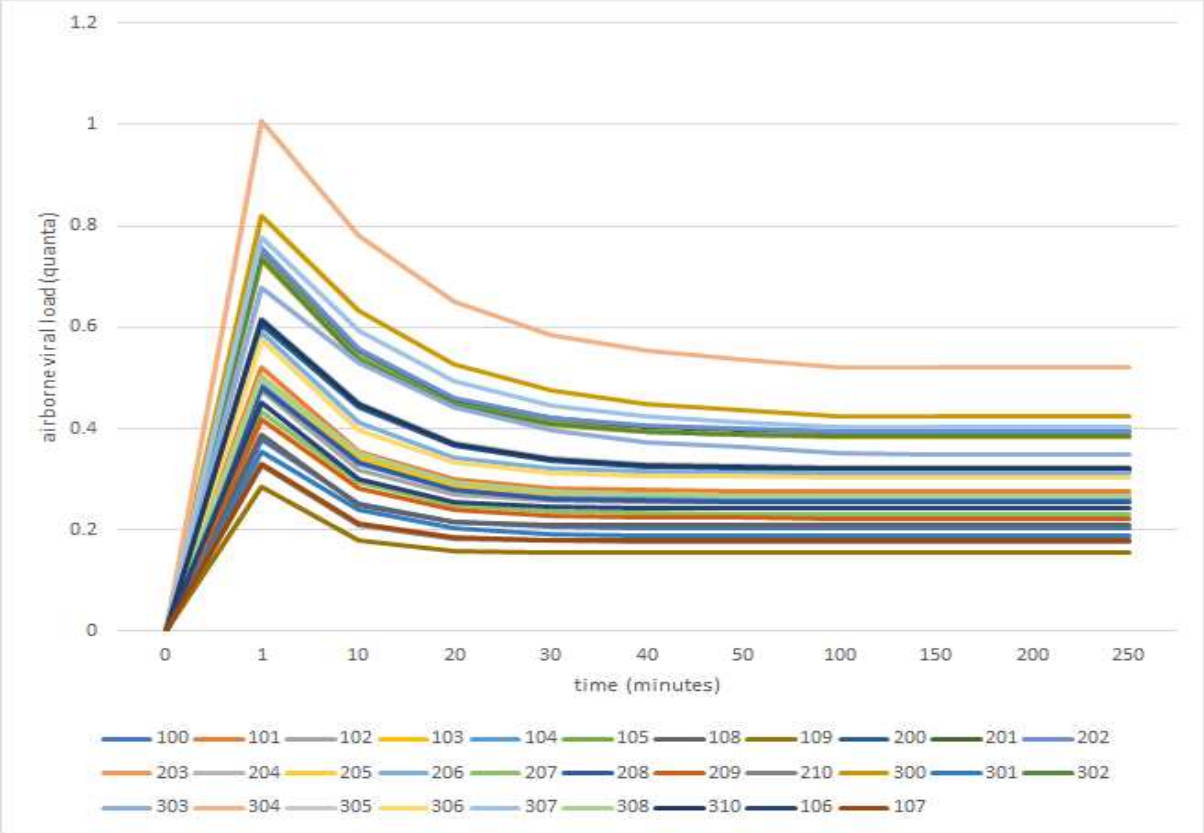

Measles at 90% occupation

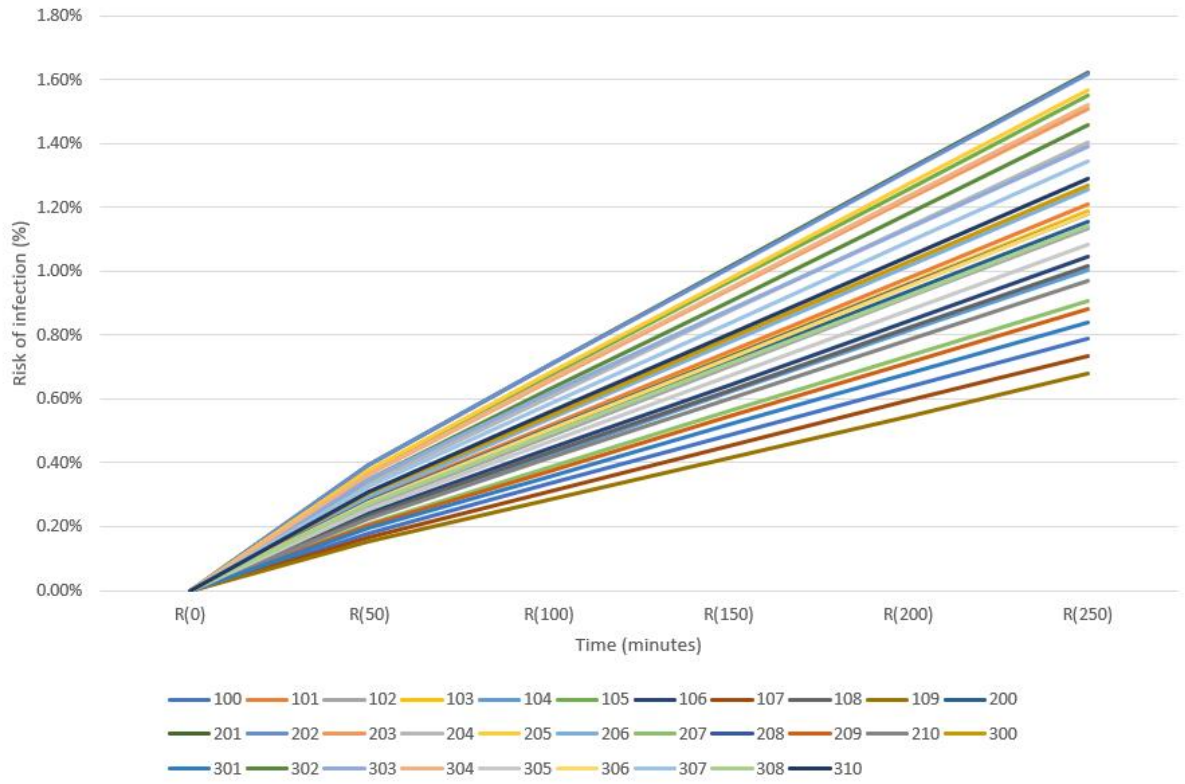

Tuberculosis Infection risk over time per classroom at 10% occupation rate

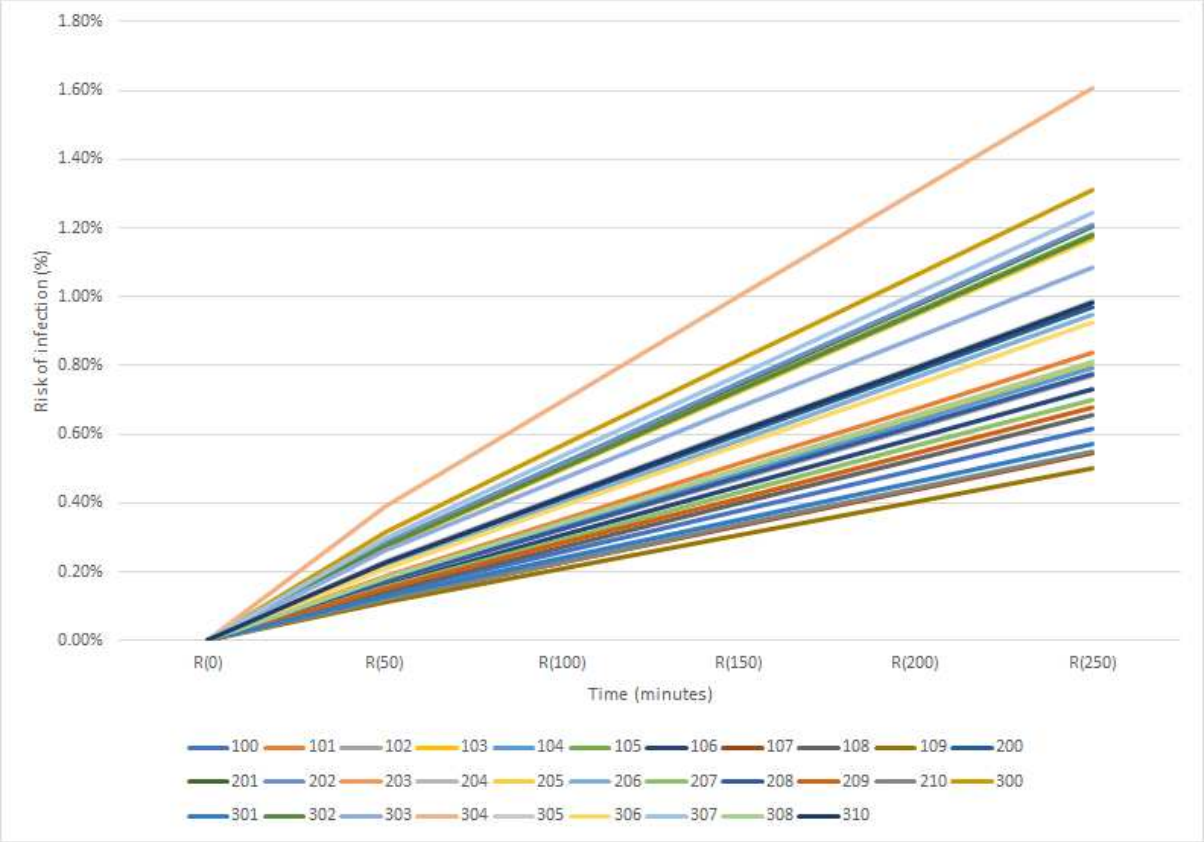

Tuberculosis Infection risk over time per classroom at 50% occupation rate

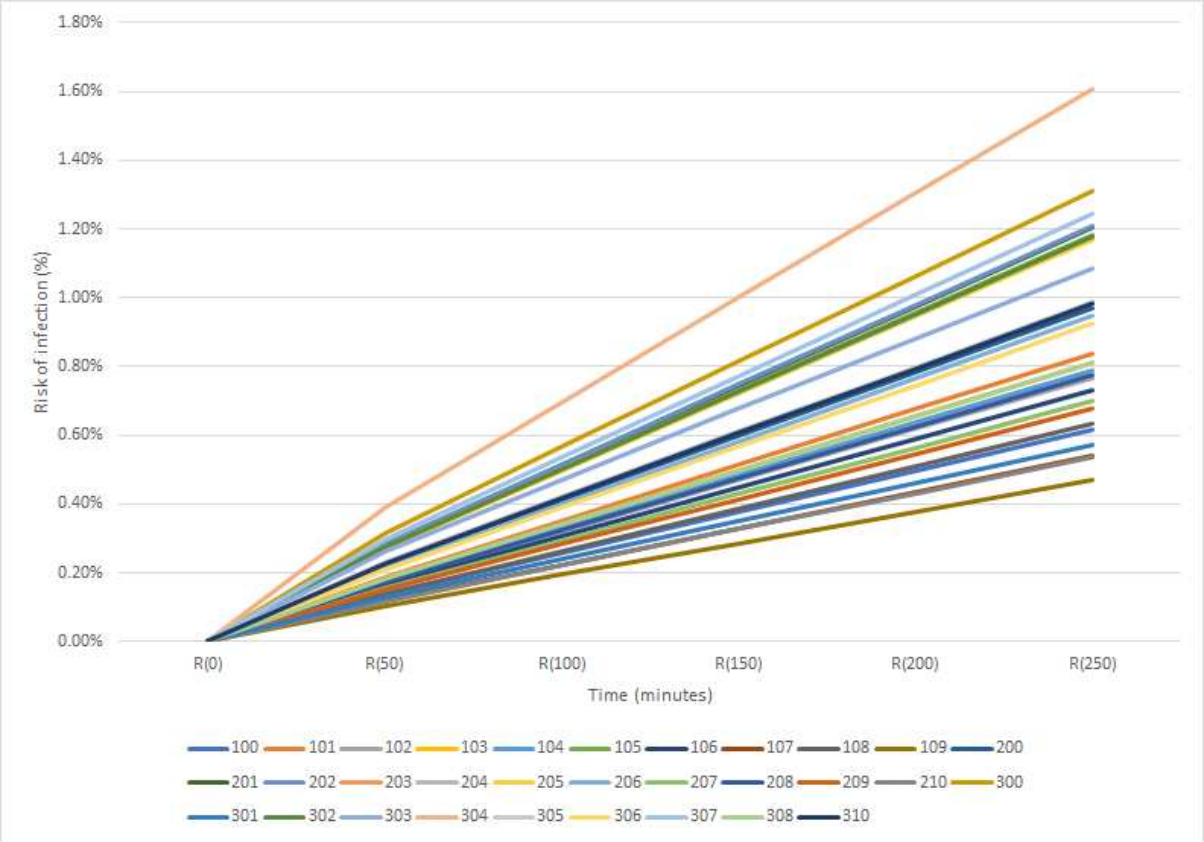

Tuberculosis Infection risk over time per classroom at 90% occupation rate

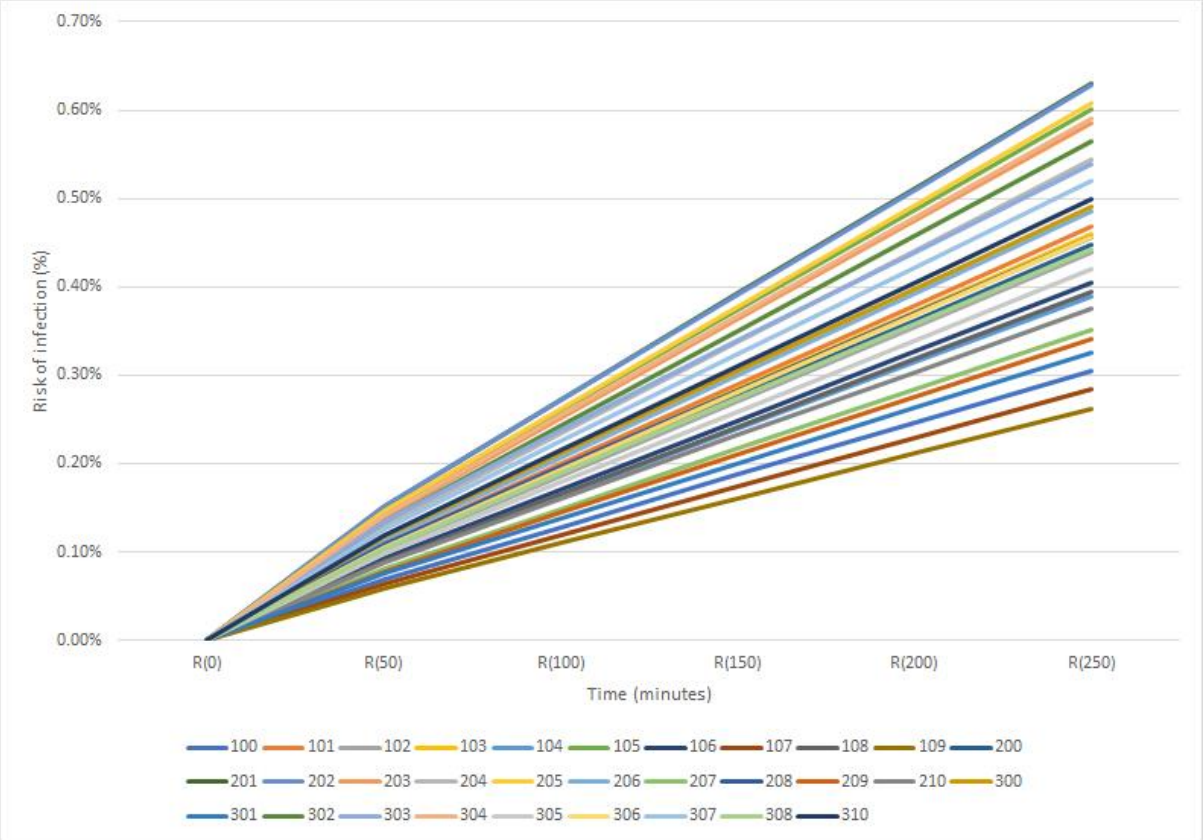

Covid-19 Infection risk over time per classroom at 10% occupation rate

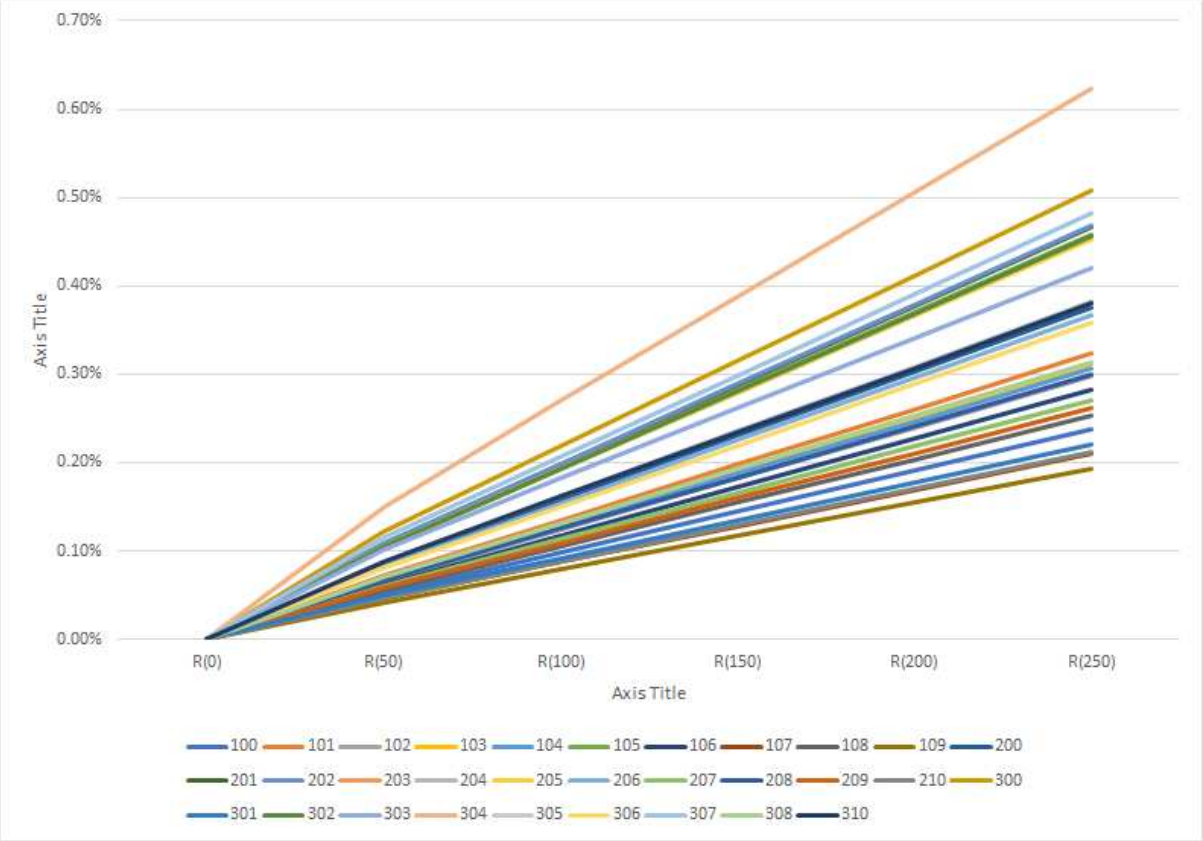

Covid-19 Infection risk over time per classroom at 50% occupation rate

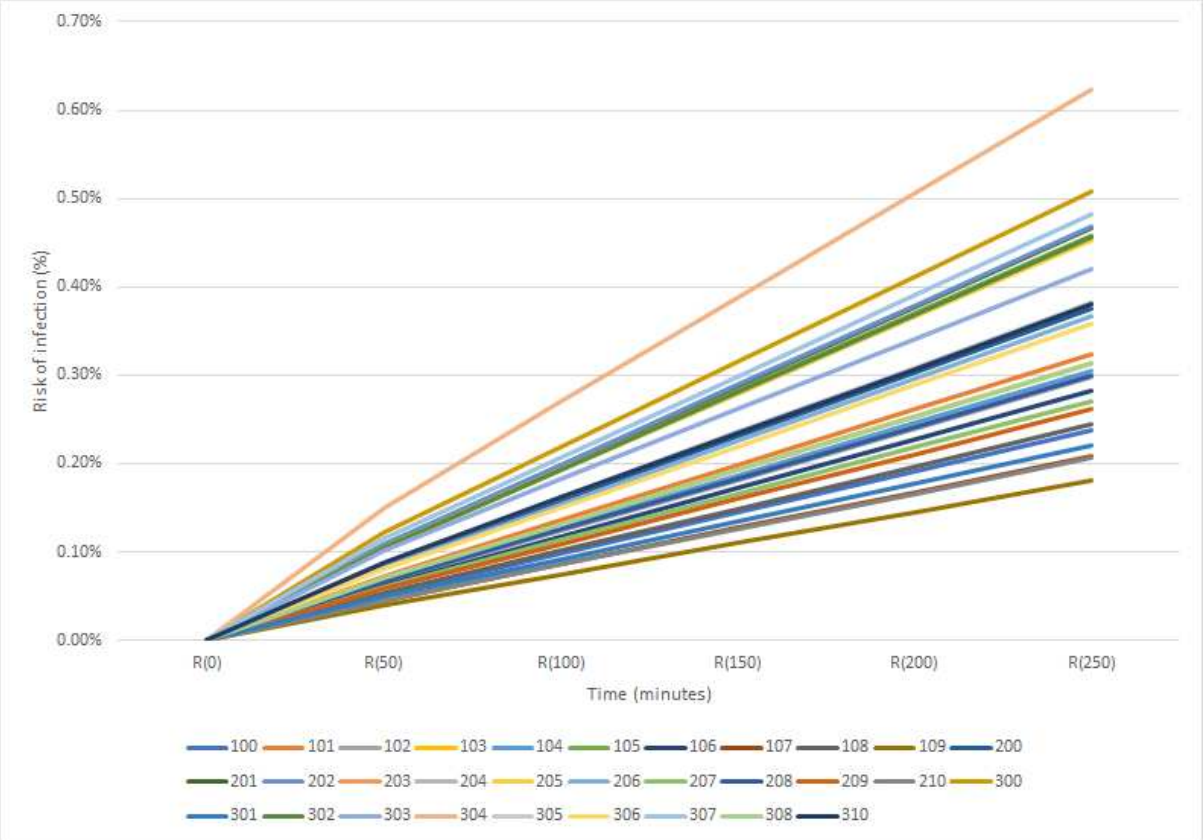

Covid-19 Infection risk over time per classroom at 90% occupation rate

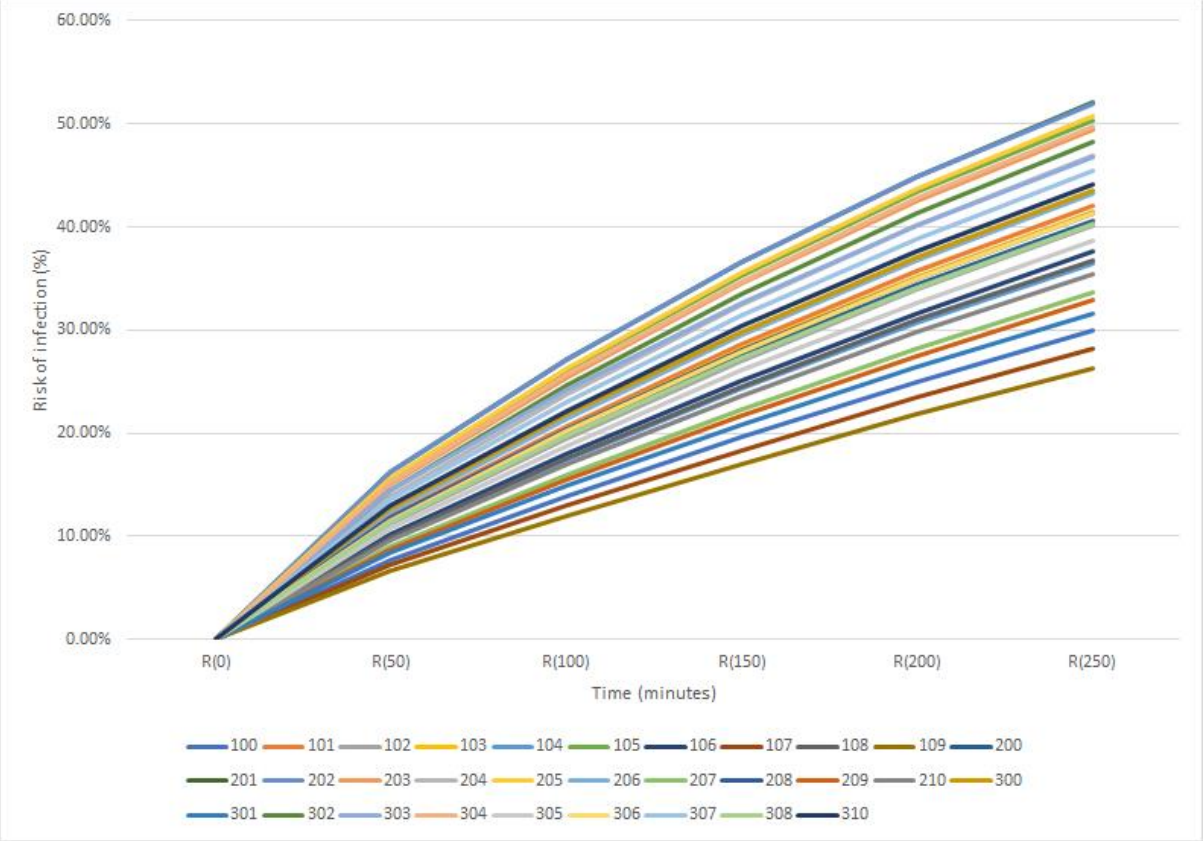

Measles Infection risk over time per classroom at 10% occupation rate

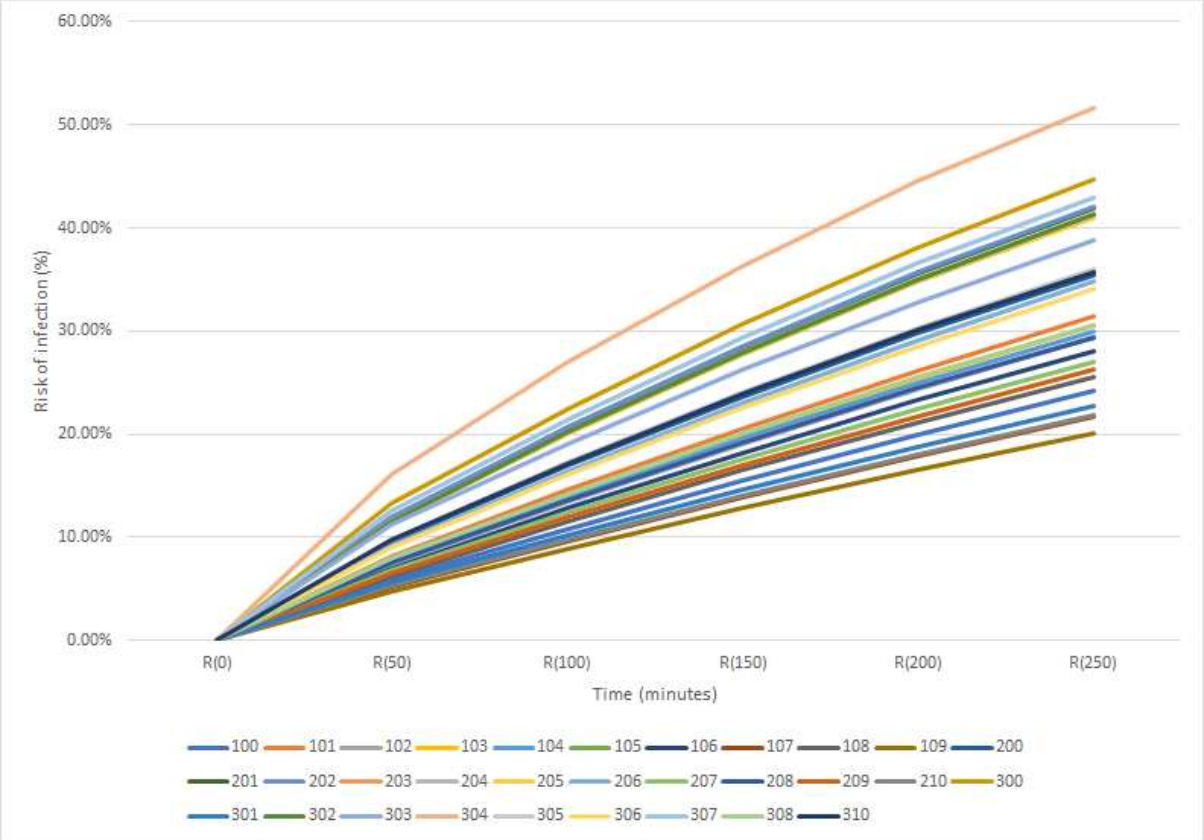

Measles Infection risk over time per classroom at 50% occupation rate

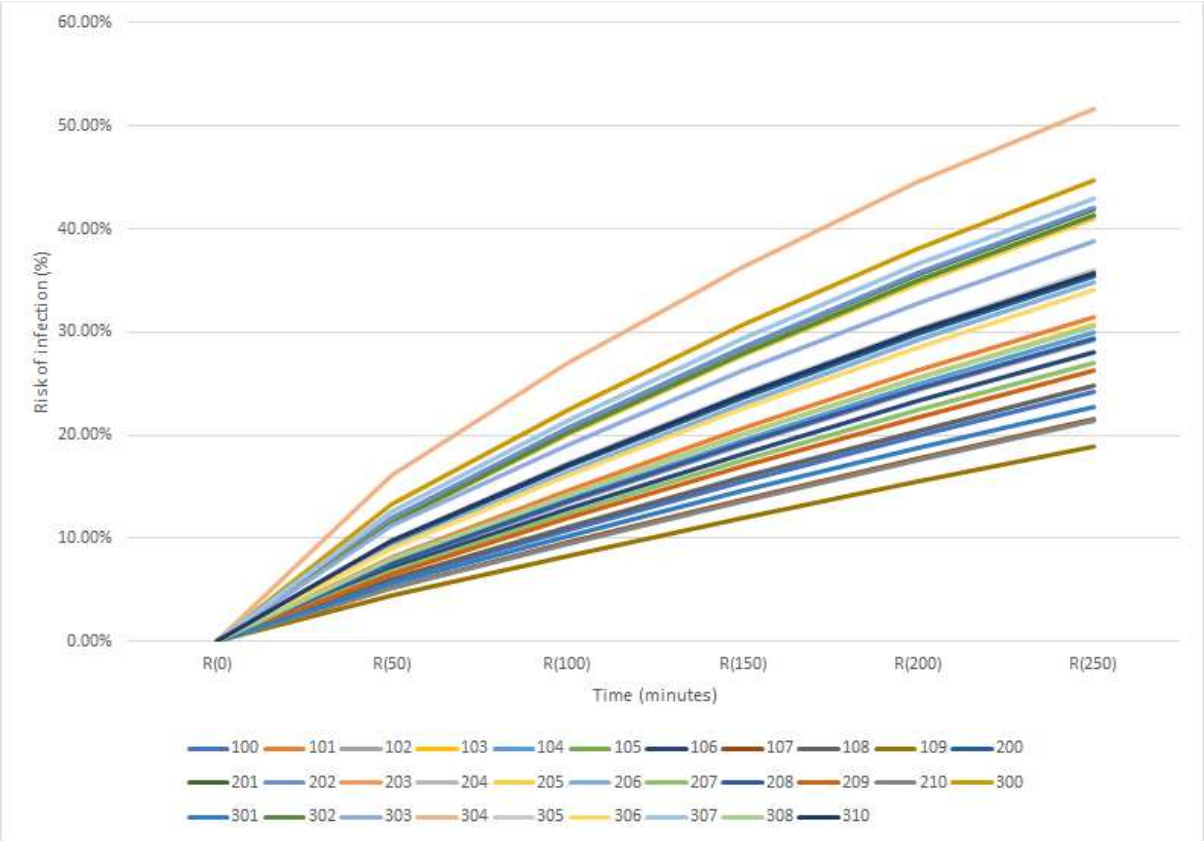

Measles Infection risk over time per classroom at 90% occupation rate